Examining the Effect of the Context of Heat-Labile Enterotoxin Presentation on the Host Immune Response

by

Halima Jane Chutkan

Department of Molecular Genetics and Microbiology
Duke University

Date:_____
Approved:

_____
Meta Kuehn, Supervisor

_____
Patrick Seed

_____
Raphael Valdivia

_____
Hiroaki Matsunami

_____
Herman Staats

Dissertation submitted in partial fulfillment of
the requirements for the degree of Doctor of Philosophy in the Department of
Molecular Genetics and Microbiology in the Graduate School
of Duke University

2011

ABSTRACT

Examining the Effect of the Context of Heat-Labile Enterotoxin Presentation on the Host Immune Response

by

Halima Jane Chutkan

Department of Molecular Genetics and Microbiology
Duke University

Date:_____
Approved:

_____
Meta Kuehn, Supervisor

_____
Patrick Seed

_____
Raphael Valdivia

_____
Hiroaki Matsunami

_____
Herman Staats

An abstract of a dissertation submitted in partial fulfillment of the requirements for the degree of Doctor of Philosophy in the Department of Molecular Genetics and Microbiology in the Graduate School of Duke University

2011

Copyright by
Halima Jane Chutkan
2011

Abstract

Enterotoxigenic *Escherichia coli* (ETEC), the leading cause of traveler's diarrhea and childhood mortality due to diarrhea in the developing world, has been shown to secrete heat-labile enterotoxin (LT) in association with outer membrane vesicles. However, studies on the effect of LT have been performed using soluble LT, which is not its physiologically relevant presentation context. The effect of LT associated with vesicles and its trafficking within human intestinal epithelial cells were compared with soluble LT. Cytokine responses and trafficking of standardized samples of soluble LT and vesicle-associated LT were evaluated in polarized intestinal epithelial cells. Using real-time PCR, immunoblotting, and ELISAs, we found that compared to soluble LT, vesicle-bound LT showed delayed kinetics in the activation of LT. Vesicles containing LT or not also produced cytokines through different signaling pathways than soluble LT. We found that this difference in signaling was due to different trafficking within the cell. Interestingly, not all LT associated with vesicles is active within cells. Vesicle-associated LT must bind to the host receptor G_{M1} in lipid rafts to be active within cells. This suggests that although vesicles can deliver large amounts of LT to a cell, much of the LT would be inactive and not produce a physiological response. To test this hypothesis, we attempted to develop animal models for ETEC-induced diarrhea. Although the models were largely unsuccessful, the mouse model appears promising for

determining the physiological response of a host to LT as fluid accumulation was observed in response to vesicles containing LT. The results in this thesis provide further understanding of the mechanism of LT-induced diarrhea and emphasize the importance of study toxins in their natural context.

For my family, innate and acquired.

Contents

Abstract iv

List of Tables xii

List of Figures xiii

1. Introduction 1

1.1 Outer Membrane Vesicles 1

1.1.1 Structure and Composition 1

1.1.2 Survival 3

1.1.3 Interbacterial Competition 3

1.1.4 Host Interactions 4

1.1.5 Vaccines 6

1.1.6 Routes of Internalization 7

1.1.7 Vesicle Internalization and Trafficking 8

1.2 Enterotoxigenic Escherichia coli 9

1.3 Heat-labile Enterotoxin 12

1.3.1 Assembly and Secretion 12

1.3.2 Regulation 14

1.3.3 Binding and Internalization 15

1.3.4 Activity 17

1.4 Diarrhea 18

1.4.1 Impact 18

1.4.2 Association with cytokines 19

1.4.3 Diarrhea models 20

1.5 Gut Immunity 23

1.5.1 Commensal bacteria 23

1.5.2 Epithelial barrier 24

1.6 Significance 26

2. Outer membrane vesicle-associated heat labile enterotoxin shows delayed PKA activation kinetics 28

2.1 Summary 28

2.2 Introduction 29

2.3 Results 32

2.4 Discussion 49

2.5 Acknowledgements 57

3. Heat labile enterotoxin- and G_{M1}-dependent intracellular trafficking and signaling of enterotoxigenic *Escherichia coli* outer membrane vesicles 58

3.1 Summary 58

3.2 Introduction 59

3.3 Results 62

3.4 Discussion 75

3.5 Acknowledgements 81

4. Exploring the physiological response to heat-labile enterotoxin 82

4.1 Summary 82

4.2 Introduction 82

4.3 Results 86

4.4 Discussion 94

4.5 Acknowledgments 97

5. Concluding remarks 99

5.1 Vesicles as delivery systems 99

5.2 Vesicles as a regulatory mechanism 101

5.3 Vesicles in a physiological context 102

5.4 Future directions 103

6. Materials and Methods 106

6.1 Bacterial strains and media 106

6.1.1 Media 108

6.1.2 LT mutants 108

6.2 Cell culture 108

6.2.1 Polarization assays 109

6.3 Toxin purification 109

6.4 Outer membrane vesicle purification and standardization 110

6.4.1 Vesicle purification 110

6.4.2 LT+ vesicle standardization to soluble LT 111

6.4.3 Lipid standardization 112

6.4.4 Flagellin immunoblotting 112

6.5 Pathway inhibitors 113

6.5.1 Signaling inhibitors 114

6.5.2 Trafficking inhibitors 114
6.6 Treatment conditions 115
6.7 Real-time PCR 115
6.7.1 Extraction of total RNA and reverse transcription 115
6.7.2 Real-time PCR 115
6.8 Nuclear extraction 117
6.9 Immunoblotting of nuclear extracts 118
6.10 Electrophoretic mobility shift assay 118
6.11 Enzyme-linked immunosorbent assays 119
6.12 Luciferase assay 119
6.13 Microscopy 120
6.13.1 Fluorescent labeling of vesicles 120
6.13.2 Internalization and co-localization experiments 120
6.14 Isolation of detergent-resistant membranes 121
6.15 Animal models 122
6.15.1 Pig Ussing chamber studies 122
6.15.2 Rabbit ligated ileal loops 123
6.15.3 Mouse studies 124
6.16 Glycosidase treatment 125
6.17 Y1 assay 125
6.18 Statistical analysis 126
Appendix A 127

References 133

Biography 149

List of Tables

Table 1: Toxins and routes of entry for selected outer membrane vesicles 4

Table 2: Strains used in this study 106

Table 3: Signaling and trafficking inhibitors 113

Table 4: RT-PCR primers used in this study 116

List of Figures

Figure 1: Model of outer membrane vesicle formation. 2

Figure 2: Overview of the internalization and trafficking of LT. 17

Figure 3: Diagram of the intestinal environment. 24

Figure 4: LT standardization of LT^+ OMVs. 33

Figure 5: Lipid standardization of vesicle preparations. 34

Figure 6: Catalytically active LT-containing treatments induce higher amounts of TNFα and IL-6 gene expression levels at 6 h. 35

Figure 7: Catalytically active LT-containing treatments elicit higher concentrations of IL-6 in the apical supernatant. 36

Figure 8: Soluble LT, but not LT^+ OMVs, induce TNFα and IL-6 gene induction through PKA. 38

Figure 9: Immunoblots and densitometry analysis of pCREB and TBP in polarized T84 cells after treatment with soluble LT and OMV treatments. 39

Figure 10: CRE activation in HEK293T cells shows delayed activation kinetics in response to LT^+ OMVs. 41

Figure 11: LT^+ OMVs show similar levels of TNFα induction at 9 h as soluble LT but significantly higher levels of IL-6 induction. 42

Figure 12: LT^+ OMVs induce TNFα and IL-6 through PKA at 9 h. 43

Figure 13: Both soluble LT and LT^+ OMVs act through ERK1/2 and p38 to induce TNFα but not IL-6. 45

Figure 14: Soluble LT but not LT^+ OMVs induce TNFα and IL-6 through AP-1. 46

Figure 15: EMSA of AP-1 activation in polarized T84 cells in response to treatments. 47

Figure 16: OMVs but not soluble LT induce IL-6 through NFκB. 48

Figure 17: Flagellin levels in vesicle preparations do not correlate with TNFα and IL-6 induction. 49

Figure 18: Overview of the different pathways through which soluble LT and LT^+ OMVS elicit TNFα and IL-6 responses in human intestinal epithelial cells. 50

Figure 19: ETEC OMVs are internalized independent of LT. 63

Figure 20: LT enhances the association of OMVs with polarized T84 cells. 64

Figure 21: LT^+ OMVs but not ΔLT OMVs colocalize with G_{M1}. 66

Figure 22: G_{M1} binding is required for the activation of LT. 68

Figure 23: OMVs interact with intact lipid rafts on polarized intestinal epithelial cells. . 70

Figure 24: OMVs that do not contain LT require clathrin to induce IL-6 73

Figure 25: LT requires ER trafficking to be active, but ΔLT OMVs do not 75

Figure 26: The transepithelial resistance between paired treatments was consistent throughout the experiment. 87

Figure 27: No Cl- secretion was observed in response to LT or CT. 88

Figure 28: Rabbit ileal loops showed no difference in gut density after treatment with soluble and OMV-bound LT. 89

Figure 29: Fluid accumulation showed contradictory results from trial to trial. 90

Figure 30: Paregoric and antibiotic pre-treatment led to a significant increase in fluid accumulation in response to LT^+ OMVs. 91

Figure 31: Sodium bicarbonate resulted in decreased fluid accumulation compared to PBS. 92

Figure 32: LT^+ OMVs showed a difference in cytokine induction in a mouse model compared with soluble LT. 94

Figure 33: Overview of the trafficking and signaling pathways of soluble and OMV-bound LT. 104

Figure 34: LT in ETEC2 vesicles show a different mobility compared to soluble LT. 127

Figure 35: The slowly migrating band is not an aggregate or glycosylated. 129

Figure 36: The vesicle-associated modified protein does not bind to galactose. 130

Figure 37: ETEC2 is toxic to Y1 adrenal cells. 132

1. Introduction

1.1 Outer Membrane Vesicles

Outer membrane vesicles are spherical structures that bud naturally from all Gram-negative bacteria studied to date. Vesicles were first identified in the 1960s in cultures of *Escherichia coli* grown under lysine-limiting conditions but were thereafter observed in cultures of normally growing bacteria (Bishop & Work, 1965). Vesicles have also been isolated from some Gram-positive bacteria (Prados-Rosales et al, 2011; Rivera et al, 2010). Vesicle production is a natural process and is not a result of membrane instability (McBroom et al, 2006). Vesiculation has been shown to occur in planktonic cultures, biofilms and in vivo (Ciofu et al, 2000; Hellman et al, 2000; Schooling & Beveridge, 2006). Although the exact mechanism of vesicle formation is unknown, vesicles from a variety of species have been shown to play roles in survival and host interactions.

1.1.1 Structure and Composition

Vesicles are roughly 50 – 200 nm and are composed of a lipid bilayer derived from the outer membrane of Gram-negative bacteria (Kulp & Kuehn, 2010). Outer membrane proteins are also inserted into the vesicle membrane, and the lumen of the vesicle contains periplasmic components (Kuehn & Kesty, 2005). As shown in Figure 1, vesicles bud off and release from the surface of Gram-negative bacteria. Outer membrane vesicles show a similar protein profile to outer membrane proteins, but there

are some differences. Proteomics studies have shown that depending on the strain and growth conditions, certain outer membrane proteins are enriched or excluded from vesicles (Horstman & Kuehn, 2000; Kato et al, 2002; Wensink & Witholt, 1981). LPS has also shown enrichment in vesicles compared to the whole bacteria. Lipid profiling has shown that *P. aeruginosa* OMVs are enriched in a particular form of LPS that is found in small amounts in the outer membrane of *P. aeruginosa* (Kadurugamuwa & Beveridge, 1996). DNA has also been found to be associated with *P. aeruginosa* and *E. coli* vesicles, and these vesicles were able to mediate the transfer of DNA from one strain to another (Kolling & Matthews, 1999; Renelli et al, 2004).

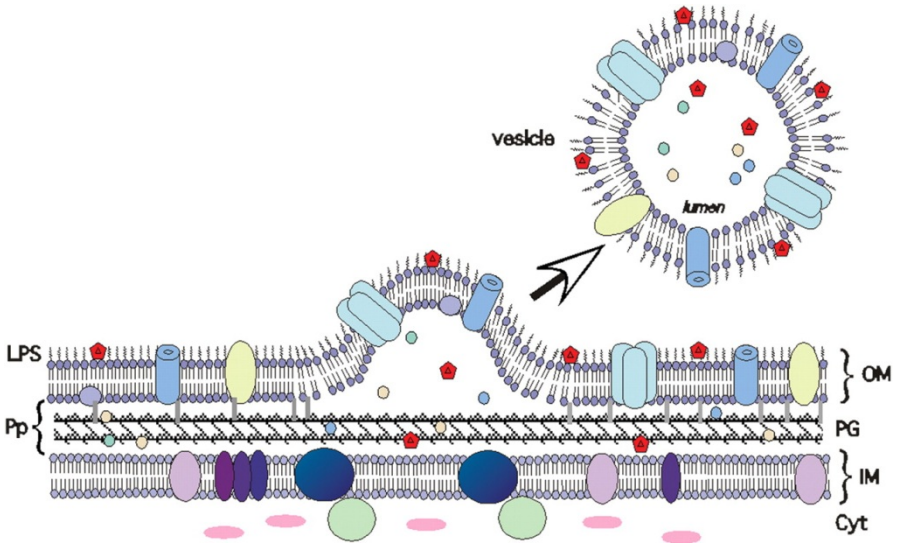

Figure 1: Model of outer membrane vesicle formation.
A general model of outer membrane vesicle formation in Gram-negative bacteria. The vesicle bulges from the outer membrane and pinches off to form spherical membranous structures containing both outer membrane and periplasmic components. Reproduced from (Kuehn & Kesty, 2005).

1.1.2 Survival

Outer membrane vesicles have also been shown to be protective against a variety of stressors, both external and internal.

Because vesicles are composed of outer membrane components, they can act as decoys against membrane-targeting agents, such as antimicrobial peptides and lytic phage (Manning & Kuehn, in press). In addition to acting as decoys to bind membrane-targeting agents and increase the survival of bacteria, outer membrane vesicles can also contain enzymes, such as β-lactamase in *P. aeruginosa* vesicles, that inactivate these agents (Ciofu et al, 2000).

In addition to protection against extrinsic factors, internal stress can also lead to increased vesicle production to promote survival. Studies have shown that an accumulation of misfolded periplasmic proteins leads to increased vesicle production and the enrichment of these misfolded proteins into these vesicles (McBroom & Kuehn, 2007). Indeed, hypervesiculating mutants have been shown to survive better under conditions of both internal and external stress (McBroom & Kuehn, 2007).

1.1.3 Interbacterial Competition

Outer membrane vesicles can also deliver proteins to other bacteria. Vesicles can fuse with other bacteria to deliver proteases and hydrolases to lyse competitors, providing a growth advantage (Kadurugamuwa & Beveridge, 1996; Kadurugamuwa & Beveridge, 1999).

1.1.4 Host Interactions

In addition to interacting with other bacteria in the environment, outer membrane vesicles can interact with host cells to aid the bacteria in infection and colonization. Outer membrane vesicles have been shown to be associated with virulence factors, including outer membrane proteins, toxins, and pathogen-associated molecular patterns (PAMPS), including flagellin and the major constituent of outer membrane vesicles, LPS. Table 1 shows some of the toxins that have been identified to be associated with outer membrane vesicles.

Table 1: Toxins and routes of entry for selected outer membrane vesicles

Bacterium	***Toxin***	***Method of Entry***	***Reference***
Shigella flexneri	-	Phagocytosis	(Kadurugamuwa & Beveridge, 1998)
Helicobacter pylori	VacA	Clathrin	(Parker et al, 2010)
Enterotoxigenic *E. coli*	LT	Lipid raft, caveolin	(Kesty et al, 2004)
E. coli O111:H-	ClyA	-	(Wai et al, 2003)
E. coli O157:H7	Stx	-	(Kolling & Matthews, 1999)
E. coli	α-hemolysin	-	(Balsalobre et al, 2006)

Table 1: Toxins and routes of entry for selected outer membrane vesicles (continued)

Bacterium	*Toxin*	*Method of Entry*	*Reference*
Porphrymonas gingivalis	-	Lipid raft	(Furuta et al, 2009)
Pseudomonas aeruginosa	Cif	Lipid raft	(Bauman & Kuehn, 2009; Bomberger et al, 2009)
Moraxella catarrhalis	-	Lipid raft, TLR, caveolin, flotillin	(Schaar et al, 2011)
Non-typeable *Haemophilus influenzae*	-	Caveolae	(Sharpe et al, 2011)
Campylobacter jejuni	CDT	-	(Lindmark et al, 2009)
Acinetobacter baumannii	OmpA	Lipid rafts	(Jin et al, 2011)
Aggregatibacter actinomycetemcomitans	LktA	-	(Kato et al, 2002)
A. actinomycetemcomitans	CDT	Lipid rafts	(Rompikuntal et al, 2011)

Outer membrane vesicles can serve as efficient delivery molecules through their interactions with host cells. Proteins that are secreted extracellularly are susceptible to degradation by host proteases. However, outer membrane vesicles may protect complexed proteins from degradation by proteases, allowing the secreted proteins to be

more effectively delivered to host cells (Kulp & Kuehn, 2010). In addition, adhesins that mediate binding to host cells have been found to be associated with outer membrane vesicles (Holm et al, 2004; Kesty et al, 2004). For example, toxins can act as adhesins; both LT from ETEC and VacA from *H. pylori* can enhance the association of vesicles with host cells (Kesty et al, 2004; Parker et al, 2010). Vesicles may also deliver a larger dose of associated toxin to host cells than soluble toxin, acting as "toxin bombs" (Mudrak & Kuehn, 2010).

1.1.5 Vaccines

In addition to their natural roles in interactions with bacteria and host cells, vesicles have also been investigated for their ability to induce an immune response when administered as a vaccine. The role of vesicles in protecting proteins from proteases may better preserve antigenic epitopes and elicit a stronger immune response (van der Ley et al, 1991). Vesicles can also contain adjuvants to help promote an immune response, such as LPS, flagellin, and outer membrane proteins. Vaccines derived from outer membrane vesicles have been shown to be more effective immunogens than corresponding outer membrane proteins (Chen et al, 2010; Muralinath et al, 2011; Peeters et al, 1996) and heat-killed bacteria (Park et al, 2011; Roberts et al, 2008). Outer membrane vesicles can also be engineered to incorporate specific proteins for presentation as antigenic epitopes (Koeberling et al, 2006) and to make both LPS and

proteins less toxic in an effort to make vaccines more effective and safer for human use (Asensio et al, 2011; Taxt et al, 2010; Van der Ley & Van den Dobbelsteen, 2011).

1.1.6 Routes of Internalization

How do vesicles interact with host cells? The internalization of large molecules, such as pathogens and outer membrane vesicles, into host cells can occur through a variety of mechanisms. The primary mechanisms associated with vesicle entry include lipid rafts, caveolae, and clathrin-mediated endocytosis.

Lipid rafts are discrete sphingolipid- and cholesterol-rich microdomains in the plasma membrane of eukaryotic cells (Lajoie & Nabi, 2010). These domains can play roles in the endocytosis of pathogens and their products, polarization, signaling and secretion (Vieira et al, 2010). Several methods have been used to study lipid rafts and their associated proteins. One method is through the differential centrifugation of detergent-resistant membrane preparations using sucrose density gradients (Vassilieva et al, 2008; Vieira et al, 2010; Wolf et al, 2002). Another method is the pharmacological depletion of cholesterol from the plasma membrane using methyl-β-cyclodextrin (Vieira et al, 2010). Molecular markers that have been used to identify lipid raft microdomains include G_{M1} and flotillin-1 (Badizadegan et al, 2000; Vieira et al, 2010).

Another marker that may be associated with lipid rafts in certain cell types is caveolin-1. Internalization through these caveolin-associated lipid rafts, also known as caveolae, leads to the formation of flask-shaped invaginations of the plasma membrane

(Schlegel et al, 1998). Although caveolae are readily found in endothelial cells, adipocytes, muscle cells and fibroblasts (Schlegel et al, 1998), caveolin-1 is not associated with detergent-resistant membranes in intestinal epithelial cells. In fact, caveolin-1 is only expressed at very low levels in these cells and is not associated with G_{M1} in apical membranes (Badizadegan et al, 2000). Unlike caveolin-independent lipid raft endocytosis, caveolae require dynamin (Oh et al, 1998). However, both caveolae and lipid raft-dependent endocytosis are sensitive to cholesterol depletion (Parton & Simons, 2007).

Clathrin, a coat protein, mediates the internalization of receptors, membrane and cargo (Kaksonen et al, 2006). In this process, cargo binds to specific host receptors, which then bind to adaptor proteins. Clathrin associates with adaptor proteins to form a coat at the site of internalization and leads to membrane invagination that then buds to form an intracellular vesicle (Kaksonen et al, 2006). Like caveolae, the fission of the intracellular vesicle requires dynamin (McMahon & Boucrot, 2011). The vesicles then fuse with endosomes, which may then traffic their cargo to late endosomes and lysosomes and recycle receptors back to the plasma membrane (Kaksonen et al, 2006).

1.1.7 Vesicle Internalization and Trafficking

Outer membrane vesicles have been shown to be internalized in host cells through a variety of mechanisms, depending on the strain from which vesicles were isolated and the host cell (Table 1). The major routes of outer membrane vesicle

internalization are mediated by clathrin, caveolae, and clathrin- and caveolin-independent lipid rafts. Intriguingly, *P. gingivalis* bacteria take advantage of lipid rafts to subvert innate defense mechanisms (Hajishengallis et al, 2008), and their vesicles also interact with host cells through lipid raft domains, possibly through the same fimbrial adhesin (Furuta et al, 2009). In addition to these pathways, vesicles from *S. flexneri* have been shown to be internalized through phagocytosis (Kadurugamuwa & Beveridge, 1998).

Once vesicles have been internalized, the pathways through which they are trafficked are as varied as the internalization mechanisms. Although *P. aeruginosa* vesicles from a cystic fibrosis clinical isolate were shown to colocalize with ER markers, vesicles from a burn wound isolate trafficked within early endosomes and did not require ER translocation for toxicity (Bauman & Kuehn, 2009; Bomberger et al, 2009). Our lab has shown that LT^+ vesicles from ETEC do not get internalized within acidified compartments, which excludes trafficking within endosomes and lysosomes (Kesty et al, 2004).

1.2 Enterotoxigenic Escherichia coli

Diarrheal diseases account for over two million deaths annually in developing countries, particularly in children less than five years old (Svennerholm & Steele, 2004). Diarrheal outbreaks in developing countries can be caused by several pathogens, including *Vibrio cholerae,* enterotoxigenic *E. coli* (ETEC), *Shigella* spp., *Campylobacter*

jejuni, *Salmonella enterica* serovar *typhi,* other non-ETEC *E. coli*, rotavirus, and *Entamoeba histolytica* (Holmgren & Svennerholm, 1998; Svennerholm & Steele, 2004). However, ETEC accounts for the majority of diarrheal cases. A 30-year study of diarrhea in developing countries showed that ETEC accounted for 280 million cases of diarrhea annually in children less than five years old (Wenneras & Erling, 2004). Mortality due to ETEC-associated diarrhea has been estimated at 170,000 annually (Niyogi, 2005).

ETEC and *V. cholerae* produce similar diarrheal symptoms. Both infections produce a sudden onset of watery diarrhea and vomiting that may last for several days and may lead to dehydration and malnutrition in young children. In addition, dry mouth, lethargy, and muscle cramps may accompany fluid loss (Qadri et al, 2005). ETEC-induced diarrhea may range from mild to severe cholera-like illness (Qadri et al, 2005). Some studies have shown differences in the timeframe, magnitude and severity of dehydration between ETEC and *V. cholerae*, but these differences may be strain-specific (Qadri et al, 2005; Sack, 1975). ETEC is a secretory, non-inflammatory diarrhea that is usually self-limiting (Daniels, 2006).

E. coli was first associated with diarrheal disease in a nursery outbreak in the 1940s (Bray, 1945). In 1957, an *E. coli* strain isolated from patients with a diarrhea-like disease was shown to produce fluid accumulation in rabbit ileal loops, similar to *V. cholerae* (De et al, 1956). However, ETEC was not identified until 1967, when it was isolated from young animals with diarrhea (Sack, 1975). In 1968, ETEC was isolated

from adults in Calcutta suffering from a *Vibrio*-like cholera illness but showed no signs of *V. cholerae* (Sack et al, 1971). These patients showed the characteristic symptoms of cholera but over a shorter timeframe, and the researchers were able to isolate a heat-labile enterotoxin (LT) from small bowel samples (Sack et al, 1971).

Since this first report, ETEC has been isolated from patients in developing countries, such as Bangladesh, Mexico, Peru, Argentina, and Nicaragua (Qadri et al, 2005). ETEC is endemic in these countries due to poor sanitation procedures and inadequate clean water (Qadri et al, 2005), and pre-existing malnutrition can lead to a more severe manifestation of the disease (Brown, 2003). Both *V. cholerae* and ETEC have been isolated from the surface waters of Bangladesh and Bolivia, and transmission has been shown to occur through the fecal-oral route through bathing or ingesting contaminated food or water (Begum et al, 2005; Ohno et al, 1997).

ETEC is also the leading cause of traveler's diarrhea worldwide (Black, 1990), and it has been estimated to cause 10 million cases of traveler's diarrhea annually (Steffen et al, 2005). In fact, approximately 60% of all U.S. residents traveling to Mexico are expected to develop traveler's diarrhea (Flores et al, 2008).

The most common treatment option for diarrhea caused by ETEC and *V. cholera* is rehydration therapy, and antibiotics are usually only used in cases of traveler's diarrhea (Qadri et al, 2005). ETEC strains have shown increasing multidrug resistance in several areas of the world, making antibiotic therapy less effective (Chakraborty et al,

2001; Qadri et al, 2005). However, infection with ETEC usually provides immunity to future infections, which is reflected in the majority of cases being associated with children in endemic areas (DuPont et al, 1981). This immunity has been thought to be associated with increased antibody production against the B subunit of LT, blocking the binding of LT to host ganglioside receptors (DuPont et al, 1981).

1.3 Heat-labile Enterotoxin

ETEC produces diarrhea through many virulence factors, including toxins and colonization factors. ETEC elaborates heat-stable enterotoxins (STs) and LT either alone or in combination (Croxen & Finlay, 2010). ST is a small (approximately 2 kDa), non-immunogenic toxin that is plasmid encoded (Taxt et al, 2010). ST has been shown to produce a more severe disease than LT in multiple studies (Qadri et al, 2000). ST binds reversibly to guanylyl cyclase C, which leads to an increase in cyclic GMP levels and fluid secretion (Rao, 1985). Unlike CT, a closely related toxin, LT is plasmid encoded, and both subunits are transcribed into a single mRNA (Dallas et al, 1979). Because CT and LT are so closely related, many of the studies performed on this type of heat-labile enterotoxin have focused on CT, and the data have been extrapolated to LT.

1.3.1 Assembly and Secretion

LT is a multi-subunit 87 kDa toxin composed of five identical 11.6 kDa B subunits arranged in a pentameric ring and one catalytically active 27 kDa A subunit. LTA is further composed of two domains, LTA1 and LTA2, which are covalently linked

by a disulfide bridge (Dallas & Falkow, 1980; Moss et al, 1981). The LTA2 subunit is responsible for binding to the pentameric B subunit ring, and the LTA1 subunit is catalytically active (Dallas & Falkow, 1980). LT is highly functionally and phenotypically similar to cholera toxin (CT) and shares approximately 80% sequence homology (Dallas & Falkow, 1980).

The first efforts to purify LT showed that LT co-purified with endotoxin and outer membrane fragments (Jacks et al, 1973; Lariviere et al, 1973). Early studies showed that unlike CT, LT was a periplasmic protein that was not efficiently secreted from the cell (Hirst et al, 1984a; Wensink et al, 1978). However, in 1995, Wai et al. showed that LT was released at the same time as outer membrane vesicles (Wai et al, 1995). Further studies performed in our lab showed for the first time that LT was tightly associated with vesicles and was enriched in vesicles compared to the periplasm (Horstman & Kuehn, 2000). The results suggested that LT was present on both the outer leaflet of vesicles and within the lumen (Horstman & Kuehn, 2000). Both LT and CT can bind to LPS from *E. coli* but not *V. cholerae*, and this binding site has been shown to be independent of the G_{M1}-binding site (Horstman & Kuehn, 2000; Mudrak et al, 2009).

A study examining the toxicity of vesicle-associated LT compared with LT from vesicle-free supernatant suggested that >95% of the toxic activity of LT was vesicle-associated (Horstman & Kuehn, 2002). Both LTA and LTB are synthesized in the cytoplasm and translocated across the inner membrane into the periplasm through the

Sec pathway (Palva et al, 1981). The B subunit then assembles into a pentamer and binds to the A subunit to form the holotoxin, which is then secreted through the general secretory pathway (Hofstra & Witholt, 1984; Hofstra & Witholt, 1985; Horstman & Kuehn, 2002). Once secreted, LTB binds to Kdo2-lipid A on the outer leaflet of the outer membrane (Horstman et al, 2004). Vesicles containing LT bound to the surface and within the periplasm of the bacterial cell can then bud from the cell and interact with host cells.

1.3.2 Regulation

LT production can be regulated in a variety of ways. In vitro studies have shown that LT is maximally produced at 37°C at a pH of 7.5-8.0 and that LT is induced in the presence of glucose (Kunkel & Robertson, 1979; Mundell et al, 1976). LT appears to be maximally produced under conditions that mimic the environment of the small intestine, its location of action (Mudrak & Kuehn, 2010). Likewise, LT production appears to be inhibited under conditions that mimic other less-favorable locations of the body. For example, LT production is inhibited by short-chain fatty acids, which are produced in the colon (Takashi et al, 1989). Short-chain fatty acids can lead to the adsorption of fluid in the colon, which would make LT inefficient (Binder, 2010).

The transcription of LT may also be regulated by a feedback loop. A consensus sequence that binds to cAMP receptor protein (CRP) is located at -31.5 bp upstream of the LT transcriptional start site (Bodero & Munson, 2009). Once bound to this upstream

region, CRP leads to the repression of LT transcription. However, CRP cannot bind without its cofactor, cAMP, which is produced by host cells in response to LT (Bodero & Munson, 2009). This negative feedback loop may reduce the damage produced by LT and maximize the resources available to the bacteria. Confirming the results on the induction of LT in the presence of glucose, high levels of glucose suppress cAMP synthesis, inhibiting the action of CRP and resulting in LT transcription (Bodero & Munson, 2009).

1.3.3 Binding and Internalization

Like CTB, the LTB subunit mediates toxin binding to the host ganglioside receptor G_{M1} (Moss et al, 1981). Unlike CTB, LTB has also been shown to bind to other receptors on host cells, including glycoproteins, polyglycosylceramides, G_{M2}, and asialo-G_{M1}, albeit with less affinity (Holmgren et al, 1985; Teneberg et al, 1994). However, binding to other receptors, such as G_{D1a}, has been shown to render the toxin inactive in polarized intestinal epithelial cells because G_{D1a} is not associated with lipid rafts (Wolf et al, 1998). LT has also been shown to bind to blood sugar residues of the A-type blood antigen (Holmner et al, 2007).

G_{M1} is located in cholesterol-rich domains within the host cell membrane. Pharmacologically depleting cholesterol to disrupt the organization of lipid rafts has been shown to inhibit the internalization of vesicles containing LT (Kesty et al, 2004). In addition, cholesterol depletion has been shown to inhibit the toxicity of CT (Wolf et al,

2002). However, although cholesterol depletion has been shown to disrupt the trafficking of CT, CT was still found in lipid raft domains at the plasma membrane (Wolf et al, 2002). The internalization pathways of LT depend on the cell type and age. Neonates are considered more sensitive to LT because as cells mature, LT uptake switches from rapid and clathrin-dependent to slower and caveolin-dependent (Lu et al, 2005; Viswanathan et al, 2009). Once LT binds to G_{M1}, it is internalized into an endocytic compartment and trafficked in a retrograde manner through the Golgi apparatus and the endoplasmic reticulum (ER) (Figure 2). Both CT and LT show a lag time in the activation of adenylate cyclase, which is assumed to be the time required for these toxins to enter the cell and be retro-translocated to the Golgi and ER (Fishman, 1980). Studies have shown that the entire CT holotoxin is transported to the ER and remains associated with G_{M1} in lipid rafts in the ER membrane (Fujinaga et al, 2003).

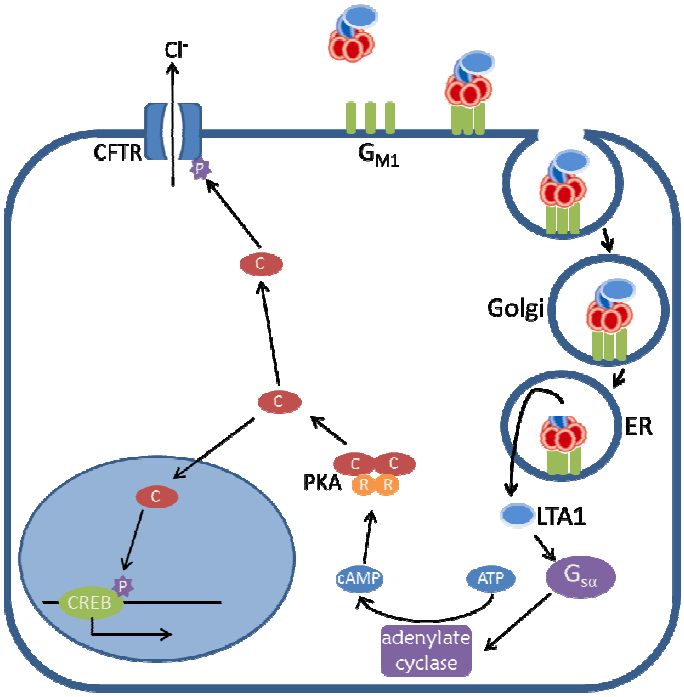

Figure 2: Overview of the internalization and trafficking of LT.

LT binds to G_{M1} on host cells and leads to Cl- and fluid efflux from the cell. See text for more details.

1.3.4 Activity

As shown in Figure 2, after LT is transported to the ER, the LTA1 fragment is translocated to the host cytosol through the ER-associated degradation pathway (Viswanathan et al, 2009). LTA1 then ADP-ribosylates an arginine residue of the $G_{s\alpha}$ subunit of adenylate cyclase, which leads to an increase in cyclic adenosine monophosphate (cAMP) levels (Gill & Richardson, 1980). cAMP is a regulator of protein kinase A (PKA), a multi-functional kinase that is composed of two regulatory and two catalytic subunits. The regulatory subunits of PKA are released through cAMP, and the

catalytic subunits perform two important roles: transcriptional regulation and the activation of the cystic fibrosis transmembrane regulator (CFTR).

In the first role, the catalytic subunit of PKA is transported into the nucleus and phosphorylates the cAMP response element-binding protein (CREB). Active phosphorylated CREB then binds to cAMP response elements (CREs) within the promoter regions of certain genes, including IL-6 and TNFα, and induces transcription.

In its second role, the catalytic subunit of PKA phosphorylates the CFTR, allowing for the efflux of Cl^- ions into the intestinal lumen. In addition, high levels of cAMP decrease sodium uptake (Sánchez & Holmgren, 2005). The combination of increased chloride efflux and decreased sodium influx leads to sodium and water efflux and diarrhea (Sánchez & Holmgren, 2005).

In addition to its role in inducing diarrhea, LT has been shown to confer a colonization advantage to ETEC in both murine and porcine intestine (Allen et al, 2006; Berberov et al, 2004). In vitro studies have shown that LT may confer this advantage by increasing the adherence of ETEC to host cells through an increase in cAMP levels (Johnson et al, 2009).

1.4 Diarrhea

1.4.1 Impact

Diarrhea can lead to death and illness in the short term, but even those who survive diarrheal episodes can have lasting repercussions. In the long term, repeated bouts of

diarrhea in the first two years of life, regardless of the cause, can lead to cognitive impairment and lower physical fitness (Guerrant et al, 1999). Repeated bouts of diarrhea can also lead to a loss of 10 IQ points (Petri et al, 2008). In addition, in a cohort of Brazilian children, the age of starting school was significantly delayed in children with repeated bouts of diarrhea compared to children with less diarrheal illnesses (Guerrant et al, 2002). These long-term effects are linked with malnutrition induced by diarrhea.

1.4.2 Association with cytokines

Few studies have been performed to determine the association of cytokines with diarrhea in humans, and of these studies, even less have been performed specific to ETEC diarrhea. Serum samples from children with diarrhea caused by rotavirus have shown an increase in the production of several cytokines, including IL-6, IL-10 and IFNγ (Jiang et al, 2003). High levels of TNFα, which is involved in chloride secretion, have also been correlated with the number of diarrheal episodes (Jiang et al, 2003; Oprins et al, 2000). In clinical settings, both IL-6 and TNFα have been found in the stools of children who had diarrhea that was caused by another enteric pathogen, *Shigella dysenteriae* (de Silva et al, 1993). In addition, in children with enterocolitis, serum IL-6 has been shown to be discriminative of bacterial etiology from viral etiology (Yeung et al, 2004). A study on the cytokine profile of fecal samples from patients with traveler's diarrhea caused by ETEC, EAEC, *Shigella* and *Salmonella* showed increased levels of IL-6, IL-8, TNFα, IFNγ, and IL-1β (Greenberg et al, 2002).

Although IL-6 is a pro-inflammatory cytokine, ETEC-induced diarrhea is not inflammatory. IL-6 receptors are expressed on both apical and basolateral surfaces of intestinal epithelial cells; however, the signal-transducing component of the IL-6R, gp130, is expressed mostly on the basolateral membrane (Wang et al, 2003). Once bound, the IL-6R can lead to both pro- and anti-inflammatory responses. IL-6R can activate the JAK/STAT pathway, leading to pro-inflammatory responses, and then lead to the activation of SOCS3, an inhibitor of the JAK/STAT pathway, leading to an anti-inflammatory response (Wang et al, 2003). The basolateral activation of the IL-6R leads to activation of the JAK/STAT pathway more than the apical pathway (Wang et al, 2003).

1.4.3 Diarrhea models

One of the limitations of studying LT under physiological conditions is the lack of an appropriate model. Indeed, this lack of an animal model has hampered the development of vaccines against ETEC (Walker et al, 2007). Experiments to study the effect of ETEC in the host have been performed in humans, but these experiments are limited and expensive and have not contributed to a clearer understanding of the pathogenesis of ETEC (DuPont et al, 1971). In addition, because of the risks posed, studies cannot be performed in children. Studies have also been performed in non-human primates, but these studies require specialized expertise and are also very expensive (Jones et al, 2006). However, other ex vivo and in vivo models have been used to study the physiological response of LT in a limited manner.

Ussing chambers. Ussing chambers can be used to examine the effect of certain substances on the net ion transport in whole tissue. Intestinal tissues are harvested from an animal, cleaned, and mounted in the Ussing chamber with a distinct boundary between the apical and basolateral side, allowing the toxins to be added in a manner that recapitulates the recognition of the toxin by the intestinal epithelia. These tissue explants are maintained at 37°C in Ringer solution to provide an isotonic environment. The benefit of using Ussing chambers is the ability to study interactions in a whole-tissue and more physiologically relevant context than a mono-culture of cells in vitro. In addition, a smaller dose of toxin can be used because the target tissue is accessible and the toxin does not have to pass through an animal first. Although the tissue cannot be maintained for an extended time before degradation occurs, toxin responses have been shown to occur within an hour. In addition to providing measurements of the net ion secretion across tissue, histology can also be evaluated in Ussing chamber explants. Previous studies have shown that Ussing chamber experiments using porcine intestinal explants showed an increase in Cl^- secretion in response to soluble LT after 1 h (O'Donnell et al, 2000). Ussing chamber studies using the same concentration of LT in rabbit explants found an increase in Cl- secretion beginning at 20 min (Mynott et al, 1997).

Rabbit ligated loop model. Rabbit ileal loops can be used to measure fluid accumulation in response to toxins. In this procedure, the rabbit is anesthetized, and the

intestine is removed from the body cavity without being surgically excised. Segments of the intestine are then ligated on either end to form small loops without disrupting the blood flow to these areas. Test substances can then be injected into the loops, and the intestine is replaced within the rabbit. After a given time, the rabbit is euthanized, and the gut density within the loops is measured. Like Ussing chambers, histology can also be determined from the experiment. Unlike Ussing chambers, the intestine remains intact and attached to nerves and underlying substructures. This allows for the evaluation of the infiltration of immune cells, such as neutrophils. The rabbit ligated ileal loop method has been used to determine fluid accumulation in response to LT, CT and ETEC (Triadafilopoulos et al, 1989). The maximal level of fluid accumulation is seen 18 h after inoculation (Sack, 1975). One advantage to this method is that up to 20 loops can be obtained from a single animal, reducing animal-to-animal variation. However, rabbit ileal loops are expensive and time-consuming to monitor. In addition, current guidelines for rabbit ileal loops limit the time that rabbits can be maintained in this condition to 8 h, which is before the maximal induction of fluid accumulation.

Mouse models. Mice are not naturally susceptible to ETEC, due in part to the inability of ETEC to sufficiently adhere to the intestinal epithelium (Zhang et al, 2008). A mouse model has successfully been used to investigate the colonization of mouse intestines by ETEC and the role that various virulence factors play in adherence to the intestine (Allen et al, 2006). However, even in this model, no diarrhea is observed. An

infant mouse model has also been used to evaluate diarrheal pathogenicity, with mortality as the endpoint (Bertin, 1985; Duchet-Suchaux, 1988). This model is mostly ineffective in response to human ETEC strains, which may also be due to the lack of colonization factors (Duchet-Suchaux et al, 1990).

1.5 Gut Immunity

ETEC acts in the intestine, a unique niche within the body. Unlike most other areas of the body, the intestine is home to a variety of commensal flora that play beneficial roles in digestion and protection from infection. Because of this symbiotic relationship, the intestinal environment has developed an immune system that shows tolerance to commensal bacteria to prevent an overwhelming inflammatory response to beneficial bacteria. Pathogenic bacteria can subvert these defenses in a variety of ways, and ETEC is very effective in causing disease.

1.5.1 Commensal bacteria

The intestinal tract contains approximately 10^{13}-10^{14} commensal bacteria of a variety of genera, including *Bacteroides, Eubacterium, Clostridium* and *Ruminococcus* (Jarchum & Pamer, 2011; Round et al, 2010). These bacteria contribute to metabolism, nutrient acquisition, and intestinal immune homeostasis. Because of the presence of these commensals, the intestine has developed mechanisms to reduce the immune reaction to beneficial bacteria. Commensals can secrete products to preserve the epithelial barrier.

1.5.2 Epithelial barrier

The intestinal surface is lined with a columnar layer of epithelial cells that show distinct polarized apical and basolateral surfaces (Artis, 2008). These polarized epithelial cells form a barrier between the intestinal lumen and the host connective tissue (Figure 3) (Artis, 2008). Intestinal epithelial cells can express different molecules at different developmental stages. For example, epithelial cells from newborns express more TLR4 and clathrin, which is the primary mechanism through which LT is internalized in newborns (Gribar et al, 2008; Lu et al, 2005).

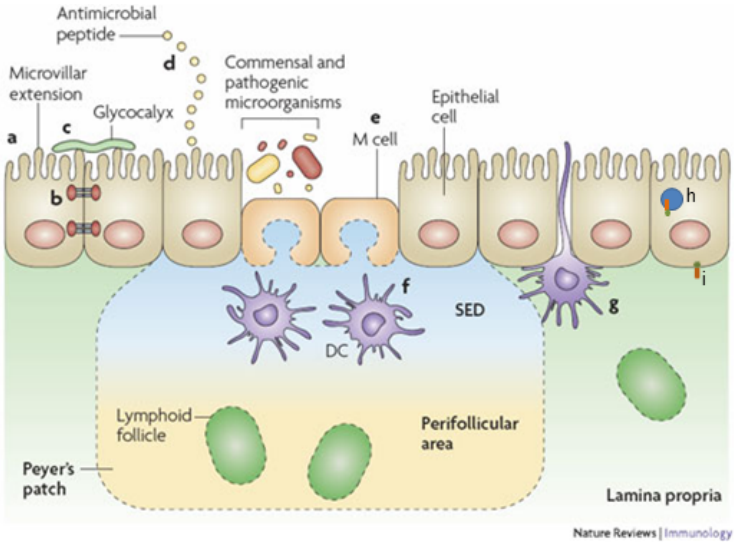

Figure 3: Diagram of the intestinal environment.
A schematic of the intestinal milieu showing intestinal epithelial cells with microvilli (a). IECs form tight junctions between cells (b) to maintain a tight physical barrier. IECs secrete mucous-like glycocalyx (c) to help prevent attachment of bacteria. M cells (e) are dispersed in Peyer's patches, which also contain dendritic cells (f). Dendritic cells also lay outside of Peyer's patches (g) that extend dendrites into the intestinal lumen to sample antigens. IECs express Toll-like receptors subcellularly within endosomes (h) and at the basolateral surface (i). Adapted from (Artis, 2008).

Polarized cells show distinct protein expression profiles at the apical and basolateral surfaces. For example, in polarized intestinal epithelial cells, the transferrin receptor is located only on the basolateral membrane, and caveolin is expressed mostly on the basolateral membrane and is not associated with apical lipid rafts (Beatty et al, 1999; Ivanov et al, 2004). In addition, to prevent a constant inflammatory reaction to commensals, polarized intestinal epithelial cells express little to no Toll-like receptor (TLR) 4 or 2, which primarily recognize LPS and lipoteichoic acid, respectively, on their apical surface (Abreu et al, 2001; Artis, 2008). While normal healthy intestinal immune cells express little or no TLR4 or TLR2, these receptors have been found to be upregulated in patients with inflammatory bowel disease and ulcerative colitis (Cario & Podolsky, 2000). Furthermore, TLR5, which recognizes flagellin, is only expressed on the basolateral surface extending into the lamina propria. Therefore, TLR5 only recognizes invasive bacteria that have crossed the epithelial barrier, which would not occur with commensals (Gewirtz et al, 2001). The ability of the intestinal epithelium to differentiate between friend and foe leads to the production of cytokines and other signaling factors that either maintain intestinal homeostasis or lead to an immune response. Pathogenic bacteria and their products generally lead to an increase in inflammatory responses that are mediated by a variety of cells, including neutrophils.

Other antigen-presenting cells are also present in the epithelial barrier. Dendritic cells that lay just below the polarized monolayer express tight junction proteins and

extend dendrites through the monolayer into the lumen of the intestine to sample the bacteria and other products present in the lumen (Artis, 2008). M cells are specialized cells found in Peyer's patches in the intestine that also sample the intestinal lumen. M cells can present mucosal antigens to dendritic cells in Peyer's patches through transcytosis (Artis, 2008).

1.6 Significance

ETEC is a worldwide public health problem that is responsible for thousands of death in the developing world, particularly in children. Although LT is a primary effector in the induction of diarrheal disease, it has never before been studied in its natural context of presentation. The results in this thesis have contributed to the understanding of the mechanism of this toxin in a physiologically relevant in vitro model. In Chapter 2, we show that when equal amounts of toxin are presented to polarized intestinal epithelial cells, vesicle-associated LT shows delayed kinetics in the activation of PKA and CREB. In Chapter 3, we show that similar to soluble LT, LT associated with vesicles require both a trafficking motif and a scaffolding motif to be active within cells. Vesicle-associated LT must bind to G_{M1} in lipid rafts to be trafficked to the ER and activate CREB. This suggests that vesicle-mediated delivery may be a method of post-translational regulation of LT activity to prevent an overwhelming host response that could be deleterious to ETEC. In Chapter 4, we use available models to study the consequences of toxin presentation in a whole-tissue context and attempt to

develop a practical model to do so. These studies show the importance of studying toxins in their natural context of presentation.

2. Outer membrane vesicle-associated heat labile enterotoxin shows delayed PKA activation kinetics

2.1 Summary

Enterotoxigenic *Escherichia coli* (ETEC) is the leading cause of traveler's and children's diarrhea worldwide. Among its virulence factors, ETEC produces heat-labile enterotoxin (LT). Most secreted LT is associated with outer membrane vesicles that are rich in lipopolysaccharide. The majority of prior studies have focused on soluble LT purified from ETEC periplasm. We investigated the hypothesis that the extracellular vesicle context of toxin presentation might be important in eliciting immune responses. We compared the polarized epithelial cell response to apically applied soluble LT and LT-containing vesicles (LT^+ OMVs) and controls using a catalytically inactive mutant of LT and OMVs lacking LT. Although OMV treatments with no or catalytically inactive LT induced a modest amount of IL-6, samples containing catalytically active LT elicited higher levels. A combination of soluble LT and LT-deficient OMVs induced significantly higher IL-6 than either LT or LT^+ OMVs alone. The responses to LT^+ OMVs were found to be independent of the canonical LT pathway because the inhibition of cyclic AMP response element-binding protein (CREB) phosphorylation did not lead to a decrease in cytokine gene expression levels. Furthermore, soluble LT caused earlier phosphorylation of CREB and the activation of CRE compared with LT^+ OMVs. Soluble LT also led to the activation of activator protein 1, whereas LT^+ OMV IL-6 responses appeared to be

mediated by NFκB. In summary, the results demonstrate that soluble LT and OMV-bound LT elicit similar cytokine responses through different activation pathways.

2.2 Introduction

Enterotoxigenic *Escherichia coli* (ETEC) is the leading cause of traveler's diarrhea (Black, 1990), and it has been estimated to cause approximately 10 million cases of traveler's diarrhea worldwide (Steffen et al, 2005). ETEC is also the leading cause of morbidity and mortality due to diarrhea in children in developing countries. A total of 280 million cases of diarrhea associated with ETEC were found in children less than five years old in outpatient clinics in developing countries (Wenneras & Erling, 2004), and mortality due to ETEC has been estimated at 170,000 deaths annually (Niyogi, 2005). Heat-labile enterotoxin (LT) is a major virulence factor produced by ETEC and is known to contribute to the disease (Kaper et al, 2004).

LT shares approximately 80% homology with cholera toxin (CT), which is produced by *Vibrio cholerae* (Spangler, 1992). LT is an AB5 toxin that is composed of a pentameric B subunit, which binds to host receptors, and a catalytically active A subunit. The B pentameric ring binds to the Galβ1,3GalNAcβ1(NeuAcα2,3),4Galβ1,4Glc ceramide (G_{M1}) ganglioside on host cells, which mediates internalization. Studies using soluble LT purified from the periplasm have led to a detailed understanding of its complex trafficking pathway and activation inside mammalian cells. Once internalized, LT is trafficked to the Golgi and the endoplasmic reticulum (ER), in which the A subunit

is further processed. The modified A subunit then catalyzes the ADP-ribosylation of the Gsα subunit in the adenylate cyclase pathway. This ribosylation leads to an increase in cyclic adenosine monophosphate (cAMP) levels and an efflux of water and electrolytes into the lumen of the intestine (Fleckenstein et al, 2010). Both CT and LT activate protein kinase A (PKA), which phosphorylates the cystic fibrosis transmembrane regulator (CFTR) and cAMP response element (CRE)-binding protein (CREB) to transport Cl^- into the intestinal lumen and induce gene transcription (Sánchez & Holmgren, 2005).

Most secreted LT is found on the surface and in the lumen of outer membrane vesicles (OMVs) that are rich in lipopolysaccharide (LPS) (Horstman & Kuehn, 2000), whereas the majority of secreted CT is soluble (Hirst et al, 1984b). OMVs are spherical structures secreted from all Gram-negative bacteria studied to date (Kulp & Kuehn, 2010). OMVs are enriched in outer membrane components, and the lumen of OMVs contains periplasmic components. OMVs contain biologically active components and immunomodulatory molecules (also known as pathogen-associated molecular patterns; PAMPs), such as LPS and flagellin, that interact with and influence host cells (Ellis & Kuehn, 2010).

Other toxins from a variety of pathogenic bacteria have also been shown to be enriched in OMVs, including cytolysin A (ClyA) from *E. coli* (Wai et al, 2003), leukotoxin A (LktA) from *Aggregatibacter actinomycetemcomitans* (Kato et al, 2002), vacuolating toxin (VacA) from *Helicobacter pylori* (Fiocca et al, 1999), and cytolethal distending toxin (CDT)

from *Campylobacter jejuni* (Lindmark et al, 2009). Previous studies have demonstrated differences in mammalian cell toxicity based on the presentation of those toxins (e.g., in the context of OMVs versus soluble toxin). Wai et al. showed that compared to equal amounts of ClyA purified from the periplasm, OMV-associated ClyA induced higher cytotoxic activity in HeLa cells (Wai et al, 2003). The OMV context of ClyA presentation was shown to facilitate the active oligomerized state of ClyA, leading to its higher activity (Wai et al, 2003). *H. pylori* has been shown to secrete VacA in both a free soluble form and associated with OMVs (Fiocca et al, 1999). Ricci et al. demonstrated that although OMV-associated VacA accounted for approximately 25% of secreted toxin, the OMV-bound toxin showed lower vacuolating activity than soluble VacA (Ricci et al, 2005). However, because OMVs are complex entities, the OMV association of toxins is likely to affect host cells beyond the differences in toxin potency.

The gut is a unique environment that has developed tolerance to native microbiota. The intestinal epithelium forms tight intracellular junctions and microvilli that inhibit the attachment and invasion of intestinal organisms (Artis, 2008). Tight junctions also play a role in the polarization of epithelial cells, resulting in distinct apical and basolateral surfaces (Kohler & Zahraoui, 2005). Commensal tolerance is further maintained through a variety of mechanisms, including the subcellular localization of Toll-like receptors (TLRs) and the inhibition of immune responses to commensal products, such as LPS (Artis, 2008). Pathogenic bacteria subvert these defenses in a

variety of ways, including epithelial cell internalization and the elaboration of virulence factors, such as toxins (Rumbo et al, 2004). OMVs can also penetrate the epithelial cell barrier. ETEC OMVs have been found to enter cultured intestinal epithelial cells via a specific LT-mediated pathway (Kesty et al, 2004).

We hypothesize that in addition to modulating its toxicity, the context of toxin presentation is important in determining the host response. In particular, OMV-associated toxin is likely to elicit a different inflammatory response than soluble toxin because of the presence of LPS and other PAMPs. To investigate this theory, we compared the response of polarized human intestinal epithelial cells to apically applied soluble LT, catalytically inactive LT (S63K), OMVs containing either catalytically active LT (LT^+ OMVs) or catalytically inactive LT (S63K OMVs), and OMVs without LT (ΔLT OMVs). We found significant differences in the kinetics of responses induced by soluble LT compared with OMV-bound LT. Our results show that soluble LT and LT^+ OMVs elicit different responses and act through different mechanisms.

2.3 Results

Standardization of LT in LT^+ OMVs. To fully understand the context-dependent presentation effects of LT, the amount of LT in LT^+ OMVs had to be determined[1]. Two-fold dilutions of soluble toxin purified from the periplasm of secretion-deficient *E. coli* were analyzed alongside two-fold dilutions of LT^+ OMVs using immunoblotting (Figure

[1] Detailed methods for the entire thesis can be found in Chapter 6.

4). Standardization was based on the B subunit. To ensure that the B subunit was not complexed, samples were run in 4 M urea. On average, 1 μg of LT+ OMVs (as measured using protein content) contained approximately 43.75 ng LT.

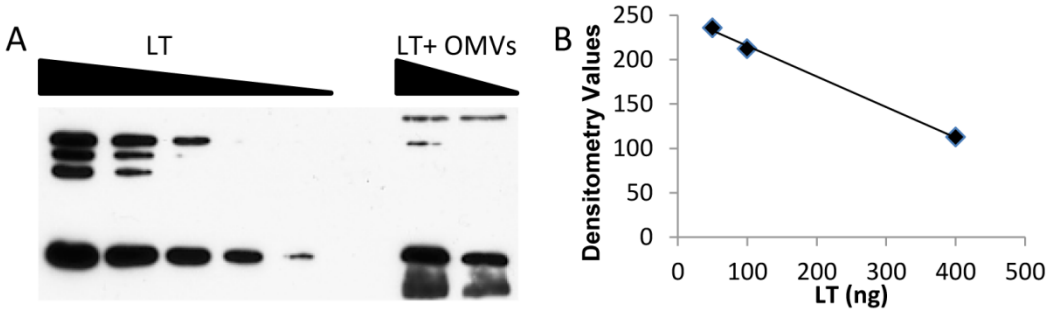

Figure 4: LT standardization of LT+ OMVs.

(A) Representative immunoblot of the standardization of LT in LT+ OMVs. Two-fold dilutions of soluble LT starting at 400 ng were run alongside 1 μg and 0.5 μg LT+ OMVs on a 15% SDS gel and immunoblotted using a cross-reactive polyclonal CT antibody. **(B)** Densitometry analysis to determine a standard curve of LT. Bands in (A) were quantified using ImageJ software.

Standardization of lipid content in vesicle preparations. LPS is the most predominant immunostimulatory molecule in OMVs. Therefore, to ensure that an equal amount of OMVs was added to cells, vesicles were standardized to LT+ OMVs by their lipid content (Figure 5). Two-fold dilutions of OMV preparations were incubated with FM4-64, a lipophilic dye that binds to the lipids in vesicles, and standard curves were constructed for each preparation. The lipid concentration of LT+ OMVs and S63K OMVs were similar based on their protein content. However, ΔLT OMVs had a lower lipid content to protein ratio, which means that the concentration of ΔLT OMVs used in our experiments had lower protein content than the other OMV preparations.

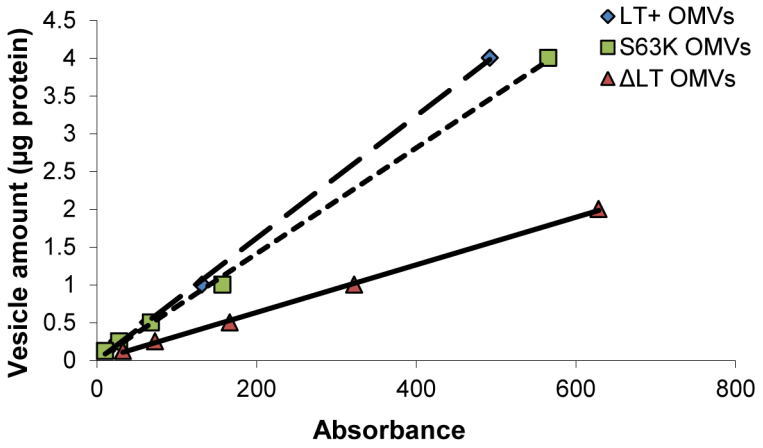

Figure 5: Lipid standardization of vesicle preparations.

Two-fold dilutions of OMV preparations were incubated with FM4-64, and standard curves were calculated for each preparation.

Catalytically active LT-containing treatments induce higher expression levels of IL-6 and TNFα than other treatments. To investigate whether the context of LT presentation affected the host response to LT, we treated polarized cultures of human T84 intestinal epithelial cells with either soluble LT or equivalent concentrations of LT in the context of OMVs. Cytokine induction in response to either LT or OMVs has been widely studied using a variety of cultured mammalian cells (Bowman & Clements, 2001; Cheng et al, 2000; Ellis & Kuehn, 2010; Schaar et al, 2011; Soriani et al, 2002). However, no studies on the pathways involved in cytokine responses to LT^+ OMVs have been performed using the more physiologically relevant polarized epithelial cell model.

As shown in Figure 6A, whereas all treatments induced TNFα expression, soluble LT, LT^+ OMVs and the combination of LT/ΔLT OMVs induced higher gene expression levels of TNFα than the other treatments. This induction appeared to be

dependent on the catalytic activity of LT because the catalytically inactive S63K LT treatments and the ΔLT OMVs did not induce TNFα to the same level, even at the higher 1 nM dose (Figure 6A).

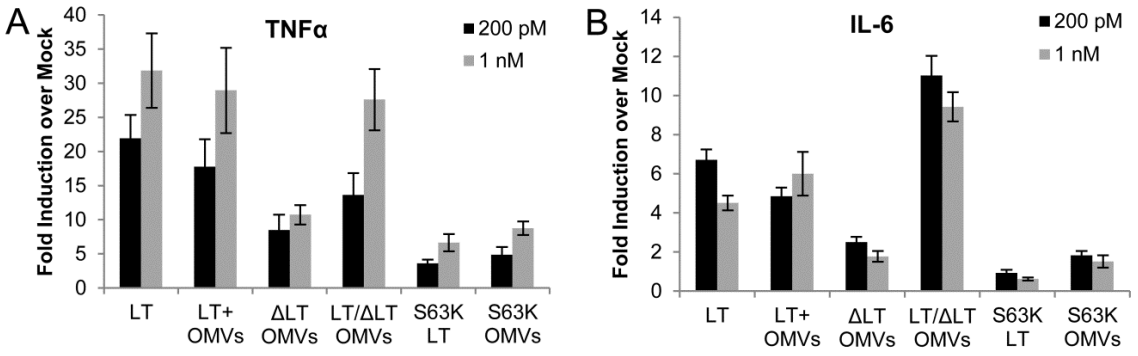

Figure 6: Catalytically active LT-containing treatments induce higher amounts of TNFα and IL-6 gene expression levels at 6 h.

Polarized T84 cells were apically treated with samples equivalent to 200 pM or 1 nM LT for 6 h. The gene expression level of **(A)** TNFα and **(B)** IL-6 was determined using RT-PCR. Each experiment was performed in triplicate.

As shown in Figure 6B, the catalytically active LT-containing treatments induced higher gene expression levels of IL-6 than the other treatments at both 1 nM and 200 pM. In addition, both concentrations of LT induced equivalent amounts of IL-6, suggesting that the 200 pM treatment already produced the maximal effect. Both ΔLT and S63K OMVs induced a modest amount of IL-6, whereas S63K LT did not induce IL-6 expression over mock. In contrast to TNFα, whose expression was not significantly different between the LT-containing treatments, the combination of LT and ΔLT OMVs led to significantly higher IL-6 levels than either soluble LT or LT$^+$ OMVs at both concentrations (ANOVA; $p < 0.01$ at 1 nM; $p < 0.001$ at 200 pM). This induction was

synergistic because the level of induction was more than the combined results of LT and ΔLT OMVs. The amount of IL-6 gene induction was not significantly different between soluble LT and LT+ OMVs at either concentration.

To determine if induction was also present at the protein level, the levels of TNFα and IL-6 in the apical and basolateral supernatants were measured using ELISAs. IL-6 ELISA results shown in Figure 7 confirmed that the induction of gene expression also resulted in an increase in protein concentration in the apical compartment. No IL-6 was found in the basolateral supernatants, indicating the polarized secretion of this cytokine. TNFα protein expression was not found in the supernatants of our treated cells, which may be due to a low level of TNFα expression. Overall, these results indicated that catalytically active LT, presented either solubly or as a component of OMVs, elicited substantial but indistinguishable TNFα and IL-6 responses in polarized epithelial cells.

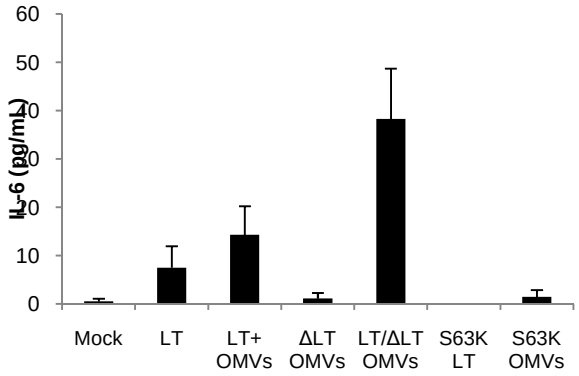

Figure 7: Catalytically active LT-containing treatments elicit higher concentrations of IL-6 in the apical supernatant.

Figure 7 (continued). Polarized T84 cells were apically treated with samples corresponding to 1 nM LT, and apical and basolateral supernatants were collected. IL-6 protein levels were measured using an IL-6 ELISA. Each experiment was performed in triplicate.

LT^+ OMVs do not induce cytokine gene expression through CREB at 6 h. To further examine the role of the catalytic activity of LT in inducing IL-6 and TNFα gene expression, we used Rp-camps and H89 to inhibit the action of PKA. Rp-camps prevents the dissociation of the catalytic subunits of PKA from their regulatory subunits and abolishes PKA activity. As expected, Rp-camps significantly inhibited the induction of TNFα and IL-6 in response to soluble LT (Figure 8A and B). However, the inhibition of PKA activity notably did not have an effect on the responses induced by LT^+ OMVs at 6 h (Figure 8A and B). The combination of LT/ΔLT OMVs showed an intermediate response to inhibition by Rp-camps: Rp-camps pretreatment significantly inhibited IL-6 gene induction but had no effect on TNFα gene induction. H89 inhibits the phosphorylation of CREB by PKA and thereby inhibits PKA activity. H89 led to a significant and more substantial reduction in IL-6 expression in response to soluble LT and the combination of LT/ΔLT OMVs but showed no effect on IL-6 gene induction in response to LT^+ OMVs (Figure 8B). However, whereas H89 showed similar effects as Rp-camps in TNFα induction for most treatments, it led to a significant inhibition of TNFα expression in response to LT^+ OMVs. In sum, it was notable that differences in the presentation of similar concentrations of LT (LT^+ OMVs compared with soluble LT) resulted in differences in the kinetics of activation of PKA.

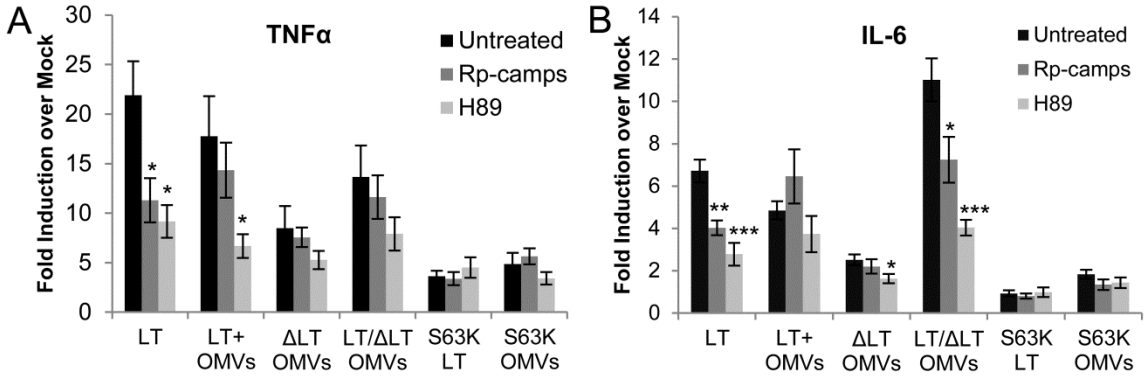

Figure 8: Soluble LT, but not LT⁺ OMVs, induce TNFα and IL-6 gene induction through PKA.

Polarized T84 cells were pretreated for 1 h with either Rp-camps or H89, and samples corresponding to 200 pM LT were added to the apical chamber for 6 h. The gene expression levels of **(A)** TNFα and **(B)** IL-6 were measured using RT-PCR. *, $p<0.05$; **, $p<0.01$; ***, $p<0.005$ compared to untreated levels (n=4).

To examine the phosphorylation of CREB, immunoblots of nuclear extracts were performed to determine the levels of pCREB present in cells incubated with our samples. TATA-binding protein (TBP) was used as a loading control for all immunoblots. Immunoblots showed that at 4 h, CREB was phosphorylated in response to soluble LT and the combination of LT/ΔLT OMVs but not phosphorylated in response to LT⁺ OMVs (Figure 9A, upper panels). However, when assayed 2 h later, CREB was phosphorylated in response to LT⁺ OMVs, soluble LT and the combination of LT/ΔLT OMVs (Figure 9A, lower panels).

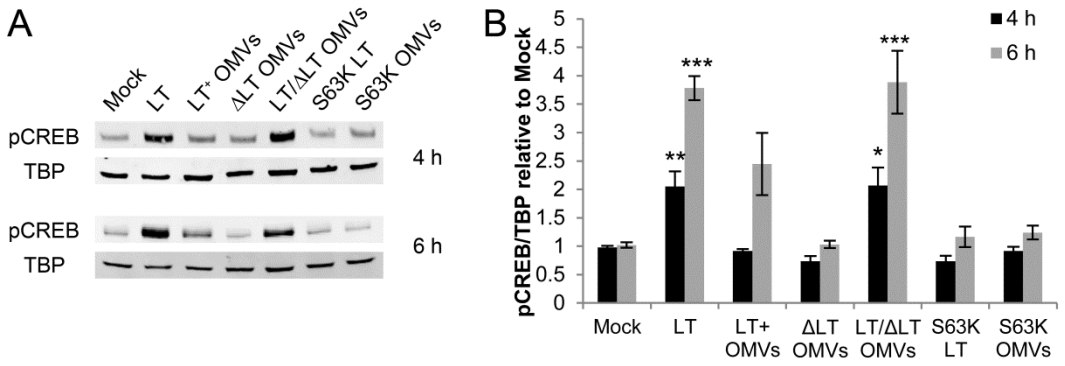

Figure 9: Immunoblots and densitometry analysis of pCREB and TBP in polarized T84 cells after treatment with soluble LT and OMV treatments.

Polarized T84 cells were treated with samples corresponding to 1 nM LT for the indicated times, and nuclear proteins were extracted and analyzed using immunoblotting. **(A)** Representative images of nuclear extracts immunoblotted with an anti-pCREB antibody. An anti-TBP antibody was used as a loading control. Each experiment was performed in triplicate. **(B)** Densitometry analysis of three independent immunoblots for each time. Each sample was first normalized to TBP and then standardized to the respective mock. *, $p<0.05$; **, $p<0.01$; ***, $p<0.005$.

Densitometry analysis of the immunoblots showed that pCREB was significantly increased approximately 2 fold in response to LT and LT/ΔLT OMVs compared to the other treatments at 4 h and approximately 3.75 fold at 6 h (Figure 9B). LT^+ OMV treatment led to a substantially higher CREB phosphorylation than mock at 6 h, but this increase was not statistically significant. At both timepoints, both soluble LT and the combination of LT/ΔLT OMVs induced significantly higher levels of pCREB than LT^+ OMVs. Therefore, treatment with LT in its native OMV-associated state appeared to activate CREB more slowly compared with treatments containing soluble LT.

We next used an independent assay to further examine the differences in the kinetics of cAMP activation. We compared the effects of soluble LT and OMV-bound LT

on the activation of CRE genetic elements using a dual luciferase reporter system. This assay provides a more sensitive detection of the downstream effects of cAMP activation than densitometry. Because we found it technically unfeasible to transfect T84 cells and maintain their ability to form a polarized monolayer, we used HEK293T cells for these assays. HEK293T cells were transfected with a reporter plasmid containing the CRE promoter fused to firefly luciferase. To control for transfection efficiency, cells were co-transfected with a plasmid that constitutively expressed *Renilla* luciferase. The results were consistent with the kinetics of CREB activation. Although LT^+ OMVs stimulated CRE activity approximately five fold at 4 h, this induction was not significantly above mock-treated cells ($p > 0.05$; Figure 10). However after only 4 h, both soluble LT and the combination of LT/ΔLT OMVs significantly induced CRE activity above mock (approximately 15- and 22-fold higher than mock, respectively; Figure 10), and the response to the combination of LT/ΔLT OMVs levels was significantly higher than for the same amount of soluble LT ($p < 0.01$). At 6 h, CRE activity was significantly induced by all of the treatments containing active LT: soluble LT (~35 fold), LT^+ OMVs (~19 fold) and the combination of LT/ΔLT OMVs (~28 fold; Figure 10). These results confirm that the LT present in native LT^+ OMVs is delayed in causing the phosphorylation of CREB and activating CRE. Further, the data suggest that the delayed activation of CREB by LT^+ OMVs does not account for the TNFα and IL-6 gene expression levels observed at 6 h.

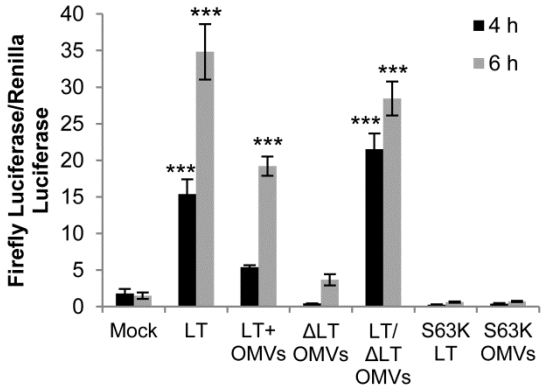

Figure 10: CRE activation in HEK293T cells shows delayed activation kinetics in response to LT$^+$ OMVs.

HEK293T cells were transfected with a reporter plasmid containing the CRE genetic element fused to a firefly luciferase reporter. A plasmid containing constitutively expressed *Renilla* luciferase was also transfected to control for transfection efficiency. Transfected cells were then treated with samples corresponding to 1 nM LT for the indicated times, and the firefly activity was determined and normalized to *Renilla* luciferase values. Asterisks indicate significant differences from the respective mock control at the corresponding time. ***, $p<0.005$ (n=3).

To confirm that the activation of PKA and CREB in response to LT+ OMVs showed delayed activation kinetics and was not just decreased, we determined the induction of TNFα and IL-6 at 9 h (Figure 11). We found that TNFα responses appeared to peak at 6 h and were decreased at 9 h. Both soluble LT and LT+ OMVs showed similar amounts of TNFα induction, which were higher than treatments containing catalytically inactive or no LT (Figure 11A). However, IL-6 levels were constant between 6 h and 9 h, except for LT+ OMVs, which showed a large up-regulation of IL-6 at 9 h (Figure 11B). This induction was significantly higher than LT ($p<0.05$).

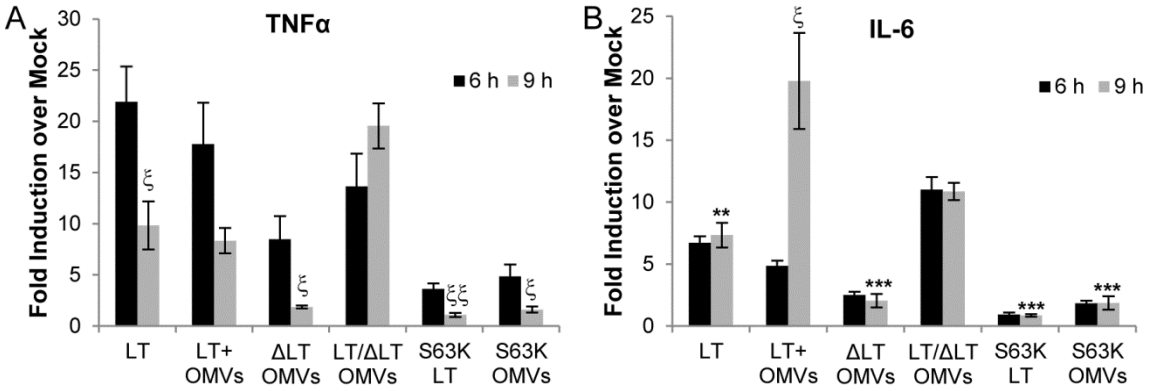

Figure 11: LT+ OMVs show similar levels of TNFα induction at 9 h as soluble LT but significantly higher levels of IL-6 induction.

Polarized T84 cells were treated with samples corresponding to 200 pM LT for 9 h, and the gene expression levels of **(A)** TNFα and **(B)** IL-6 were determined using RT-PCR ($n\geq2$). Asterisks indicate significant differences from LT+ OMVs at 9 h for IL-6. * $p<0.005$ and * $p<0.001$. ξ indicates significant differences of the 9 h treatment from the 6 h treatment. ξ $p<0.05$, ξξ $p<0.005$. Not all significant differences are shown.

We used Rp-camps to determine whether TNFα and IL-6 induction in response to LT+ OMVs at 9 h was dependent on PKA activation. As shown in Figure 12A, the induction of TNFα by soluble LT, LT+ OMVs, and LT/ΔLT OMVs was significantly

reduced by pre-treatment with Rp-camps. Figure 12B shows that the induction of IL-6 by soluble LT and LT+ OMVs was significantly inhibited by PKA inhibition. These results confirm that LT+ OMVs show delayed rather than decreased PKA activation kinetics.

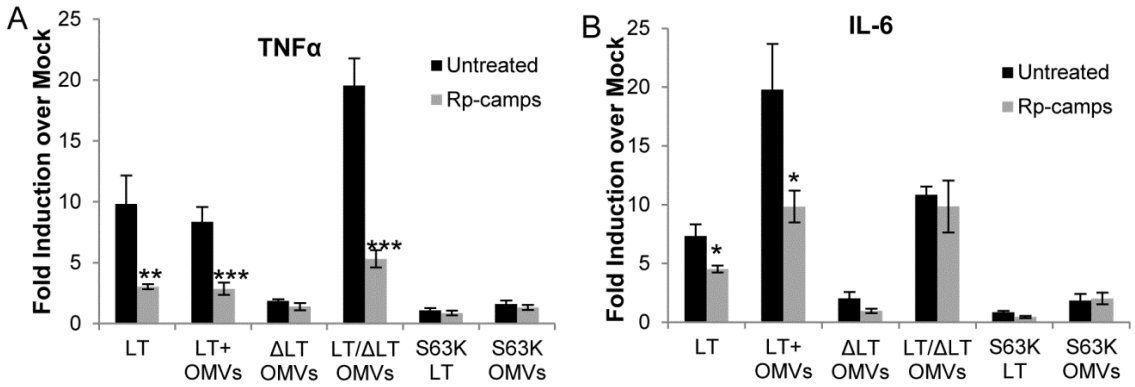

Figure 12: LT+ OMVs induce TNFα and IL-6 through PKA at 9 h.

Polarized T84 cells were pretreated for 1 h with Rp-camps, and samples standardized to 200 pM LT were added for 9 h. The gene expression levels of **(A)** TNFα and **(B)** IL-6 were determined using RT-PCR. *, $p<0.05$; **, $p<0.01$; ***, $p<0.005$ compared to untreated levels ($n\geq3$).

The induction of TNFα, not IL-6, depends on ERK1/2 and p38 MAP kinases.

Although LT+ OMVs showed delayed kinetics in activating CREB, they still induced high levels of IL-6 and TNFα gene expression at 6 h. Therefore, we investigated the pathways through which LT+ OMVs induced the expression of TNFα and IL-6. MAP kinases, including p38, ERK1/2 and JNK, have long been known to play a role in the induction of cytokines in response to stimuli. Specific inhibitors of MEK1/2 and p38 were used to determine whether ERK1/2 and p38, respectively, played a role in the induction of TNFα and IL-6 by LT and OMVs. We found that p38 and ERK1/2 had

similar roles in the induction of TNFα and that neither played a role in IL-6 induction. MEK inhibition significantly reduced the induction of TNFα by soluble LT, LT$^+$ OMVs, and the combination of LT/ΔLT OMVs (Figure 13A). p38 inhibition also significantly reduced the induction of TNFα by soluble LT and LT$^+$ OMVs but, notably, did not affect the response to the combination of LT/ΔLT OMVs (Figure 13B). Neither inhibitor significantly reduced the induction of IL-6 by soluble LT, LT$^+$ OMVs, or ΔLT OMVs (Figure 13C and D). Interestingly, p38 and ERK1/2 seemed to play, if anything, opposite roles in the induction of IL-6 in response to the combination of LT/ΔLT OMVs. The inhibition of ERK1/2 resulted in a significant decrease in IL-6, whereas p38 inhibition significantly upregulated IL-6 expression (Figure 13C and D). Together, these data demonstrate that both ERK1/2 and p38 play a role in the induction of TNFα in response to both LT and LT$^+$ OMVs, but the induction of IL-6 in response to these treatments is independent of these MAP kinases.

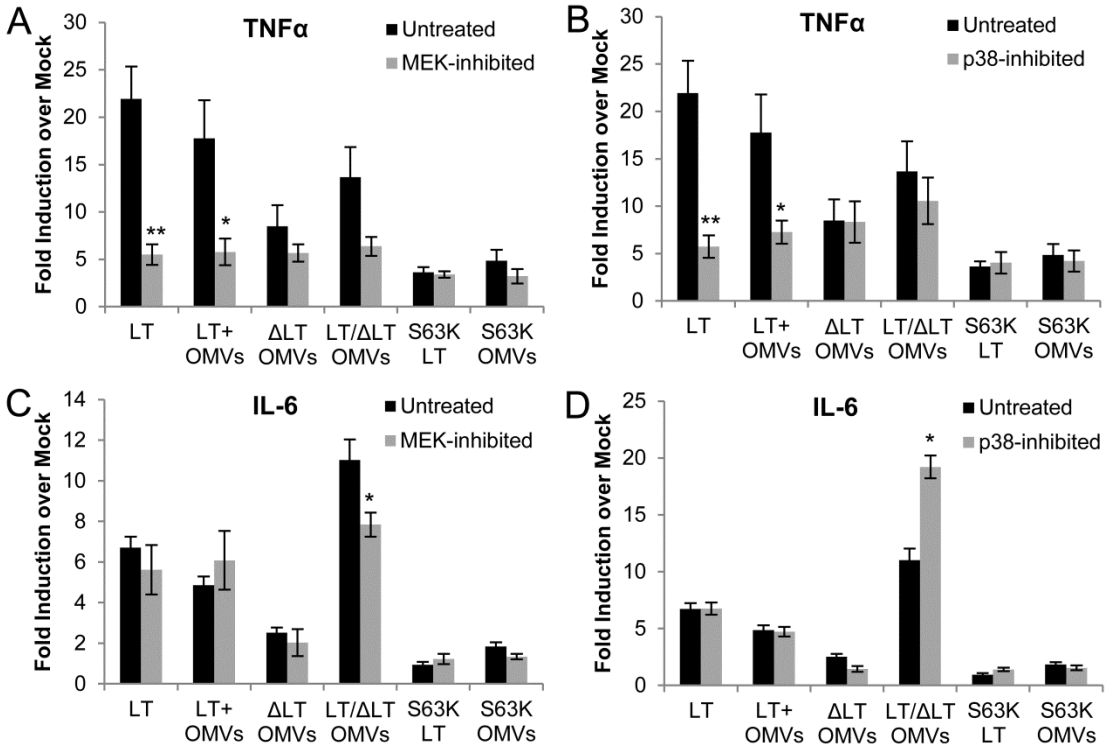

Figure 13: Both soluble LT and LT⁺ OMVs act through ERK1/2 and p38 to induce TNFα but not IL-6.

Polarized T84 cells were pre-treated with inhibitors of MEK1/2 or p38 for 1 h, and samples standardized to 200 pM LT were added to the apical compartment for 6 h. The gene expression levels of **(A-B)** TNFα and **(C-D)** IL-6 were determined using RT-PCR. *, $p<0.05$; **, $p<0.01$; ***, $p<0.005$ compared to untreated levels (n=3).

AP-1 is involved in the induction of TNFα and IL-6 in response to soluble LT but not LT⁺ OMVs. We also determined the role of the JNK MAPK pathway in the induction of TNFα and IL-6 in response to soluble LT and LT⁺ OMVs. JNK pathway inhibition led to a significant decrease in the level of expression of TNFα in response to soluble LT, but no significant differences were observed for any of the other treatments (Figure 14A). JNK pathway inhibition also led to a significant decrease in the level of expression of IL-6 in response to soluble LT (Figure 14B). In contrast to TNFα, the

expression levels of IL-6 induced in response to ΔLT OMVs and the combination of LT/ΔLT OMVs were significantly reduced with inhibition of the JNK pathway. In fact, JNK inhibition in cells treated with LT$^+$ OMVs and the combination of LT/ΔLT OMVs resulted in similar IL-6 levels (Figure 14B), suggesting that JNK inhibition removes the contribution of soluble LT to the induction of IL-6 by LT/ΔLT OMVs. It is not clear why the same effect did not occur for TNFα induction by LT/ΔLT OMVs (Figure 14A), but TNFα and IL-6 may be induced through different mechanisms. Together, these results show that the JNK pathway plays no role in the LT$^+$ OMV induction of either TNFα or IL-6 at 6 h, and this contrasts with the significant role JNK plays in their induction by soluble LT.

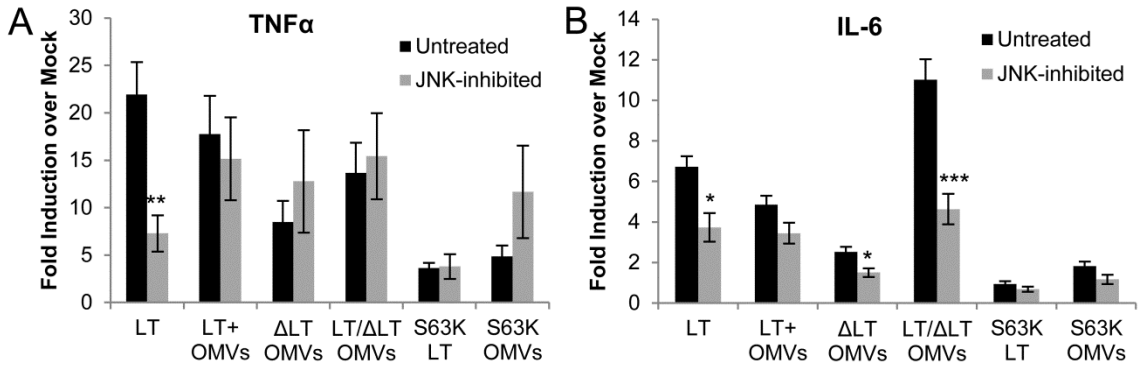

Figure 14: Soluble LT but not LT$^+$ OMVs induce TNFα and IL-6 through AP-1.

Polarized T84 cells were pre-treated with a JNK inhibitor for 1 h, and samples standardized to 200 pM LT were added to the apical compartment for 6 h. The gene expression levels of **(A)** TNFα and **(B)** IL-6 were determined using RT-PCR. *, $p<0.05$; **, $p<0.01$; ***, $p<0.005$ compared to untreated levels (n=3).

To confirm that soluble LT activates the JNK pathway, we performed an electrophoretic mobility shift assay to determine the activation status of AP-1, a

downstream effector of JNK. Our results showed that AP-1 was induced in response to both soluble LT and the combination of LT/ΔLT OMVs at 6 h (Figure 15), which is consistent with our RT-PCR results. Taken together, our results show that AP-1 plays a role in the induction of IL-6 in response to soluble LT but not OMV-associated LT, providing further evidence that soluble LT and LT^+ OMVs act through different mechanisms to induce IL-6 gene expression. Unlike pCREB, which showed delayed activation, AP-1 was not activated in response to LT^+ OMVs at 6 h.

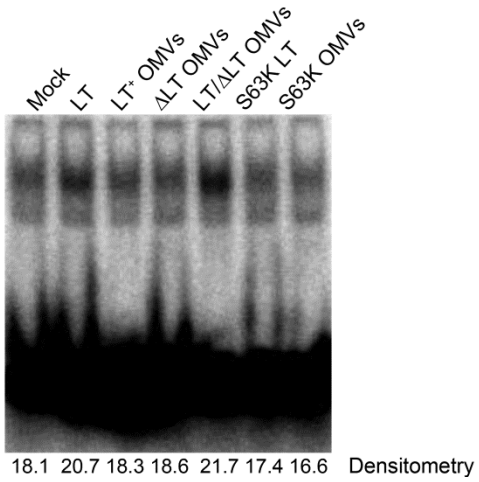

Figure 15: EMSA of AP-1 activation in polarized T84 cells in response to treatments.

Representative AP-1 EMSA of nuclear extracts of polarized T84 cells treated with samples standardized to 1 nM LT. Each experiment was performed in triplicate.

NFκB inhibits TNFα production for all treatments but has no role in the induction of IL-6 by LT and the combination of LT and LT^+ OMVs. To examine the role of NFκB in the induction of TNFα and IL-6 by LT treatments, we inhibited the activation of NFκB using PDTC, which prevents the binding of NFκB to DNA. NFκB

inhibition resulted in the downregulation of TNFα for all samples that contained catalytically active LT (Figure 16A). However, PDTC differentially effected IL-6 induction. NFκB inhibition significantly decreased IL-6 induction by LT$^+$ OMVs, ΔLT OMVs and S63K OMVs to basal levels (Figure 16B). However, NFκB inhibition did not reduce IL-6 gene induction in response to soluble LT. Furthermore, we noted a PDTC-dependent decrease in the levels of IL-6 induced by the combination of soluble LT/ΔLT OMVs to a level comparable to that of soluble LT. Thus, NFκB inhibition appeared to act on the OMV contribution towards IL-6 induction but had no effect on the contribution of soluble LT. These results further support our findings that soluble LT and a comparable concentration of OMV-bound LT induce IL-6 through different pathways.

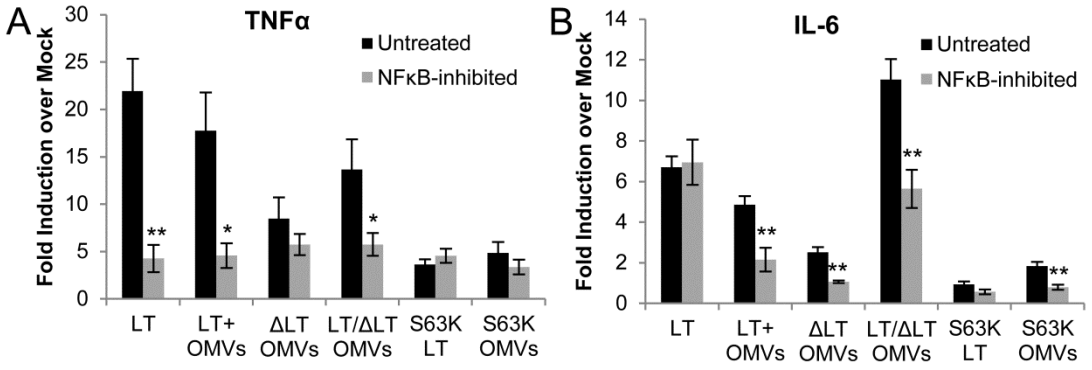

Figure 16: OMVs but not soluble LT induce IL-6 through NFκB.

Polarized T84 cells were pre-treated with an NFκB inhibitor for 30 min, and samples standardized to 200 pM LT were added to the apical compartment for 6 h. The gene expression levels of **(A)** TNFα and **(B)** IL-6 were determined using RT-PCR. *, $p<0.05$; **, $p<0.01$; ***, $p<0.005$ compared to untreated levels (n=3).

Flagellin does not contribute to the difference in TNFα and IL-6 levels between OMVs. Flagellin has been shown to induce cytokine expression and to be

associated with OMVs (Galka et al, 2008; Park et al, 2011; Subramanian et al, 2008). We analyzed the relative amounts of flagellin associated with the vesicle treatments using immunoblotting. The amount of vesicles analyzed correlated to the amount of vesicles added to the T84 cells. As shown in Figure 17, LT^+ OMVs and S63K OMVs had similar levels of flagellin, which were substantially higher than the amount of flagellin present in ΔLT OMVs. Although the flagellin present in OMVs might contribute to the induction of TNFα and IL-6, the levels of flagellin did not correlate with the differences in the levels of induction between OMV samples.

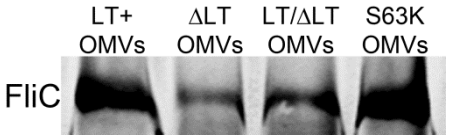

Figure 17: Flagellin levels in vesicle preparations do not correlate with TNFα and IL-6 induction.

Flagellin was detected in preparations of LT+ OMVs, ΔLT OMVs, LT/ΔLT OMVs and S63K OMVs through immunoblotting with anti-FliC. The preparations were concentrated to allow for the detection of flagellin, but the concentration was proportional to those used in the experiments.

2.4 Discussion

Because ETEC is an important agent of disease worldwide, studies to elucidate the mechanisms of its virulence factors, including LT, are important. Most studies on LT have been performed on its soluble form in many different cell lines. However, recent studies have demonstrated that LT has the propensity to bind LPS and thus become associated with secreted OMVs (Horstman & Kuehn, 2000; Horstman & Kuehn, 2002;

Mudrak et al, 2009). In addition, LT acts in the gut lumen, where tight barriers generated by the epithelium allow only apical exposure of cells to toxin. Therefore, we determined the response of polarized intestinal epithelial cells to LT presented in soluble and insoluble contexts.

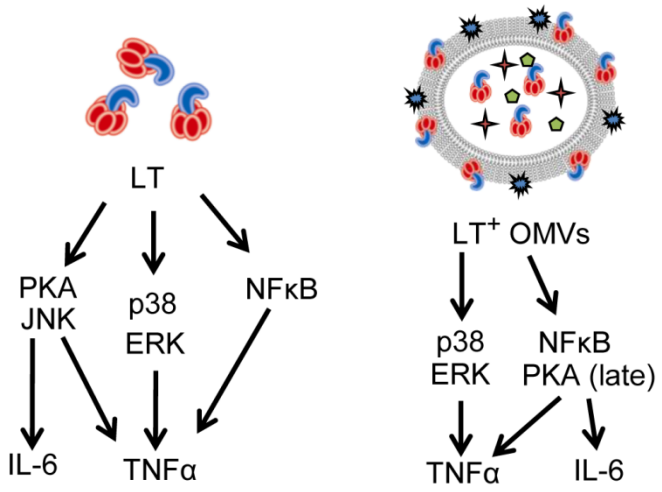

Figure 18: Overview of the different pathways through which soluble LT and LT+ OMVS elicit TNFα and IL-6 responses in human intestinal epithelial cells.

We found significant differences in the mechanisms and kinetics of TNFα and IL-6 gene induction elicited by soluble LT and LT+ OMVs. As summarized in Figure 18, soluble LT elicited IL-6 through two pathways, PKA and JNK. However, LT+ OMVs only induced IL-6 through an independent pathway involving NFκB at early times. Although both OMV-bound and soluble LT elicited TNFα through some shared pathways, the PKA and JNK pathways were still unique to soluble LT. At later times, both LT and LT+ OMVs acted through the PKA pathway (Figure 12). Whereas catalytically active LT-containing treatments (soluble LT, LT+ OMVs, and a combination of LT/ΔLT OMVs)

elicited substantially higher levels of TNFα and IL-6 expression at 6 h than non-catalytically active treatments, this higher induction did not depend on the activation of CREB. This result was unexpected. LT acts through the ADP-ribosylation of the Gsα subunit of adenylate cyclase, which results in an increase in cAMP levels. cAMP then activates PKA, which leads to Cl^- efflux and the phosphorylation of CREB. As shown in Figure 9 and Figure 10, LT^+ OMVs showed delayed kinetics of CREB phosphorylation and CRE gene activity compared to soluble LT and the combination of LT/ΔLT OMVs. Our data suggest that delayed kinetics rather than decreased induction occurs for OMV-associated LT activation because at 9 h, LT^+ OMVs elicited significantly higher levels of IL-6 than soluble LT ($p<0.001$), and this increase was significantly inhibited by Rp-camps (Figure 12). Because PKA activation is also responsible for phosphorylating the CFTR, resulting in Cl^- and water efflux into the intestinal lumen, our results also suggest that the onset of diarrhea may also be delayed in response to LT^+ OMVs compared to soluble toxin.

There are many reasons why LT in its native OMV presentation might elicit different responses than soluble LT. Multiple LT molecules are complexed with an OMV, thus fewer host cells may become intoxicated by OMV-bound LT than soluble LT. By containing multiple LT molecules, a few LT^+ OMVs could elicit maximal CREB activation, whereas soluble LT would elicit a more gradual, proportional response depending on how many individual LT molecules were encountered by each cell. In

addition, OMV internalization and trafficking could occur via a different pathway than soluble LT, leading to differences in the efficiency of the intracellular processing of LT. The delayed kinetics of activation could also suggest the inaccessibility of the toxin bound to OMVs. Removing the LT bound to LPS on the OMVs to allow it to progress through the canonical LT pathway may be inefficient inside of a host cell. Further studies are ongoing to elucidate the mechanistic basis for the observed differences.

H89, which inhibits CREB phosphorylation by PKA at low concentrations, was used as an independent method to demonstrate the role of CREB in the induction of IL-6 and TNFα. H89 showed similar results as Rp-camps, which inhibits PKA activity, except that it led to a significant decrease in TNFα induction in response to LT^+ OMVs. However, this decrease may not be dependent on CREB. In addition to its role as a CREB inhibitor, H89 has also been shown to play a role in the inhibition of mitogen stress kinase 1 (MSK1) (Hokari et al, 2005; Vermeulen et al, 2003), which phosphorylates NFκB to induce NFκB-mediated gene transcription (Vermeulen et al, 2003). However, we did not find any indication of MSK1 phosphorylation or NFκB phosphorylation in any of our samples using immunoblotting (data not shown), which suggests that MSK1 does not play a role in the induction of TNFα by LT^+ OMVs. H89 has also been shown to inhibit protein kinase D (PKD), which plays a role in Golgi-to-ER transport (Lee & Linstedt, 2000; Prestle et al, 1996). After binding to the host receptor ganglioside G_{M1}, LT is internalized and transported to the Golgi and the ER, in which the catalytic subunit is

processed. H89 may interfere with this activation by inhibiting the translocation of cargo from the Golgi to the ER, and this inhibition may also play a role in inhibiting the TNFα response to LT^+ OMVs.

This is the first study to show a role for AP-1 in the host response to LT. AP-1 only played a role in the induction of IL-6 by soluble LT and did not affect OMV responses, even at later times. In addition, AP-1 was not activated in response to LT^+ OMVs, even at later time points. No previous studies have shown activation of AP-1 by LT, although IL-6 induction in response to increased cAMP levels has been shown to be mediated, at least in part, by AP-1 (Dendorfer et al, 1994). Dendorfer et al. also showed that cAMP induced IL-6 through different mechanisms than LPS, and the IL-6 response to LPS was completely abrogated by mutations in NFκB-binding sites (Dendorfer et al, 1994). We found significant differences not only between soluble LT and LT^+ OMVs but also among overall OMV responses. A significant inhibition of IL-6 responses in response to NFκB inhibition was only observed for treatments containing OMVs. In fact, in the combination of LT/ΔLT OMVs, NFκB inhibition appeared to remove the OMV contribution to IL-6, resulting in an IL-6 level similar to that induced by soluble LT alone. These results suggest a vesicular component responsible for activating NFκB to induce IL-6. Although NFκB is an important contributor to IL-6 induction, the IL-6 promoter contains multiple regulatory elements, including binding sites for AP-1, NFκB, and NF-IL-6 (Lieb et al, 1998). Additionally, previous studies have shown that NFκB is

not required for IL-6 induction and that this induction can be mediated by MAPKs (Kondo et al, 2001; Pearson et al, 2008). Taken together, our results emphasize the different mechanisms through which soluble LT and OMV treatments induce TNFα and IL-6 responses.

OMVs were standardized according to lipid content, in consideration of the fact that LPS would probably cause a dominant cytokine response. As a consequence of different protein:lipid ratios in OMVs, however, this normalization process resulted in the protein concentrations of LT^+ OMVs and S63K OMVs being more than twice as high as the amount of protein in ΔLT OMVs. This could have caused the differences in the levels of TNFα and IL-6 induction. However, we propose that differences in OMV protein concentration were not a major factor in the observed responses. First, despite similar levels of protein in LT^+ OMVs and S63K OMVs, the induction of cytokines in response to LT^+ OMVs was significantly higher than S63K OMVs. Second, S63K OMVs, with over two-fold higher protein levels, produced similar levels of TNFα and IL-6 as ΔLT OMVs. Third, we used samples standardized to two concentrations of LT, 1 nM and 200 pM. Although the amount of protein in the ΔLT OMVs at the 1 nM treatment was twice that of LT^+ OMVs at 200 pM, LT^+ OMVs induced significantly more IL-6 than ΔLT OMVs.

Our results suggest that the response to the combination of LT/ΔLT OMVs is not merely additive. IL-6 and TNFα responses induced by the combination of LT/ΔLT OMVs were not equivalent to the combined responses of soluble LT and ΔOMVs. These

results may be due to the fact that the combination of LT/ΔLT OMVs actually consists of three distinct populations: soluble LT, ΔLT OMVs, and LT bound to the surface of ΔLT OMVs. Although LT may bind to the surface of ΔLT OMVs, this is not the native presentation because native LT^+ OMVs also contain LT in the lumen of the vesicle. The proportion of these populations, and therefore their individual contribution, is difficult to determine. Nevertheless, it was valuable to use this treatment as it allowed us to determine that the context of toxin presentation (i.e., in both the lumen and on the surface of OMVs) was important in eliciting TNFα and IL-6 responses, which were not merely a result of the presence of equivalent amounts of soluble LT and ΔLT OMVs.

IL-6 and TNFα are pro-inflammatory cytokines that can mediate acute inflammation. In addition to their role as pro-inflammatory mediators, IL-6 and TNFα may also play protective roles in the intestine, such as tissue repair after injury and protection from apoptosis (Saleh & Trinchieri, 2011; Tebbutt et al, 2002). Because ETEC does not cause disease in mice, mouse models to study the *in vivo* effects of ETEC are not available. In addition, little data have been published on the cytokine response of patients with diarrhea caused by ETEC. However, other enteric pathogens have been shown to elicit TNFα and IL-6 responses. Using *in vivo* studies, Dann et al. showed that IL-6 was produced in mouse intestines in response to *Citrobacter rodentium* and that this induction was important in preventing infection-induced apoptosis in the colonic epithelium (Dann et al, 2008). In clinical settings, both IL-6 and TNFα have been found

in the stools of children who had diarrhea that was caused by another enteric pathogen, *Shigella dysenteriae* (de Silva et al, 1993). In addition, in children with enterocolitis, serum IL-6 has been shown to be discriminative of bacterial etiology from viral etiology (Yeung et al, 2004). Although the mechanisms of IL-6 and TNFα induction in these studies have not been elucidated, these data show the relevance of IL-6 and TNFα induction by enteric pathogens.

The role of IL-6 in ETEC-induced diarrhea is unknown because ETEC is not an inflammatory diarrhea (Daniels, 2006). Although the IL-6 receptor is expressed on intestinal epithelial cells and may lead to the down-regulation of IL-6, we do not believe that this pathway is relevant in our results. First, the timeline of IL-6 induction, 6 h, was chosen because this was the first timepoint in which IL-6 was significantly induced compared to mock treatment, and the effects of this interaction with the IL-6 receptor would not be reflected in such a short timeframe. Additionally, the IL-6 receptor is primarily expressed at the basolateral membrane (Wang et al, 2003), and our ELISA results at 24 h showed IL-6 secretion only in the apical supernatant.

In summary, we show that whereas OMV-bound LT is not as effective at inducing CREB activation at early times as soluble LT, LT^+ OMVs can induce similar amounts of cytokine gene expression. These differences in CREB activation may be due to different trafficking mechanisms within the cell. Previous studies to determine the effects of LT

and vaccination strategies for ETEC have used soluble LT. Our study emphasizes the importance of studying virulence factors in their native context.

2.5 Acknowledgements

The authors thank Dr. James Fleckenstein for strain H10407Δ*eltA*; Stefanie Hartman for assistance with EMSAs; Dr. Ben Mudrak for cloning help; Dr. Patrick Seed for providing the anti-H7 antibody; and Dr. Hiroaki Matsunami, Kyla Selvig, and Dan Rodriguez for piloting the CRE-Luciferase assay.

3. Heat labile enterotoxin- and G_{M1}-dependent intracellular trafficking and signaling of enterotoxigenic *Escherichia coli* outer membrane vesicles

3.1 Summary

Enterotoxigenic *Escherichia coli* (ETEC) is responsible for approximately ten million cases of traveler's diarrhea and is the leading cause of mortality and morbidity due to diarrhea in children in developing countries. Heat-labile enterotoxin (LT) has been implicated in this process, and it is secreted from ETEC through association with outer membrane vesicles. Previously, we showed that vesicle-associated LT showed delayed kinetics in activation and the differential activation of signaling pathways compared to soluble LT. To determine whether these differences in activation were a consequence of differential internalization and trafficking, we examined the internalization in polarized intestinal epithelial cells of ETEC vesicles with and without associated LT. We found that vesicles induced interleukin-6 in cells through a lipid raft-dependent mechanism regardless of the ability to bind to G_{M1}, but that the presence of LT provided a more efficient route of internalization. Vesicles associated with LT that harbored a G_{M1}-binding mutation in the LTB subunit were internalized; however, these vesicles did not lead to phosphorylation of the cyclic AMP response element-binding protein, despite the internalization of the LTA subunit. We also found that the inhibition of ER translocation did not fully inhibit the production of IL-6, suggesting that not all vesicle components are translocated to the ER and supporting the hypothesis that the

LT-G_{M1} complex is stripped from the vesicle before trafficking to the ER. These results suggest that ETEC may deliver LT via vesicles as a method of the post-translational regulation of LT activity.

3.2 Introduction

Enterotoxigenic *Escherichia coli* (ETEC) is the leading cause of traveler's diarrhea (Black, 1990) and morbidity and mortality due to diarrhea in children in developing countries. ETEC has been estimated to be responsible for 170,000 deaths annually (Niyogi, 2005). ETEC acts through the elaboration of several virulence factors, including heat-stable enterotoxin (ST) and heat-labile enterotoxin (LT), which contribute to the disease (Kaper et al, 2004). Bacterial outer membrane vesicles (OMVs) are ubiquitously produced by Gram-negative bacteria (Ellis & Kuehn, 2010; Kulp & Kuehn, 2010) and have been identified as a means of secreting complexes of bacterial insoluble and soluble components, including virulence factors such as LT, as well as other molecules which activate responses in eukaryotic cells. OMVs are spherical bi-layer structures that are composed of both outer membrane and periplasmic components, and they are produced independent of membrane instability (McBroom et al, 2006). OMVs play roles in protecting bacteria from both internal and external stress, communicating with other bacteria, and interacting with and delivering bacterial factors to host cells (Ellis & Kuehn, 2010; Kulp & Kuehn, 2010).

Although most studies on elucidating the function and characteristics of LT have been performed on soluble LT, previous studies from our lab have shown that the majority of secreted LT is associated with OMVs, both in the lumen of the OMVs and bound to the surface through an interaction with lipopolysaccharide (LPS), a major component of OMVs (Horstman & Kuehn, 2000; Mudrak et al, 2009). In addition to LPS and LT, OMVs have been associated with numerous virulence factors. Toxins that have been identified to be active and enriched in OMVs include cytolethal distending toxin (CDT) from *Campylobacter jejuni* (Lindmark et al, 2009), leukotoxin A (LktA) from *Aggregatibacter actinomycetemcomitans* (Kato et al, 2002), and vacuolating toxin (VacA) from *Helicobacter pylori* (Fiocca et al, 1999; Ismail et al, 2003).

Although OMVs have been shown to be effective delivery vehicles for virulence factors, the mechanisms through which OMVs enter host cells are varied and appear to depend on the strain from which the OMVs were produced, the target cell, and the presence of virulence and adherence factors (Ellis & Kuehn, 2010). *Shigella flexneri* has been shown to be internalized within a phagosome in intestinal epithelial cells (Kadurugamuwa & Beveridge, 1998). *H. pylori* OMV internalization within gastric adenocarcinoma cells has been shown to be clathrin-dependent and lipid raft-independent, and association was shown to be enhanced by VacA (Parker et al, 2010). In contrast, *Porphrymonas gingivalis* OMVs have been shown to be internalized within HeLa cells and gingival cells through a lipid raft-dependent mechanism that is independent of

clathrin, caveolin and dynamin (Furuta et al, 2009). Likewise, *Pseudomonas aeruginosa* OMV internalization within lung cells has been shown to be lipid raft-dependent and clathrin- and caveolin-independent, and this association was enhanced by an aminopeptidase (Bauman & Kuehn, 2009; Bomberger et al, 2009).

Once internalized, the pathways through which OMVs are trafficked are also varied. *P. gingivalis* OMVs have been shown to traffic from early endosomes to lysosomes, in which they can persist for twenty-four hours (Furuta et al, 2009). *P. aeruginosa* OMVs from a cystic fibrosis clinical isolate have been shown to colocalize with ER makers (Bauman & Kuehn, 2009), whereas OMVs from a highly virulent burn wound isolate were shown to traffic within early endosomes and did not require trafficking to the ER for the activation of a toxin within the OMVs (Bomberger et al, 2009).

Our lab has shown that the association of ETEC OMVs with non-polarized intestinal epithelial cells is increased by the presence of LT (Kesty et al, 2004). LT^+ OMV internalization was shown to be lipid raft-dependent, and OMVs were shown to colocalize with caveolin but not clathrin. In addition, these LT^+ OMVs did not appear to be trafficked within acidic compartments (Kesty et al, 2004).

The route of LT trafficking is well understood. LT binds with high affinity to the G_{M1} ganglioside (Galb1-3GalNAcb1-4(NeuAca2-3)Galb1-4Glcb1-1ceramide) (De Haan & Hirst, 2004). LT can be internalized through caveolin-associated or –independent lipid

rafts (De Haan & Hirst, 2004). Once internalized, LT is trafficked to the *trans*-Golgi network (TGN) and retrograde transported from the TGN to the ER. However, little is known about the trafficking of LT^+ OMVs and ΔLT OMVs in the physiologically relevant polarized epithelial cell model. Polarized epithelial cells express very little caveolin, and most caveolin is found on the basolateral membrane, which would not be accessible to OMVs in the intestinal lumen (Badizadegan et al, 2000). In addition, although LT has been shown to increase the association of OMV with non-polarized intestinal epithelial cells, whether LT is required for the internalization of ETEC OMVs has not been determined. In this paper, we determined that ETEC OMVs were internalized independent of LT, although at significantly lower levels than LT+ OMVs. In addition, we found that LT+ OMVs bound predominantly to G_{M1} and lipid raft domains, and this binding was necessary for the induction of IL-6 in response to OMVs.

3.3 Results

ETEC OMVs are internalized independent of LT. A previous study by our lab using a K12 strain of *E. coli* showed that the association of OMVs produced by this non-pathogenic strain was enhanced with LT, but the internalization of OMVs derived from an ETEC strain deficient in LT (ΔLT OMVs) was not determined (Kesty et al, 2004). The outer membrane components of ETEC are expected to be quite different from those of K-12 E. coli, and these are likely to impact ETEC OMV interactions with host cells as well as intracellular trafficking. To determine whether ΔLT OMVs could be internalized by

polarized T84 cells, the polarized cells were incubated with fluorescently labeled LT+ OMVs or ΔLT OMVs, F-actin was stained using phalloidin, and confocal Z-stack images were obtained. Representative images are shown in Figure 19 along with xz and yz projections. Both LT+ OMVs and ΔLT OMVs were found to be both bound to the surface of (yellow; asterisks) and internalized within T84s (red; arrows).

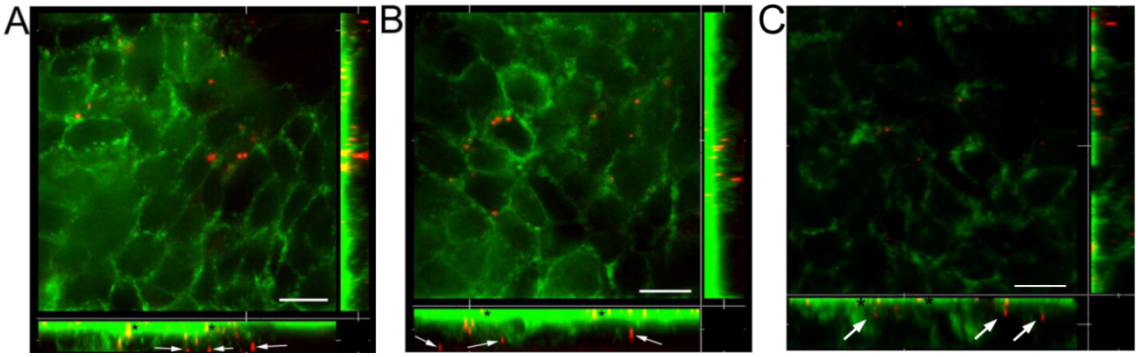

Figure 19: ETEC OMVs are internalized independent of LT.

ETEC OMVs are internalized within polarized T84 cells independent of LT. **(A-C)** Polarized T84 cells were grown on clear permeable filters and incubated with 1 μg of Alexa Fluor 555 fluorescently labeled **(A)** LT+ OMVs, **(B)** ΔLT OMVs, and **(C)** G33D OMVs at 37°C for 4 h. The cells were washed, fixed, and labeled with Alexa Fluor 488-labeled phalloidin to label actin. The filters were excised and mounted on glass slides, and Z-stacks were obtained using confocal microscopy. A representative section and XZ and YZ slices are shown for each sample. The black asterisks indicated surface-bound OMVs (yellow), and the white arrows indicate internalized OMVs (red). Scale bars indicate 5 μm.

We then determined the amount of cell-associated OMVs fluorescence for each condition to establish whether LT contributed significantly to the binding and internalization of ETEC OMVs. As shown in Figure 20A, the total amount of cell-associated fluorescence for cells that had been incubated with ΔLT OMVs was significantly lower than for LT+ OMVs. These values include both surface-bound and

internalized OMVs. We verified that both LT+ and ΔLT OMVs were fluorescently labeled to equivalent extents so that quantitative comparisons could be performed (data not shown). To examine the ratio of internalized OMVs to surface-bound OMVs, the percentage colocalization of OMV-associated fluorescence with actin staining was determined using Imaris software. Figure 20B shows that although the total amount of OMV-associated fluorescence was different between LT+ OMVs and ΔLT OMVs, the percentage of OMV-associated fluorescence that colocalized with phalloidin staining was not significantly different. These results clearly indicate that although LT is not required for the internalization of ETEC OMVs, LT increases the amount of OMVs that interact with polarized intestinal epithelial cells.

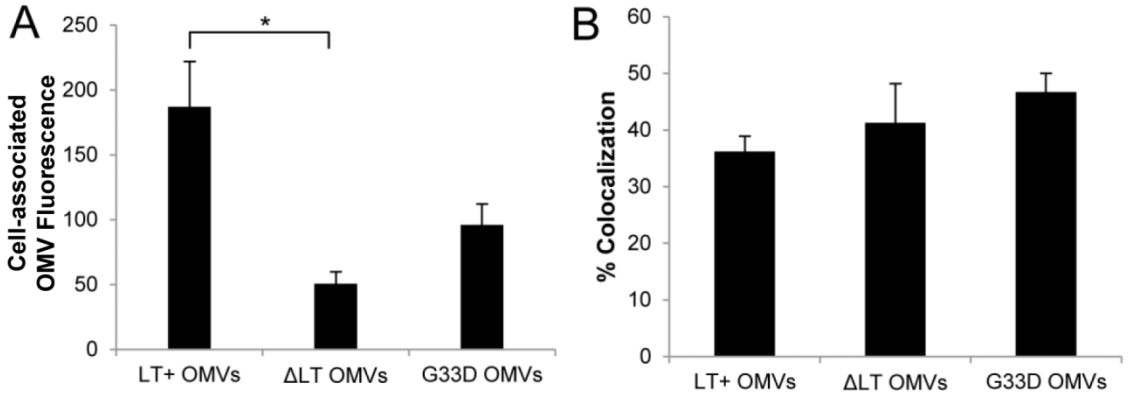

Figure 20: LT enhances the association of OMVs with polarized T84 cells.

Samples were treated as in Figure 19. **(A)** The amount of punctate fluorescent dots was quantified in at least six fields of each sample. *$p<0.05$. **(B)** The percentage of colocalization of red fluorescence with green fluorescence was determined in at least six fields per sample.

Intriguingly, although the total amount of LT+ OMVs was higher, the percentage of OMVs bound to the surface of cells was the same among all treatments. This may

suggest that while LT^+ OMVs may bind more quickly and with higher affinity to host cells than ΔLT OMVs, once OMVs are bound, they are internalized at the same rate. However, another possibility may be that once LT^+ OMVs are bound, they may traffic within cells more efficiently and they may become processed. It should be noted that a critical level of aggregation of OMVs is necessary for OMV visualization within cells. The average size of punctate fluorescence within our cells was approximately 700 nm, which is at least three times larger than the OMVs observed using electron microscopy. Whether this aggregation occurs once the OMVs bind to the cell surface or before is unclear.

LT^+ OMVs bind to G_{M1} and this binding is required for IL-6 induction and CREB phosphorylation. LT binds to the host ganglioside receptor G_{M1} on host cells as well as other terminal galactose-containing glycolipids and glycoproteins (Fukuta et al, 1988). Previous studies in our laboratory have shown that the pre-incubation of LT^+ OMVs with G_{M1} significantly reduced the association and internalization of OMVs with HT29 cells (Kesty et al, 2004). To determine whether OMVs bound directly to G_{M1} on the apical surface of polarized T84 cells, we examined the colocalization of fluorescently labeled OMVs with G_{M1} using microscopy. As shown in Figure 21, LT^+ OMVs almost completely colocalized with G_{M1}. ΔLT OMVs also colocalized somewhat with G_{M1};

however, this colocalization was not as extensive.

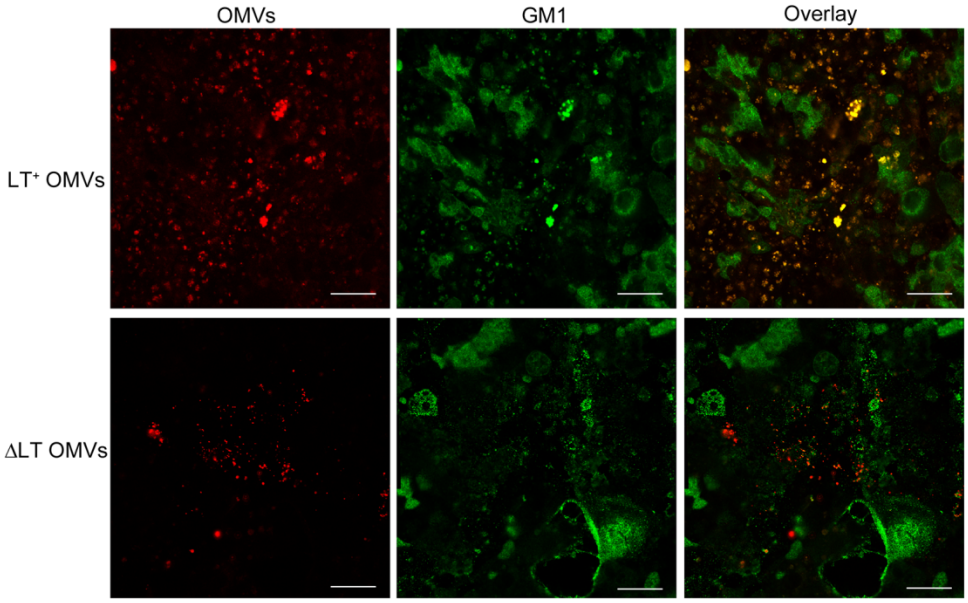

Figure 21: LT+ OMVs but not ΔLT OMVs colocalize with G_{M1}.

Polarized T84 cells were incubated at 4°C for 2 h with LT+ OMVs (upper row) and ΔLT OMVs (lower row), washed, and fixed. The cells were incubated with a primary antibody against GM1 and a 488-labeled secondary antibody. The filters were excised, mounted on glass slides, and visualized using confocal microscopy. Scale bars indicate 10 μm.

To investigate whether G_{M1} binding was important in the signaling events elicited in response to OMVs, we isolated OMVs from a strain containing a G_{M1}-binding LT mutant. The well-characterized G33D mutation in the B subunit of LT abolishes binding to G_{M1}, and previous results suggest that it may abolish binding to GD1a (Wolf et al, 1998). The G33D mutation results in decreased Y1 adrenal cell cytotoxicity and fluid accumulation in a mouse model compared to wild-type LT (Guidry et al, 1997).

Interestingly, cAMP induction has been shown to be similar between wild-type and G33D LT suggesting that LT is still active within cells (Guidry et al, 1997) Previously, we showed that IL-6 is induced in response to LT^+ OMVs (Chutkan & Kuehn, 2011). To determine the role of G_{M1} binding in the induction of IL-6 in response to LT^+ OMVs, we isolated G33D OMVs from an isogenic strain and determined IL-6 levels using RT-PCR. The amount of LT in G33D OMVs was standardized to 200 pM LT, which was similar to LT^+ OMVs. As shown in Figure 22, although similar amounts of LT were added, the G33D OMVs showed a significantly reduced induction of IL-6 compared to wild-type LT OMVs and the level was similar to that elicited by ΔLT OMVs. We have also previously shown that LT^+ OMVs lead to the activation of CREB (Chutkan & Kuehn, 2011). Therefore, we examined whether G33D OMVs could activate CREB despite showing reduced levels of IL-6. As shown in Figure 22, although soluble LT and LT^+ OMVs led to an increase in the phosphorylation of CREB, neither ΔLT OMVs nor G33D OMVs showed activation of CREB. These results suggest that binding to G_{M1} is necessary for the induction of IL-6 and the activation of CREB in response to LT^+ OMVs, possibly due to intracellular, G_{M1}-directed trafficking of the OMVs.

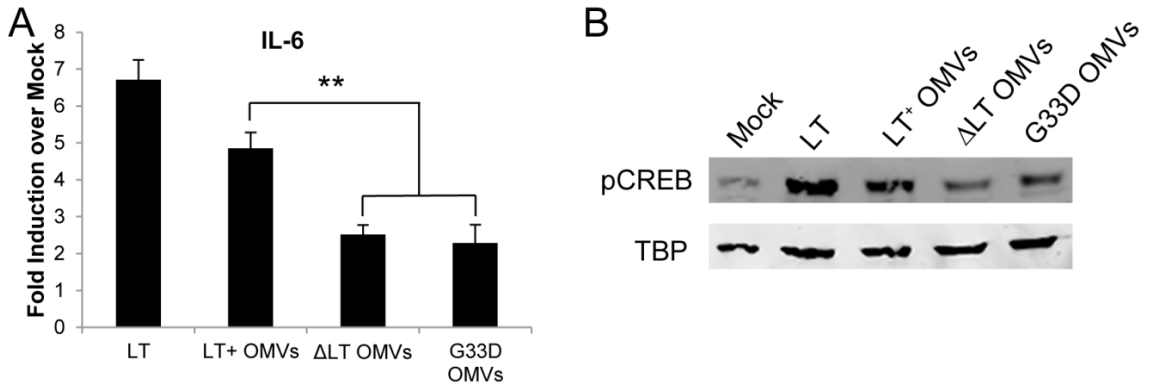

Figure 22: G_{M1} binding is required for the activation of LT.

(A) Polarized T84 cells were incubated with standardized amounts of LT, LT+ OMVs, ΔOMVs, and G33D OMVs for 6 h, and the gene expression levels of IL-6 were measured at using RT-PCR. **p<0.01 (*n*=3). **(B)** Nuclear extracts were prepared from polarized T84 cells incubated with samples standardized to 1 nM LT for 6 h, and immunoblots were performed to determine the phosphorylation status of CREB. TBP was used as a loading control. The image shown is representative of three independent experiments.

To determine the levels of association of G33D OMVs with polarized T84 cells, we fluorescently labeled G33D OMVs and assessed internalization at 4 h. As shown in Figure 19C, G33D OMVs were internalized within polarized T84 cells. Although the total amount of OMV-associated fluorescence was approximately 2-fold lower than LT^+ OMVs, this decrease was not statistically significant (Figure 20A). G33D OMVs showed no difference in the percentage of surface-bound OMVs compared to LT^+ OMVs and ΔLT OMVs (Figure 20B). These results show that although the total amount of OMV-associated fluorescence and the amount of internalized OMVs was not significantly different between LT^+ OMVs and G33D OMVs, G33D OMVs still elicited significantly lower amounts of IL-6, suggesting the importance of G_{M1} binding to the activity of LT^+ OMVs.

OMVs induce IL-6 through a lipid raft-mediated mechanism. Previous results from our lab have shown that LT^+ OMVs are internalized in non-polarized intestinal cells via a lipid raft-mediated pathway and that these OMVs colocalize weakly with caveolin, suggesting the role of caveolae in internalization (Kesty et al, 2004). However, polarized intestinal epithelial cells only weakly express caveolin, and this expression is restricted to the basolateral membrane (Badizadegan et al, 2000). Furthermore, caveolin does not colocalize with lipid raft markers in polarized intestinal epithelial cells (Badizadegan et al, 2000). To determine whether lipid raft-mediated internalization pathways contributed to the host immune reaction in response to OMVs, we pharmacologically disrupted lipid rafts in polarized T84 cells and measured the induction of IL-6. As shown in Figure 23A, disrupting lipid rafts by depleting membrane cholesterol led to a significant decrease in IL-6 induction in response to soluble LT, LT^+ OMVs, and ΔLT OMVs and a substantial decrease in response to G33D OMVs.

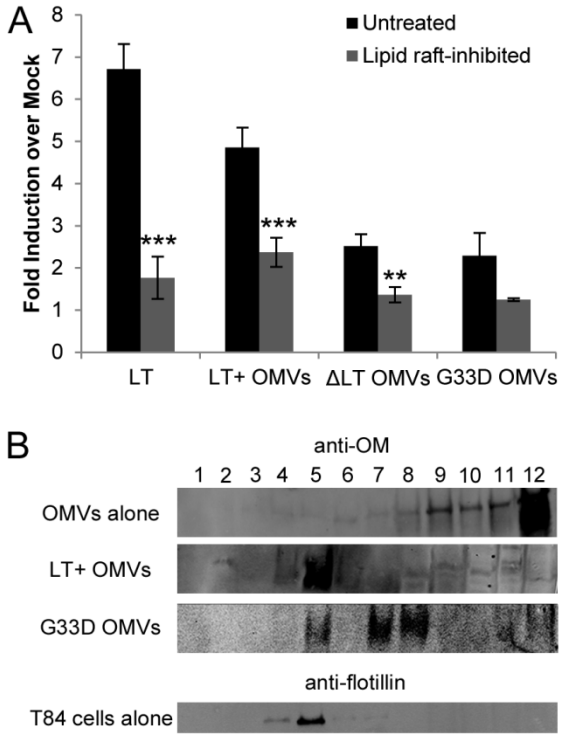

Figure 23: OMVs interact with intact lipid rafts on polarized intestinal epithelial cells.

(A) Polarized T84 cells were pretreated with 4 mM MβCD for 1 h and incubated with samples corresponding to 200 pM LT. After 6 h, the levels of IL-6 gene induction were evaluated using RT-PCR. Asterisks indicate significant differences from the respective untreated sample. **$p<0.01$, ***$p<0.005$ (n=3). **(B)** The association of LT+ OMVs and G33D OMVs with detergent-resistant lipid raft microdomains was determined using sucrose density centrifugation. Polarized T84 cells were incubated with the indicated OMVs for 1 h, and detergent-insoluble membranes were isolated using sucrose density centrifugation. Fractions were collected, and the protein was precipitated using TCA and acetone and analyzed using immunoblotting. Fractions were analyzed using a polyclonal anti-*E. coli* outer membrane antibody and a polyclonal anti-flotillin antibody.

Previous studies have shown that although soluble LT can bind to receptors other than G_{M1}, such as G_{D1a}, this binding does not lead to LT activation because G_{D1a} does not associate with lipid rafts and results in the improper trafficking of the toxin (Wolf et al, 1998). However, our data suggest that G33D OMVs may still associate with

lipid rafts. To further examine the role of lipid rafts in OMV internalization, we incubated T84 cells with OMVs for 1 h and performed sucrose density centrifugation to isolate detergent-resistant membranes. Because of the low amount of OMVs produced by the ΔLT strain, it was not technically feasible to purify enough ΔLT OMVs to perform this experiment.

Figure 23B shows that when OMVs alone were applied to the density gradient, a majority of the OMV antigen signal was detected in the high-density fraction. A protein band was observed in fraction 5 of all of the samples containing T84 cells and reacted to the anti-flotillin antibody (Figure 23B), suggesting that this fraction contained lipid rafts. For cells incubated with LT^+ OMVs, the peak of the OMV antigens were found in fraction 5, suggesting that LT^+ OMVs interact with lipid rafts. Interestingly, when G33D OMVs were incubated with T84 cells, the signal was split among fractions 5, 7 and 8. A previous study has suggested that fraction 8 may correspond to the cytosol or apical membrane (Chen et al, 2006). Together, these results suggest that while G33D OMVs can interact with lipid rafts, the majority of the OMVs interact with non-lipid raft domains after 1 h co-incubation.

IL-6 induction by LT^+ OMVs is not dependent on clathrin. We hypothesized that distinct OMV-induced signaling would reflect distinct OMV internalization pathways. To elucidate the role of OMV trafficking on signaling in polarized cells, we determined whether clathrin inhibition would change the response to OMVs. Previous

data from our lab showed no colocalization of LT^+ OMVs with clathrin in non-polarized cells (Kesty et al, 2004). However, another study has shown a role for the clathrin-mediated internalization of OMVs from a different pathogen (Parker et al, 2010). We pharmacologically disrupted clathrin-mediated endocytosis using non-toxic concentrations of chlorpromazine and PAO (Lu et al, 2005; Nazli et al, 2006).

The inhibition of clathrin-mediated internalization using chlorpromazine and PAO showed no difference in the induction of IL-6 in response to soluble LT and actually led to increased IL-6 induction in response to LT^+ OMVs (Figure 24A). Although G33D OMVs showed no difference in the induction of IL-6 in response to the disruption of clathrin-mediated internalization, ΔLT OMVs showed a slight but significant decrease when PAO was used. To further examine the role of clathrin and caveolae in OMV endocytosis, we inhibited dynamin using dynasore. Dynamin is necessary for the scission of endocytic vesicles produced during both clathrin-mediated and caveolae-mediated internalization. Confirming the results obtained using PAO, dynasore led to a significant reduction in the level of IL-6 produced by ΔLT OMVs (Figure 24B). However, there was no significant difference in IL-6 induction in response to LT^+ OMVs. Our results suggest that ETEC OMVs are internalized through a lipid-raft dependent mechanism that is independent of caveolae.

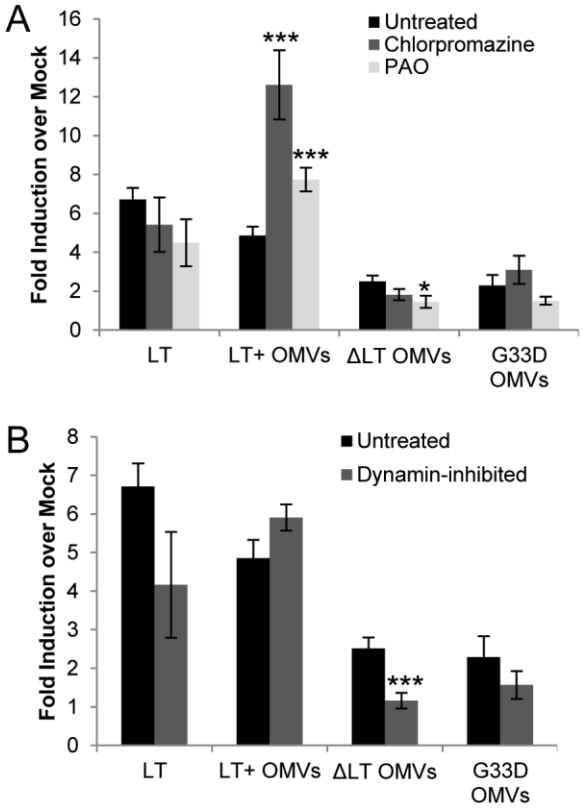

Figure 24: OMVs that do not contain LT require clathrin to induce IL-6

Polarized T84 cells were pre-treated with for 1 h with inhibitors of **(A)** clathrin (25 μM chlorpromazine or 500 nM PAO) or **(B)** dynamin (80 μM dynasore) before being incubated with samples corresponding to 200 pM LT for 6 h. IL-6 levels were measured using RT-PCR after pretreatment with the inhibitors. Asterisks indicate significant differences from the corresponding untreated sample. *$p<0.05$, ***$p<0.001$ (n=3).

IL-6 induction by soluble LT, but not LT$^+$ OMVs, requires trafficking from the Golgi to the ER. The trafficking of OMVs in polarized intestinal epithelial cells after entry could explain differences in IL-6 induction; however, OMV trafficking is not well-understood. A previous study by our lab reported that LT$^+$ OMVs were not internalized within acidic compartments in non-polarized intestinal cells (Kesty et al, 2004). In subsequent experiments using the polarized cell model, we did not find colocalization of

fluorescently labeled OMVs with any markers of early endosomes (EEA-1), late endosomes (M6PR), or lysosomes (LAMP-1, data not shown). LT trafficking, by contrast, is quite well-studied (Spangler, 1992). After LT is internalized within cells, it is trafficked from the Golgi to the ER via retrograde transport. A fragment of the LTA subunit is then translocated into the cytosol where it ADP-ribosylates the $G_{S\alpha}$ subunit of adenylate cyclase, leading to the phosphorylation of CREB. To determine if Golgi-to-ER trafficking was necessary for IL-6 induction by OMVs, T84 cells were pre-treated with Brefeldin A, which disrupts the Golgi and ER. Brefeldin A led to a significant reduction in IL-6 induction by soluble LT and LT^+ OMVs (Figure 25A). In addition, pre-treatment with Brefeldin A abolished CREB phosphorylation (Figure 25B). By contrast, Brefeldin A did not lead to a significant difference in the induction of IL-6 of CREB phosphorylation in response to ΔLT OMVs. To further determine the role of the Golgi and ER in inducing IL-6, we specifically disrupted the *cis*-Golgi network, but not the *trans*-Golgi network (TGN), using Exo1. CT has previously been shown to traffic through the TGN and not require the rest of the Golgi apparatus (Feng et al, 2004). Exo1 pretreatment did not result in any differences in IL-6 induction (Figure 25A). These results suggest that trafficking from the *cis*-Golgi to the ER is not required for the induction of IL-6 by soluble LT or by LT^+ OMVs.

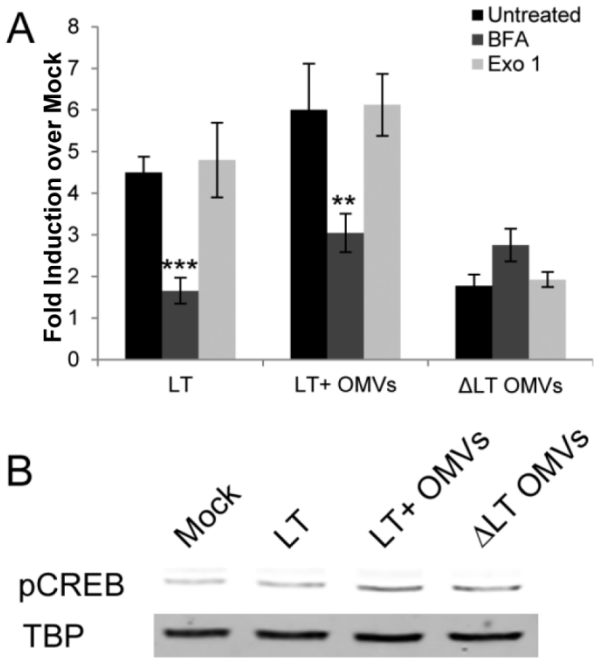

Figure 25: LT requires ER trafficking to be active, but ΔLT OMVs do not

Polarized T84 cells were pre-treated with for 1 h with inhibitors of Golgi to ER trafficking (Brefeldin A) or the *cis*-Golgi (Exo 1) before being incubated with samples corresponding to 1 nM LT for 6 h. **(A)** IL-6 levels were measured using RT-PCR after pretreatment with the inhibitors. Asterisks indicate significant differences from the corresponding untreated sample. **$p<0.01$, ***$p<0.001$ (n=3). **(B)** Nuclear proteins were extracted from T84 cells treated as described in **(A)** and immunoblotted for phosphorylated CREB and TBP as a loading control. The image shown is representative of three experiments.

3.4 Discussion

We have previously shown that LT^+ OMVs show delayed kinetics in activating CREB phosphorylation and IL-6 induction due to CREB phosphorylation compared to soluble LT (Chutkan & Kuehn, 2011). We also showed that LT+ OMVs induced IL-6 and TNFα through different signaling pathways (Chutkan & Kuehn, 2011). We hypothesized that this delay in signaling was a result of differential trafficking and internalization

within the cell. Although the internalization of LT+ OMVs has previously been examined in non-polarized intestinal epithelial cells, the link between internalization and gene induction in response to ETEC OMVs has not been determined, especially in the physiologically relevant model of polarized T84 cells.

We show that ETEC OMVs are internalized independently of LT, but this internalization is significantly higher in LT^+ OMVs compared with ΔLT OMVs. This result confirms previous results in our lab showing that LT enhanced the association of OMVs with non-polarized intestinal cells (Kesty et al, 2004). Further studies are necessary to distinguish whether OMVs are internalized at similar rates within host cells or whether LT association enhances the degradation of OMVs.

We found that LT^+ OMVs bound almost exclusively to G_{M1}. Somewhat surprisingly, ΔLT OMVs also showed weak colocalization with G_{M1}, despite not containing LT. However, as G_{M1} is a known marker of lipid rafts, this colocalization may indicate that ΔLT OMVs bind to lipid rafts by an LT/G_{M1}-independent mechanism. In support of this, we found that both LT^+ OMVs and ΔLT OMVs showed a significant inhibition of IL-6 induction in response to lipid raft disruption, and G33D OMVs showed a substantial decrease. This implies that OMVs are internalized and signal via a lipid raft-dependent mechanism. Further evidence was provided by lipid raft isolations. All of the LT^+ OMVs were colocalized with the lipid raft fraction. Interestingly, while some of the G33D OMV signal was associated with lipid rafts, the majority of these

OMVs were found in other fractions. A previous study has shown that CT remains associated with G_{M1} in lipid rafts even after it is transported through the ER and the Golgi (Fujinaga et al, 2003). In that study, CT was engineered to detect transport through the Golgi and ER, and, indeed, the CT became modified by sulfation and glycosylation, indicating transport through the Golgi and ER, respectively, This CT was also found to be associated with the lipid raft fraction in fractionated cells (Fujinaga et al, 2003). We also found that ΔLT OMVs could signal through a clathrin-dependent mechanism. OMV internalization via clathrin might be a secondary pathway, with lipid rafts being the primary mechanism. OMVs may bind to a specific host receptor that is internalized through a clathrin-mediated route, but this binding may be weaker than OMVs binding to lipid rafts, which is enhanced in OMVs containing LT because of the interaction with G_{M1}. OMVs lacking LT may bind more to the less efficient clathrin receptor because of their decreased association with lipid rafts.

Although comparable levels of LT were internalized within cells for both LT^+ OMVs and G33D OMVs, the IL-6 levels induced by G33D OMVs were indistinguishable from ΔLT OMVs, and CREB was not phosphorylated, which suggests that LT was not active within cells. Although G33D OMVs may enter cells through lipid rafts, because G33D OMVs do not bind to G_{M1}, they may not be trafficked throughout the cell via a lipid raft association, and any internalized vesicle may show up in non-lipid raft

compartments, such as the cytosol, or non-lipid raft components of the apical membrane.

LT has been shown to bind with high affinity to G_{M1} and with lower affinity to G_{D1a} and G_{M2} (Fukuta et al, 1988). However, in studies performed with LTIIb, which contains a pentameric B subunit that only binds G_{D1a} and a homologous A subunit, although the LTIIb-G_{D1a} toxin complex was internalized within polarized epithelial cells, no physiological response was observed (Wolf et al, 1998). In addition, this toxin-receptor complex did not float in the lipid raft fraction of sucrose density gradients (Fujinaga et al, 2003; Wolf et al, 1998). The authors concluded that the specificity of toxin binding was critical to the action of the toxins. In particular, the authors concluded that a major reason that G_{D1a} was not as effective as G_{M1} was because it did not associate with lipid rafts. LT G33D does not bind G_{D1a} (Wolf et al, 1998). Our results also show that the activity of LT in OMVs was critically dependent on G_{M1} binding. G33D OMVs bound to lipid rafts in low amounts, but they still lacked a trafficking signal within the cell, which once again confirms the requirement for both a trafficking motif and lipid raft association.

We have previously shown differences in the activity of soluble LT versus OMV-associated LT. Although we hypothesized that these differences may be due to trafficking, we have found many similarities between the trafficking of soluble LT and LT+ OMVs. The internalization and trafficking of LT has been well-described (Spangler,

1992). LT is internalized through a lipid raft mechanism into an early endosome, trafficked to the Golgi and then to the ER. Although OMV-associated LT still needs to be trafficked to the ER to be active, the trafficking of the other OMV components is unclear. We suggest that OMV processing might occur after internalization. Although an OMV signal is observed within cells, it is difficult to determine if this is representative of intact OMVs based solely on the fluorescent signal. If the OMV is processed within the ER, then all of the toxin would be present within the ER and available for producing a physiological response. Because the LT holotoxin remains bound to G_{M1} in the ER, it is possible to speculate that the intact OMV remains bound to G_{M1} and is also translocated into the ER. However, our results suggest that the toxin-G_{M1} complex is stripped from the OMV before being translocated. Brefeldin A treatment led to an inhibition of LT activity, but LT+ OMVs still produced an approximately three-fold increase in IL-6 induction compared to mock treatment. In addition, we did not find a difference in the induction of IL-6 in response to ΔLT OMVs with or without Brefeldin A treatment, which suggests that IL-6 inducing components of the OMV do not need to be translocated to the ER to signal. The delayed activation kinetics for OMV-associated LT may be a result of this stripping step. Further studies are needed to determine if and when OMVs are processed within cells. If OMVs are processed after internalization and the G_{M1}-bound toxin is dissociated from the OMV, then the effective concentration of active LT in LT^+ OMVs would be much lower than the actual concentration of the LT

associated with the OMVs. LT within the lumen of the OMV would not be bound to G_{M1} and therefore would not be trafficked effectively to produce a physiological response. Likewise, toxin on the exterior of the OMV that is not bound directly to G_{M1} may also be inactive once it is internalized.

The degree of intracellular processing and subsequent trafficking of OMV components could determine whether OMVs act as "bombs" to deliver large amounts of effective toxin to a cell or whether OMVs deliver large amounts of toxin to a cell, of which only a portion would be active. For some toxins associated with OMVs, intracellular toxin dissociation from the OMVs may not be necessary or play a significant a role in their activity. Thus, their effective activity would be similar to their actual concentration, and these toxins may not show delayed kinetics relative to soluble toxin.

If OMV association leads to a decrease in effective toxin activity and a delay in kinetics, why would a pathogen deliver a toxin via OMVs? OMV delivery may still be more efficient than the delivery of soluble toxin because OMVs could protect the toxin from degradation due to host proteases in the intestinal lumen (Kulp & Kuehn, 2010). Additionally, if LT has to be bound to G_{M1} and dissociated from OMVs before being trafficked to the ER, this could be a method of limiting the damage caused by exposure to large amounts of toxin. In fact, previous studies have suggested that ETEC regulates LT production through a negative feedback loop in which LT transcription is inhibited by high levels of cAMP (Bodero & Munson, 2009), suggesting that too much LT may

detrimental for ETEC, possibly through the excessive production of cAMP. Therefore, delivery of LT through OMVs could be a method of post-translational regulation of LT.

3.5 Acknowledgements

We thank Dr. James Fleckenstein for strain H10407Δ*eltA* and Dr. Ben Mudrak for cloning help. This project was supported by grant R01AI064464 from the National Institutes of Health.

4. Exploring the physiological response to heat-labile enterotoxin

4.1 Summary

The effect of heat-labile enterotoxin on the host is a complex process. In previous studies, we attempted to use in vitro methods of recapitulating the physiological environment in the intestine by using polarized intestinal epithelial cells. However, although this method gives valuable information on individual contributions, it does not account for downstream signaling events or the evaluation of the physiological consequence of LT, fluid production. Good in vivo models of ETEC-induced diarrhea are unavailable. Therefore, we attempted to develop a model for evaluating the global host response to LT using in vivo and ex vivo methods. We found that rabbit ileal loops and porcine intestinal sections were largely unresponsive to LT. In contrast, certain mouse models showed a good response to outer membrane vesicle-associated LT, but these models will require optimization.

4.2 Introduction

Enterotoxigenic *Escherichia coli* (ETEC) is an important pathogen in human health. ETEC is the leading cause of morbidity and mortality due to diarrhea in children less than five years old in developing countries. It is also the leading cause of traveler's diarrhea. ETEC induces diarrhea through the elaboration of one or a combination of two toxins, heat-labile enterotoxin (LT) and heat-stable enterotoxin (ST). Previous studies in

our lab have found that the majority of secreted LT is associated with outer membrane vesicles (OMVs), which are spherical structures that bud off the outer membrane of all Gram-negative bacteria studied to date. LT can also be found within the lumen of OMVs. We have found that compared to soluble LT, OMV-associated LT shows delayed activation kinetics in polarized T84 cells (Chutkan & Kuehn, 2011). Both soluble LT and LT^+ OMVs produce the pro-inflammatory cytokines interleukin-6 (IL-6) and tumor necrosis factor α (TNFα) in vitro, which have both been associated with diarrhea in clinical settings (Bodero & Munson, 2009; Chutkan & Kuehn, 2011). However, whether these cytokines are produced in vivo and whether there are differences in cytokine production between soluble and OMV-bound LT is unclear. In addition, whether the delay in activation kinetics has any practical consequence on the induction of diarrhea in vivo is also unknown. One of the limitations of studying LT under physiological conditions is the lack of an appropriate animal model. Indeed, this lack of an animal model has hampered the development of vaccines against ETEC (Walker et al, 2007). While experiments have been performed in human volunteers and monkeys to examine the effect of ETEC, these studies are not feasible to compare soluble LT to OMV-bound LT for a multitude of reasons (DuPont et al, 1971; Zhang et al, 2008). Therefore, we attempted to develop a model to study the physiological differences between soluble and OMV-bound LT. We considered three types of models: Ussing chambers using porcine epithelia, rabbit ligated ileal loops, and various mouse models.

Ussing chambers can be used to examine the net ion transport in whole tissue. Intestinal tissues are harvested from an animal, cleaned, and mounted in the Ussing chamber with a distinct boundary between the apical and basolateral side, allowing the toxins to be added in a manner that recapitulates the recognition of the toxin by the intestinal epithelia. The benefit of using Ussing chambers is a smaller dose of toxin can be used because the target tissue is accessible and the toxin does not have to pass through an animal first. Although the tissue cannot be maintained for an extended time before degradation occurs, responses to whole ETEC and CT have been shown to occur within an hour (Mynott et al, 1997; O'Donnell et al, 2000). In addition to providing measurements of the net ion secretion across tissue, histology can also be evaluated in Ussing chamber explants.

Rabbit ileal loops can also be used to measure fluid accumulation in response to toxins. In this procedure, the rabbit is anesthetized, and the intestine is removed from the body cavity without being surgically excised. Segments of the intestine are then ligated on either end to form small loops. Test substances can then be injected into the loops, and the intestine is replaced within the rabbit. Fluid accumulation can be measured in each individual loop. Like Ussing chambers, histology can also be determined from the experiment. Unlike Ussing chambers, the intestine remains intact and attached to nerves and underlying substructures. This allows for the evaluation of the infiltration of immune cells, such as neutrophils. The rabbit ligated ileal loop method

has been used to determine the fluid accumulation in response to LT, CT and ETEC (Triadafilopoulos et al, 1989). Using this method, the maximal level of fluid accumulation is seen 18 h after inoculation (Sack, 1975). One advantage to this method is that up to 20 loops can be obtained from a single animal, reducing animal-to-animal variation. However, rabbit ileal loops are expensive and time-consuming to monitor. In addition, current guidelines for rabbit ileal loops limit the time that rabbits can be maintained in this condition to 8 h, which is before the maximal induction of fluid accumulation.

Mice are not naturally sensitive to ETEC. A mouse model has successfully been used to investigate the colonization of ETEC and the role that various virulence factors play in adherence to the intestine (Allen et al, 2006). However, even in this model, no diarrhea is observed. An infant mouse model has been used to evaluate diarrheal pathogenicity; however, the endpoint of this model is death and may not be useful for discriminating differences (Bertin, 1985; Duchet-Suchaux, 1988). In addition, this model has been shown to be ineffective in response to human ETEC strains, which may be due to the lack of certain colonization factors (Duchet-Suchaux et al, 1990). Because soluble LT and OMV-bound LT would not be administered with the whole bug, it is likely that this model would not be responsive to these LT presentations.

Because of the lack of available options in studying LT, we sought to develop a model to determine whether differences that were observed between soluble and OMV-

bound LT in vitro were recapitulated in vivo and, if these differences were recapitulated, what the physiological consequence was. We found that explant and ex vivo methods were not useful in eliciting a response to soluble LT. We also found that a mouse model might be a promising method, but the biggest limitation that we found was the amount of LT, and therefore OMVs, needed to elicit a response.

4.3 Results

Porcine epithelia in Ussing chambers do not show a significant increase in Cl- secretion in response to LT or CT. All Ussing chamber experiments were performed in collaboration with Dr. Jody Gookin and North Carolina State University. A week-old pig was euthanized, and equal sections of porcine intestinal epithelia were harvested and mounted in Ussing chambers. Different concentrations of LT and CT or PBS were added to duplicate mucosal chambers, and measurements were taken every ten minutes for four hours. As shown in Figure 26, the transepithelial permeability was consistent between the paired treatments and either increased or remained the same throughout the experiment, which suggests that the mucosal/serosal barrier was not leaky.

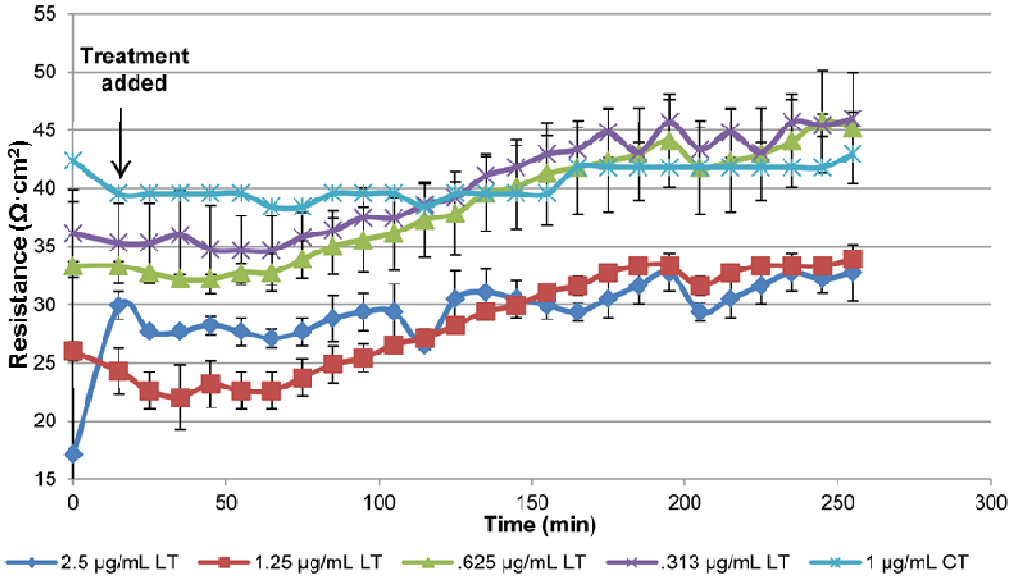

Figure 26: The transepithelial resistance between paired treatments was consistent throughout the experiment.

The intestine of a pig was excised, cleaned and mounted in Ussing chambers. Different concentrations of LT and 1 µg CT were added to duplicate explants after baseline measurements were obtained, and the potential difference was recorded every 10 min for at least 4 h. The resistance across the membranes was calculated to determine the intestinal permeability.

However, when the net ion secretion was calculated, no increase in Cl- secretion was observed for any of the LT treatment conditions (Figure 27). Secretion in response to CT trended upwards, but this increase was not significant compared to the baseline. The lack of secretion may be due to low levels of toxin. However, even at these levels of LT, the amount of OMVs needed would be technically unfeasible to prepare. Therefore, if higher concentrations of LT are necessary to see a response, then it would be very difficult to compare equal levels of soluble LT and OMV-bound LT. These results

suggest that this system is not appropriate for measuring differences in soluble and OMV-bound LT.

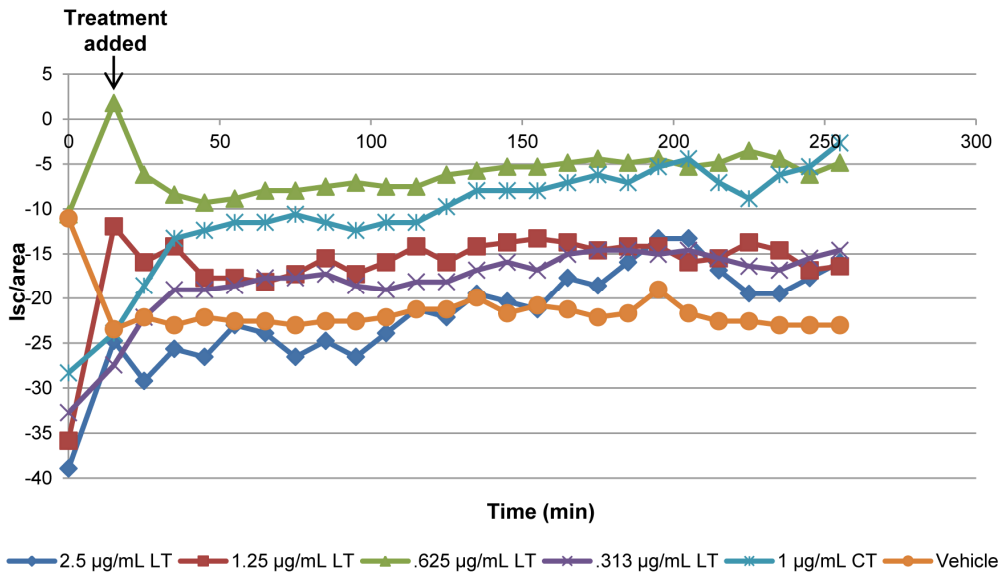

Figure 27: No Cl- secretion was observed in response to LT or CT.

Experiments were performed as in Figure 26, and the short circuit current was measured to determine the net Cl^- secretion.

Rabbit ileal loops are not an effective system for studying the response to soluble and OMV-bound LT. All rabbit experiments were performed in collaboration with Dr. Francisco Uzal at the University of California Davis. OMV samples that were standardized to 1 µg LT were injected into two loops of each of two rabbits for 8 h, and the gut density of each loop was measured. As shown in Figure 28, there was no difference in the gut density of the loops under any of the treatment conditions. In addition, the histological changes in response to the treatments were evaluated in each of the loops. Although there was a small amount of edema present in each loop, there

was no difference in the degree of edema produced in response to the treatments (data not shown). These results suggest that under these conditions, the rabbit ligated loop model is not effective in comparing the physiological response to soluble versus OMV-bound LT.

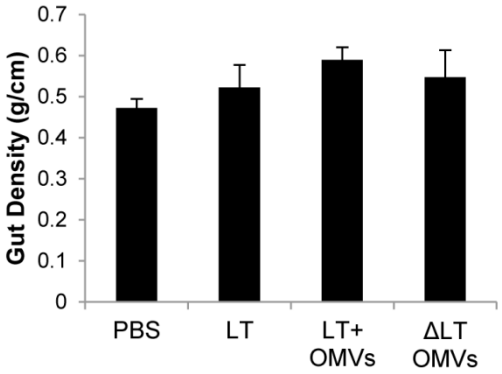

Figure 28: Rabbit ileal loops showed no difference in gut density after treatment with soluble and OMV-bound LT.

The intestines of two anesthetized rabbits were divided into 14 loops, and samples standardized to 1 μg LT or PBS were injected directly into duplicate loops of each rabbit. The intestines were then replaced within the rabbit, which maintained under anesthesia. The rabbit was sacrificed 8 h later, and the fluid accumulation within each loop was determined.

Mouse models show promising results in determining the difference in the physiological response to soluble and OMV-bound LT. All mouse experiments were conducted in collaboration with Dr. Herman Staats at Duke University. In initial experiments, groups of five mice were intragastrically administered with different concentrations of LT^+ OMVs and 10 μg LT. Because of the high concentration of LT used, OMVs were acquired from a strain that produced a large amount of OMVs. However,

we were not able to quantify the amount of LT associated with OMVs. Therefore, the samples were not standardized to soluble LT. In the initial trial of this experiment, none of the OMV treatments led to fluid accumulation, but LT led to a significant increase (Figure 29A). We attempted to increase the sensitivity of this experiment by pretreating the mice with the antibiotics streptomycin and kanamycin 20 h before inoculation to clear the intestinal flora. However, when the mice were treated with 1.25 mg LT^+ OMVs and 10 μg LT, the soluble LT showed no significant increase in fluid accumulation compared to PBS, whereas the OMVs showed a significant increase (Figure 29B). Although this model showed high variability and unreliability in determining the response to different presentations of LT, it showed that mice could respond to both soluble LT and LT^+ OMVs. Therefore, we attempted to refine this model.

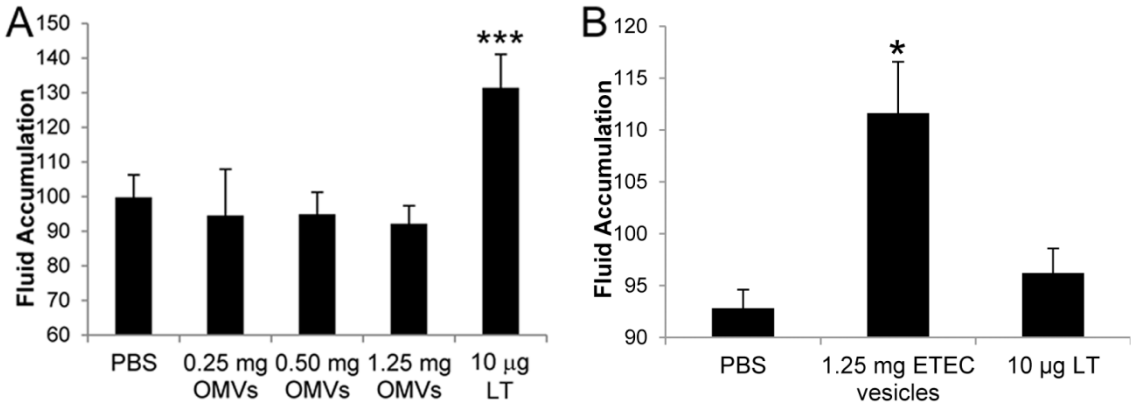

Figure 29: Fluid accumulation showed contradictory results from trial to trial.

(A) Mice were divided into groups of five mice each, and each group was intragastrically inoculated with PBS, different concentrations of LT^+ OMVs, or 10 μg LT. After 6 h, the mice were sacrificed, and the fluid accumulation was determined. **(B)** Mice were divided into groups of five mice each and allowed access to water containing streptomycin and kanamycin for 20 h before gastric inoculation with PBS,

Figure 29 (continued). 1.25 mg LT+ OMVs, or 10 μg LT. Mice were sacrificed after 6 h, and the fluid accumulation was determined.

To refine the mouse model, we intraperitoneally injected the mice with paregoric containing morphine and alcohol 2 h before inoculation. Paregoric reduces peristalsis, which may allow the toxin to remain in the intestine for longer. Experiments were performed in groups of five mice for each condition indicated, except for the 6 h treatment with 1.25 mg OMVs and PBS. This treatment was repeated once for a total of 10 mice, and Figure 30 shows the pooled results for this treatment. As shown in Figure 30A, all OMV treatments showed a significant increase in fluid accumulation compared to the PBS treatment at both 6 h and 10, although there was no significant different in gut density among treatments (Figure 30B).

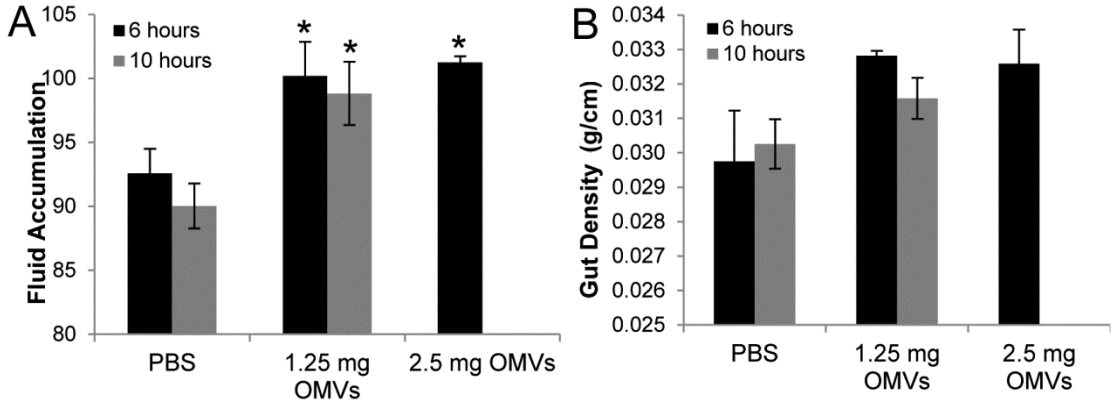

Figure 30: Paregoric and antibiotic pre-treatment led to a significant increase in fluid accumulation in response to LT+ OMVs.

Mice were divided into groups of five mice each, and each group was allowed access to water containing streptomycin and kanamycin 20 h before intragastric inoculation. At 2 h before inoculation, mice were intraperitoneally injected with paregoric containing morphine and alcohol. Mice were then inoculated with PBS, 1.25 mg LT+ OMVs,

Figure 30 (continued). or 2.5 mg LT+ OMVs. After 6 or 10 h as indicated, mice were sacrificed, and the **(A)** fluid accumulation and **(B)** gut density for each group were calculated.

We also attempted to increase the sensitivity of the model by administering the samples in sodium bicarbonate to increase the intestinal pH of the mice, providing an environment more similar to human intestinal pH. As shown in Figure 31A, the gut density of the mice was not significantly different between the treatments, but Figure 31B shows a significant decrease in fluid accumulation compared to the PBS control. However, this result is skewed by the level of fluid accumulation induced by PBS, which was much higher than the average fluid accumulation in mice treated with PBS and no sodium bicarbonate. This result demonstrates one of the greatest drawbacks to using mouse models of diarrhea, which is the high mouse-to-mouse variability.

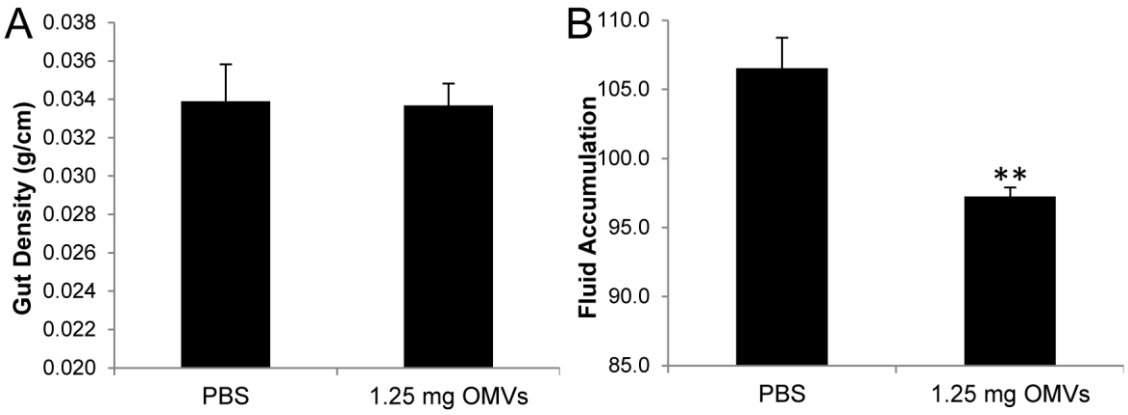

Figure 31: Sodium bicarbonate resulted in decreased fluid accumulation compared to PBS.

Mice were treated as in Figure 30 except that samples were administered in 10% sodium bicarbonate. After 6 h, the mice were sacrificed, and the **(A)** gut density and **(B)** fluid accumulation were determined for each group.

We then evaluated the cytokine production in mice fed PBS or 1.25 mg OMVs for 6 h as shown in Figure 29B. Blood was collected by cheek bleed before the addition of the toxin or OMV and again after 6 h. Lumenal fluid was also collected to determine the cytokine profile. IL-12 (p70), TNFα, IL-5, IL-4, IL-6 and IFNγ were measured in each sample using a multiplex ELISA system. Most cytokines showed no difference in induction in LT or OMV samples compared to PBS. However, as shown in Figure 32, both IL-5 and IL-6 showed a difference in expression. Although the level of IL-5 produced in LT-treated mice was similar to the amount produced by OMV-treated mice, only LT showed a significant increase after treatment compared to the pre-treated sera of the same mice (Figure 32A). Consistent with the results of fluid accumulation and gut density, there was substantial variation among the groups of mice at the baseline. IL-5 was not induced in the lumenal fluid. In contrast, interestingly, although IL-6 was produced in response to both OMVs and LT, only LT induced IL-6 in the lumenal fluid (Figure 32B). We were unable to collect lumenal fluid from mice before the treatment, so there is no baseline with which to compare. However, neither PBS- nor OMV-treated mice showed any IL-6 in the lumenal fluid. In addition, PBS-treated mice showed no IL-6 production in any of the samples tested. Our results suggest that IL-6 is an important cytokine produced in response to both OMV and LT and that it may be more important for soluble LT in the gut.

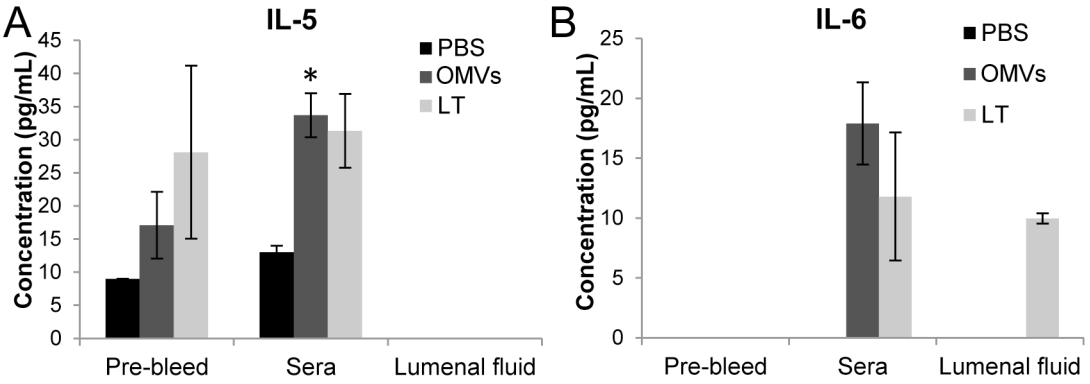

Figure 32: LT+ OMVs showed a difference in cytokine induction in a mouse model compared with soluble LT.

Mice were treated as in Figure 29B. Blood was collected before inoculation and both blood and lumenal fluid were collected after 6 h of treatment. Cytokine profiles were measured in the blood and lumenal fluid using a multiplex ELISA, and the results for **(A)** IL-5 and **(B)** IL-6 are shown.

4.4 Discussion

Studying the physiological effects of ETEC and the development of a vaccine has been hampered by the lack of an animal model for ETEC-induced diarrhea. Previous results showed that soluble LT and OMV-associated LT showed delayed kinetics in activation in polarized intestinal epithelial cells and suggested that LT delivery via OMVs might be a post-translational method of LT regulation. However, whether these kinetics are recapitulated in vivo are unknown.

Although we attempted to recapitulate the intestinal epithelium that LT would interact with during infection, the intestinal epithelium is too complex to be modeled in mono-culture. The role of TNFα and IL-6, which are produced to varying degrees in response to soluble LT and LT+ OMVs, in the intestine are unknown. In addition to the

tight barrier of intestinal epithelial cells, dendritic cells lay just below the surface of these cells and can extend their dendrites through the tight barrier to sample the contents of the intestinal lumen (Artis, 2008) (Figure 3). In addition, M cells are interspersed throughout the epithelium in Peyer's patches (Artis, 2008). These cells can also sample the lumen and deliver antigens to dendritic cells through transcytosis (Artis, 2008).

An appropriate animal model would be useful to determine the physiological responses to different contexts of LT presentation. Therefore, we attempted to develop a model that was sensitive enough to show differences in the reaction to soluble versus OMV-bound LT. We investigated Ussing chambers using porcine epithelia, rabbit ligated loops, and mouse model variations in this work and did not find a suitable model with which to study LT.

Porcine epithelia in Ussing chambers showed no response to even the highest concentration of LT, and at 4 h, the tissue had started to break down. Rabbit ileal loops showed no fluid accumulation in any of the conditions tested, which was not unexpected because the maximal level of fluid accumulation is usually observed at 18 h, and due to ethical guidelines, rabbits cannot be maintained under anesthesia for longer than 8 h.

Mice are not naturally susceptible to ETEC, and we attempted several different conditions to produce fluid accumulation. Although we showed that mice could accumulate fluid in response to soluble and OMV-bound LT, these results were

inconsistent between trials. A major disadvantage to using mice is the variability between animals. The fluid accumulation in PBS-treated mice varied widely from trial to trial, which made comparisons difficult.

Although disadvantages were present for each model, the primary problem is the concentration of LT required to elicit a reaction. Soluble LT is easy to purify; therefore, acquiring enough LT is not an issue. However, OMVs are difficult to purify in large quantities for certain bacteria, especially ΔLT OMVs. It is technically unfeasible to purify OMVs with a high enough LT content to match soluble LT, and even harder to then match these LT+ OMVs with ΔLT OMVs. In the mouse models, we purified LT^+ OMVs from a high-producing strain, but we were unable to quantify the LT concentration (see Appendix A). Therefore, when OMVs were added, they were not standardized to the amount of soluble LT, which is a limitation in trying to discriminate differences in the context of LT presentation.

We obtained interesting results using the mouse model. We demonstrated that LT^+ OMVs could induce fluid accumulation in vivo. We also found that IL-5 and IL-6 were produced in the sera of treated mice at similar levels in response to both soluble LT and LT^+ OMVs, whereas in the lumenal fluid, only soluble LT produced IL-6. Interestingly, in these mice, LT+ OMVs led a significant increase in fluid accumulation and soluble LT showed no significant difference from PBS-treated mice. These results

show that IL-6 is an important cytokine in vivo as well as in vitro, but the role of IL-6 in diarrhea is still unknown.

IL-5 is produced by Th2 cells, mast cells, eosinophils, natural killer cells, and natural killer T cells (Kouro & Takatsu, 2009). IL-5 enhances the terminal differentiation of activated B cells and the maturation of eosinophils, which may lead to inflammation (Kouro & Takatsu, 2009). The role of IL-5 in LT-induced diarrhea is difficult to determine because ETEC is not an inflammatory disease (Daniels, 2006). In addition, the IL-5 results are difficult to interpret because of the variation in the pre-bleed sample of mice that were given soluble LT. Further studies should determine the eosinophil status within the intestines of mice treated with soluble and vesicle-bound LT.

A new model of diarrhea has been developed since these studies were performed in adult Wistar rats (Bisson et al, 2010). In this model of traveler's diarrhea, adult rats are fed ETEC to induce diarrhea, fever, and weight loss, hallmarks of diarrheal illness. Future studies to determine the physiological consequence of OMV-mediated delivery of LT should investigate this possibly valuable model.

4.5 Acknowledgments

We would like to thank Dr. Jody Gookin at North Carolina State University for technical assistance in performed porcine Ussing chamber experiments, Dr. Francisco Uzal at the University of California Davis for performing rabbit ligated loop

experiments, and Dr. Herman Staats at Duke University for performing all of the mouse experiments.

5. Concluding remarks

5.1 Vesicles as delivery systems

Outer membrane vesicles are naturally produced by bacteria under a variety of conditions. In addition to their roles in communication with other bacteria, the transfer or resistance elements to other bacteria, and as a stress response system, vesicles can also interact with eukaryotic cells. An increasing amount of studies has shown the delivery of virulence factors, including LPS and toxins, to human cells, including epithelial cells and immune cells. Indeed, in some cases, vesicles may be necessary for toxin activity. Vesicles have been shown to facilitate the oligomerized state of ClyA, leading to its activity in HeLa cells. Our lab has previously shown that ETEC delivers LT in the form of vesicles, both on the surface and inside the lumen of the vesicles.

The work of this thesis shows that LT can induce significantly different immune responses when it is associated with vesicles compared to its soluble form (Figure 33). Although both vesicle-associated LT and soluble LT showed similar levels of cytokine production, vesicle-associated LT showed no LT activity, as determined by measuring CREB phosphorylation and CRE activity. At a later time, vesicle-associated LT showed significantly higher levels of cytokine production than soluble LT, which was mediated by LT activity. In addition to this delayed activation kinetics, as shown in our model in Figure 33, vesicles also induced immune responses through different signaling pathways than soluble LT, which is likely due to the vesicle component.

Vesicles were also found to traffic differently than soluble LT, leading to the ability to signal without ER trafficking. Much of our data on colocalization with cellular components is based on fluorescence microscopy. In this context, it is important to differentiate between a vesicle as an intact entity and vesicle components, which could still show a fluorescent signal within a cell independent of the vesicle. Techniques to determine the trafficking and potential processing of vesicles would be invaluable in further elucidating whether ETEC vesicles remain intact within cells.

Surprisingly, not all LT is equal. The results in this thesis show that LT associated with internalized vesicles is not active unless it is associated with both a scaffolding motif, lipid rafts, and a signaling motif, G_{M1}. As shown in Figure 33, this result means that even though LT is present within a cell, it may not be active. LT within the lumen of the vesicle and LT bound to the surface of vesicle that is not in direct contact with G_{M1} would be inert within the cell.

ETEC has developed an almost perfect toxin delivery mechanism. Vesicles contain LPS, which is a potent immunostimulatory molecule. However, in intestinal epithelial cells, vesicles containing LPS alone produced only a modest response. This may be due to the unique environment in which ETEC acts: the gut. We share our gut with billions of organisms. In a symbiotic relationship, we provide them with nutrients, and they in turn release nutrients from otherwise indigestible sources for us to use and release products that contribute to our intestinal health. To allow this symbiotic

relationship to continue, our intestines have developed a tolerance to these commensals to prevent a constant and overwhelming inflammatory response. Thus, intestinal epithelial cells are usually refractory to LPS, and this was certainly the case in our model.

5.2 Vesicles as a regulatory mechanism

Based on our results, we suggest that LT delivery through vesicles is a method of limiting the amount of LT that is active within intestinal epithelial cells, effectively acting as a regulatory mechanism. Why would ETEC regulate the amount of effective LT? LT is already regulated at the transcriptional level. LT transcription is down-regulated in the presence of high cAMP levels, a negative feedback loop that ensures that cAMP is not hyper-produced. Like all organisms, the primary goal of ETEC is to be fruitful and multiply. An overwhelming diarrheal response could lead to an overwhelming immune response against ETEC or the death of the host.

Another advantage to vesicle-mediated delivery could be protection from degradation by host proteases in the lumen. Vesicles might also increase the stability of the LT holotoxin. Although LT and CT from *Vibrio cholerae* are 80% similar to each other, and both ETEC and *V. cholerae* can produce diarrheal diseases with similar severity, in many cases, *V. cholerae* patients present with longer and more severe illness. One study attempting to determine a reason for this difference found that a 10 amino acid sequence in the A subunit conferred greater stability to the CT holotoxin. Binding to LPS might

increase the stability of the toxin, allowing it to be internalized within the cell more effectively than soluble toxin.

5.3 Vesicles in a physiological context

Our results suggest that the onset of diarrhea is delayed in response to vesicle-associated LT and decreased in comparison to soluble LT overall. The role of the cytokines produced is also unclear in a physiological context. Although IL-6 has been associated with clinical manifestations of diarrhea, the direction of cause and effect has not been established. Does IL-6 recruit inflammatory cells or upregulate immune cells, such as secretory IgA or Th17 cells? In vitro systems cannot measure diarrhea directly or account for the contribution of other cell types and the downstream effects of signaling. However, the lack of an animal model has hampered investigation into ETEC, including in the area of vaccine development. ETEC diarrheal disease is one of the diseases in which human volunteers are used. Because of the ethical guidelines and expense involved in using the human or monkey model, we attempted to develop a model to study the physiological impact of vesicle-associated LT.

One major disadvantage in animal models is the amount of LT necessary to elicit a reaction, a level that is difficult to purify in association with vesicles. In addition to the difficulty in isolating large amounts of vesicles and determining the amount of associated LT, if our hypothesis that vesicles act as a regulatory mechanism is correct, the amount of vesicles needed to elicit a response might be even higher. Another

disadvantage was the amount of time needed to determine a response, which was outside of the ethically accepted timelines for experiments. However, even in a limited mouse model, we found that IL-6 was differentially induced in response to soluble and vesicle-associated LT. These preliminary results once again suggest the importance of IL-6 in diarrheal disease and warrant further investigation.

5.4 Future directions

This thesis shows the importance of studying toxins in their native context. Much remains to be elucidated about the interaction of outer membrane vesicles with host cells. Unlike vesicles from several other pathogens, ETEC vesicles have been shown to not be trafficking within acidic compartments, such as endosomes and lysosomes. However, vesicles containing LT bind to G_{M1} in lipid rafts, and the LT is still trafficked to the ER. LT is internalized after binding to G_{M1} in lipid rafts into endosomes. Our data suggest that this localization in endosomes may not be necessary for the proper trafficking of LT. Our data also show a minor role for clathrin-mediated internalization. Further studies should determine if vesicles are internalized within compartments, and if they are, these compartments should be characterized further regarding whether vesicles are processed within these compartments and how LT is trafficked.

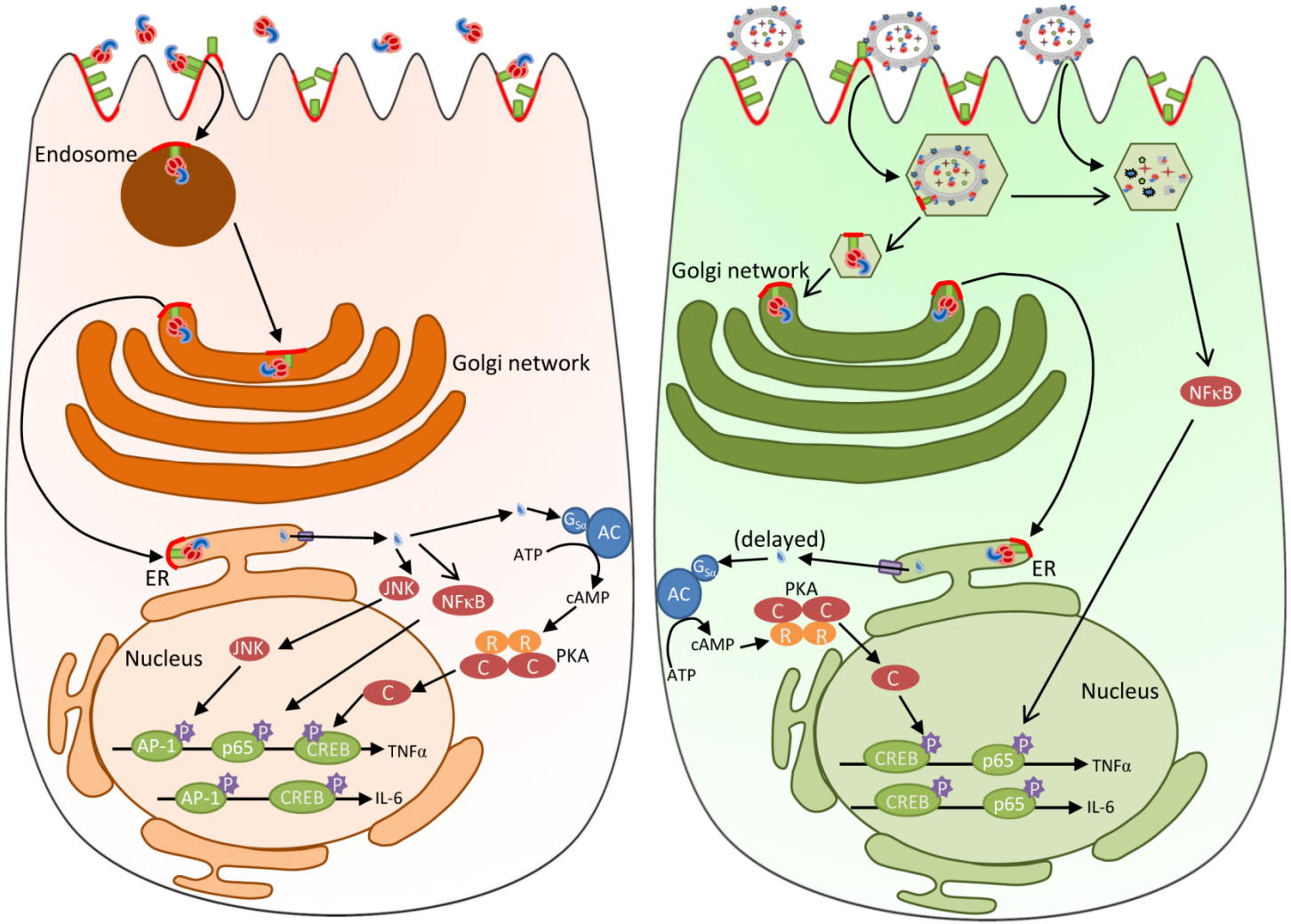

Figure 33: Overview of the trafficking and signaling pathways of soluble and OMV-bound LT.

Figure 33 (continued). The signaling and trafficking of soluble LT (left) and OMV-bound LT (right) in polarized intestinal epithelial cells is shown. Soluble LT (left) binds to GM1 (green) associated with lipid rafts (red) and is internalized within an endosome. The endosome delivers the LT-GM1 complex to the Golgi apparatus, and it is trafficked from the *trans*-Golgi network to the endoplasmic reticulum (ER). The LTA1 fragment of the LTA subunit is then translocated into the cytosol in which it ADP-ribosylates the $G_{s\alpha}$ subunit of adenylate cyclase (AC), leading to cAMP production. cAMP then interacts with the regulatory subunits (R) of protein kinase A (PKA), leading to the release of catalytic subunits (C). The catalytic subunit phosphorylated cAMP response element binding protein (CREB), leading to the induction of IL-6 and TNFα. The LTA1 fragment can also lead to the phosphorylation of c-Jun N-terminal kinase (JNK), which in turn phosphorylates activator protein 1 (AP-1), leading to the transcription of IL-6 and TNFα. Nuclear factor kappa B (NFκB) is also activated by the LTA1 fragment, leading to the transcription of TNFα. Vesicle-bound LT (right) enters the cell through binding to the host receptor G_{M1} in lipid rafts and is internalized. Clathrin-mediated internalization may occur at low levels. Once the vesicle is internalized, it is processed to release LT bound to the G_{M1}/lipid raft complex, which is trafficked similar to soluble LT, but at a later time. The LTA1 fragment also activates PKA but does not appear to activate JNK. The remaining vesicle components elicit IL-6 and TNFα through NFκB.

6. Materials and Methods

6.1 Bacterial strains and media

Bacterial strains were maintained in LB Miller broth (25 g/L) or CFA broth at 37°C with or without 100 μg/mL ampicillin (Sigma). Strains were stored at -80°C in 20% glycerol. The strains used in this study are shown in Table 2.

Table 2: Strains used in this study

Strain	*Description*	*Relevant characteristics*	*Reference*
jf570	H10407 Δ*eltA*	ETEC strain with polar insertion in *eltA* (LT deficient)	(Dorsey et al, 2006)
MK132	E9034A	ETEC strain Longus+; O8:H9; CS3; LT/ST	(Parissi-Crivelli et al, 2000)
MK171	E9034P	ETEC strain lacking the LT plasmid	(Parissi-Crivelli et al, 2000)
MK1052	H10407 Δ*eltA*/pILT	jf570 carrying inducible LT plasmid; Amp^r	(Mudrak et al, 2009)
MK1226	H10407 Δ*eltA*/pILT[S63K]	jf570 carrying inducible S63K mutant; Amp^r	This work

Table 2: Strains used in this study (continued)

Strain	*Description*	*Relevant characteristics*	*Reference*
MK1272	H10407 Δ*eltA*/pILT[G33D]	jf570 carrying inducible S63K mutant; Amp^r	This work
MK741	DH5α *degP*::Tn*5*/pDsbA/pILT	*E. coli* K12, *degP* knockout, carrying a plasmid copy of *dsbA* and an inducible LT plasmid; Kan^r Cm^r Amp^r	(Mudrak et al, 2009)
ATCC43886	ETEC2	ETEC strain isolated from diarrheic stool	(Wachsmuth et al, 1979)
MK759	ETEC2/pILT	ETEC2 carrying inducible LT plasmid; Amp^r	This work
MK1250	DH5α *degP*::Tn*5*/pDsbA/pILT[S63K]	*E. coli* K12, *degP* knockout, carrying a plasmid copy of *dsbA* and an inducible S63K plasmid; Kan^r Cm^r Amp^r	This work

6.1.1 Media

LB Miller broth

10 g/L Bacto-tryptone, 5 g/L yeast extract, 10 g/L NaCl

CFA medium

1% casamino acids, 0.15% yeast extract, 0.005% $MgSO_4$, 0.005% $MnCl_2$

6.1.2 LT mutants

LT mutants were constructed using site-directed mutagenesis using the QuikChange kit (Qiagen) according to the manufacturer's instructions. The primers used were the following: S63K sense, 5'-GACGGATATGTTTCCACTAAACTTAGTTTGAGAAGTGC-3', and S63K anti-sense, 5'-GCACTTCTCAAACTAAGTTTAGTGGAAACATATCCGTC-3'; and G33D sense, 5'-CGGAATCGATGGCAGACAAAAGAGAAATGG-3', and G33D anti-sense, 5'-CCATTTCTCTTTTGTCTGCCATCGATTCCG-3'. To induce the expression of plasmid-encoded wild-type or mutant LT, 100 μM isopropyl β-D-1-thiogalactopyranoside (IPTG) was added to cultures.

6.2 Cell culture

The human intestinal epithelial T84 cell line (American Type Culture Collection CCL-248) was maintained in a 1:1 ratio of Dulbecco's modified Eagle's medium and Ham's F12 medium (Gibco) supplemented with 10% fetal bovine serum (FBS; HyClone) and 1% penicillin–streptomycin amphotericin B (Gibco) at 37°C. Human embryonic

kidney 293T (HEK293T) cells (ATCC CRL-11268) were maintained in minimum essential medium supplemented with 10% FBS at 37°C.

6.2.1 Polarization assays

For polarization assays, 4 x 10^5 T84 cells were seeded on 1.12-cm^2 transwell inserts (Corning) and grown for 5-7 days. Tight junction formation was measured using transepithelial electrical resistance (TEER) using a Millicell-ERS (Millipore), and cells were used at TEERs ≥ 1,000 Ω·cm^2. Cells were used between passages 62-73.

6.3 Toxin purification

Toxin was prepared from DH5α *degP*::Tn5 carrying pDsbA and pILT or pILT[S63K]. Cells were diluted 1:50 from an overnight culture into CFA medium containing ampicillin and grown to an OD_{600} of approximately 1.0, at which point they were induced with 200 μM isopropyl-1-thio-β-D-galactopyranoside (IPTG; Sigma).

The next day, cells were pelleted at 10,000 g for 10 min and resuspended in 25 mL of 10 mM Tris (pH 7.5). The suspension was then sonicated twice for 90 sec each, with a 30 sec rest between sonications. Cell debris was pelleted at 9,000 g for 5 min, and the supernatant was collected. A total of 2 mL 20% immobilized D-galactose beads (Pierce) in TEN buffer (50 mM Tris, pH 7.5, 1 mM EDTA, and 200 mM NaCl) was added to the supernatant, which was incubated overnight at 4°C with rotation.

Galactose beads were then pelleted at 700 g for 3 min and washed three times with TEN. After the final wash, the beads were resuspended in 40 mL of 0.3 M galactose (Sigma) in TEN overnight at 4°C with rotation.

The beads were pelleted at 4,000 g for 5 min, and the supernatant was collected and concentrated using 10-kDa cut-off centrifuge filters (Amicon). The resulting filtrate was filter-sterilized using 0.45 μm centrifuge filters (Millipore) to remove any remaining beads, and the concentration of soluble toxin was determined using the Coomassie Plus Better Bradford Reagent (Pierce) using bovine serum albumin as a standard, according to the manufacturer's instructions. Purified toxin was assayed for purity using 10% SDS-PAGE and Ruby Red (Molecular Probes) and immunoblotting (anti-CT; Sigma). The endotoxin concentration of LT was determined using a limulus amebocyte lysate assay (Cambrex) and was found to be less than 1 EU/mL for both wild-type LT and S63K LT in the concentrations used in the assays.

6.4 Outer membrane vesicle purification and standardization

6.4.1 Vesicle purification

Outer membrane vesicles were purified from ETEC2 or strains expressing wild-type LT, LT S63K LT or no LT as described previously (Kesty & Kuehn, 2004; McBroom et al, 2006). Cells were diluted 1:50 from an overnight culture into CFA medium with (strains containing wild-type LT, G33D LT or S63K LT) or without (LT-deficient strain)

ampicillin and grown to an OD_{600} of approximately 1.0, at which point they were induced with 100 μM IPTG.

The next day, the cells were pelleted at 10,000 g for 15 min, and the supernatant was collected and concentrated to 500 mL using a 100 kDa cut-off filter using a Pall Filtration system (Cole-Parmer). The concentrated supernatant was sterile-filtered through a 0.45 μm polyvinylidene fluoride vacuum filter (Millipore) and centrifuged at 38,400 g for 3 h. The resulting pellets were resuspended in Dulbecco's phosphate buffered saline.

To remove contaminants, 1.5 mL of 60% Opti-prep solution (Sigma) was added to each 0.5 mL of vesicles. The vesicles were layered under a continuous Opti-prep gradient (40%-25%) and centrifuged at 40,600 rpm overnight at 4°C. To analyze which fractions contained purified vesicles, an aliquot of 1-mL fractions were run on a 15% SDS gel. After staining with Ruby Red, vesicle fraction were identified through the presence of OmpF/C, pooled, resuspended in DPBSS, and checked for sterility by plating a sample on an LB agar plate. The protein concentration of sterile vesicles was determined as described above.

6.4.2 LT+ vesicle standardization to soluble LT

Two-fold dilutions of LT+ vesicles and G33D vesicles starting at 1 μg were analyzed alongside two-fold dilutions of soluble LT in 4 M urea starting at 400 ng using immunoblotting. Samples were run on a 15% SDS gel, transferred to a PVDF membrane,

and blocked in TBST with milk. The blot was then incubated with the cross-reactive primary rabbit antibody anti-CT diluted 1:10,000 in TBST with milk overnight at 4°C with shaking. The blot was then incubated with a horseradish peroxidase-conjugated anti-rabbit antibody diluted 1:10,000 for 1 h and visualized using enhanced chemiluminescence (Super Signal; Pierce). The densitometry of the bands was quantified using ImageJ (NIH), and a standard curve of soluble LT was constructed. The amount of LT in LT+ vesicles was compared to the standard curve to determine the amount of LT in vesicles.

6.4.3 Lipid standardization

Two-fold dilutions of LT+ vesicles, S63K vesicles, and ΔLT vesicles were incubated with the lipophilic dye FM4-64 at 37°C for 10 min. The samples were then added in duplicate to a black 96-well plate and read using a fluorometer at an excitation of 506 nm and an emission of 750 nm. A standard curve was constructed for each vesicle sample to determine the relative amount of lipid in each sample. S63K and ΔLT vesicle concentrations were standardized to the amount of lipid in LT+ vesicles for each assay.

6.4.4 Flagellin immunoblotting

Vesicle samples were analyzed using 10% SDS-PAGE (BioRad) and transferred to a nylon membrane. The membrane was then blocked in Odyssey blocking buffer and incubated with rabbit anti-H7 (a flagellar marker originally produced by Difco, a kind gift from Dr. Patrick Seed, Duke University). The membrane was then incubated with a

fluorescently conjugated anti-mouse antibody and imaged using the Odyssey imaging system.

6.5 Pathway inhibitors

Table 3: Signaling and trafficking inhibitors

Inhibitor	*Source*	*Catalog#*	*Target*	*Concentration*
Rp-camps	Calbiochem	116814-5UMOL	PKA	100 μM
H89	Sigma	B1427	CREB	10 μM
SB203580	Calbiochem	559398-1ML	p38	10 μM
PDTC	Calbiochem	548000-100MG	NFκB	100 μM
PD98059	Calbiochem	513001-1ML	MEK1/2	10 μM
SP600125	Calbiochem	420128-5MG	JNK	10 μM
Brefeldin A	Calbiochem	203729-1MG	Golgi, ER	5 μM
Exo 1	Calbiochem	341220-25MG	cis-Golgi	100 μM
MβCD	Sigma	C4555-1G	Lipid rafts	4 mM
PAO	Sigma	P3075-1G	Clathrin	500 nM
Chlorpromazine	Sigma	C8138-5G	Clathrin	25 μM
Dynasore	Sigma	D7693-5MG	Dynamin	80 μM

6.5.1 Signaling inhibitors

Inhibitors of PKA (adenosine 3′,5′-cyclic phosphorothioate-Rp; Rp-camps), p38 (4-(4-fluorophenyl)-2-(4-methylsulfinylphenyl)-5-(4-pyridyl)1H-imidazole; SB203580), JNK (anthra[1,9-cd]pyrazol-6(2H)-one, 1,9-pyrazoloanthrone; SP600125), MEK (2′-amino-3′-methoxyflavone; PD98059) and NFκB (ammonium pyrrolidinedithiocarbamate; PDTC) were purchased from Calbiochem. The CREB inhibitor H89 (N-[2-(p-bromocinnamylamino)ethyl]-5-isoquinolinesulfonamide dihydrochloride) was purchased from Sigma-Aldrich. SB203580 (10 μM), SP600125 (10 μM), PD98059 (10 μM) and H89 (10 μM) were added bilaterally to polarized cells for 1 h, Rp-camps (100 μM) was added basolaterally for 1 h and PDTC (10 μM) was added bilaterally for 30 min before the addition of treatments.

6.5.2 Trafficking inhibitors

Inhibitors of Golgi to ER transport (1,6,7,8,9,11a,12,13,14,14a-decahydro-1,13-dihydroxy-6-methyl-4H-cyclopent[f]oxacyclotridecin-4-one; Brefeldin A) and the cis Golgi network (2-(4-fluorobenzoylamino)methylbenzoate; Exo1) were purchased from Calbiochem. Inhibitors of clathrin-mediated endocytosis (chlorpromazine and phenylsarine oxide, PAO) and dynamin (dynasore) were purchased from Sigma-Aldrich. Methyl-β-cyclodextrin was purchased from Santa Cruz Biotechnology. Brefeldin A (5 μM), Exo1 (100 μM), PAO (500 nM), chlorpromazine (25 μM), dynasore

(80 μM) and MβCD (4 mM) were added bilaterally to transwells 1 h before the addition of the samples.

6.6 Treatment conditions

The media of polarized transwell cultures were changed, and a total of 10 μL of samples standardized to either 1 nM or 200 pM LT or vehicle (PBS) were added to the apical compartment of duplicate wells of polarized T84 cells for the indicated times with or without inhibitor pre-treatment for 1 h or 30 min.

6.7 Real-time PCR

6.7.1 Extraction of total RNA and reverse transcription

Total RNA was collected using the Qiagen RNeasy kit according to the manufacturer's instructions. The RNA was reverse-transcribed into cDNA using oligo(dT) primers and SuperScript III (Invitrogen), according to the manufacturer's instructions, and the cDNA was used as the template in RT-PCR assays. As a control for possible DNA contamination, the previous step was repeated without the addition of SuperScript III. The cDNA was then cleaned up using the PCR product purification protocol supplied with the Qiagen mini-prep kit (Qiagen) and resuspended in 50 μL of elution buffer.

6.7.2 Real-time PCR

RT-PCR was performed in a total volume of 15 μL using iQ SYBR Green (Bio-Rad) and analyzed using an iCycler Real Time Detection System (Bio-Rad). Gene-

specific primers were designed using PrimerQuest (IDT). The gene-specific primers used for RT-PCR analysis are shown in Table 4. The thermocycling conditions were an initial denaturation at 95°C for 3 min followed by 40 cycles of 95°C for 1 min and 63.2°C for 30 sec. Melt curve analysis was used to confirm the specificity of the primers. Results were analyzed using the accompanying software, and gene expression was standardized to GAPDH levels. Results are shown as the fold induction of the gene in relation to the corresponding mock treatments and were measured using the $2^{-\Delta\Delta Ct}$ method.

Table 4: RT-PCR primers used in this study

Gene	*F*	*R*
IL-6	GACAGCCACTCACCTCTT	TGTTTTCTGCCAGTGCC
TNFα	CCCAGGCAGTCAGATCAT	TCAGCTCCACGCCATT
IL-1β	AGCTTGGTGATGTCTGGT	GACATGGAGAACACCACTTG
TSLP1	AGGCTATTCGGAAACTCAGA	GTGACACTTGTTCCAGACA
TGFβ	TGCTCGCCCTGTACAA	GTCATAGATTTCGTTGTGGGT
IL-8	CCATCTCACTGTGTGTAAACA	GCAAAACTGCACCTTCAC
IL-10	CAACCTGCCTAACATGCT	GCAACCCAGGTAACCCTTAA
IL-12 (p40)	GGGAACTGAAGAAAGATGTTTATG	TCCAAGGTCCAGGTGATAC
TGFβ	GGAAACCCACAACGAAATCT	GGAGCTCTGATGTGTTGAAG
GAPDH	ACATCGCTCAGACACCAT	GGGTCATTGATGGCAACA

Table 4: RT-PCR primers used in this study (continued)

Gene	*F*	*R*
APRIL	CTATAGCGCAGGTGTCTTC	GCCACTTTTTATAACACAATCACAG
RANTES	CTCCCACAGGTACCATGAA	GGCAATGTAGGCAAAGCA
HBD1	GCCATGAGAACTTCCTACCTTC	CAGAATAGAGACATTGCCCTCC
LL-37	TGTGCTTCGTGCTATAGATGG	GCACACTGTCTCCTTCACTG
NOS2	TCAGTATCACAACCTCAGCAAG	TTGATCCTCACATGCCGTG

6.8 Nuclear extraction

Nuclear protein extractions were performed as described previously (Schreiber et al, 1989), with some modifications. Briefly, 300 μL buffer A (10 mM HEPES, pH 8, 1.5 mM $MgCl_2$, 10 mM KCl and 0.5 mM dithiothreitol (DTT)) supplemented with 0.4% Igepal was directly added to cells in the transwell insert and incubated on ice for 15 min. Cells were then scraped with a pipet tip, collected, vortexed for 15 s, and centrifuged at 8,000 g for 2 min at 4°C. The supernatant was discarded, and the nuclear pellet was washed with buffer A. The nuclear pellet was then resuspended in 25 μL buffer B (20 mM HEPES, pH 7.9, 1.5 mM $MgCl_2$, 0.42 M NaCl, 0.2 mM EDTA, 25% glycerol, 0.5 mM

DTT and protease and phosphatase inhibitor cocktails (Sigma-Aldrich)) and incubated at 4°C for 2 h with shaking.

6.9 Immunoblotting of nuclear extracts

Nuclear extracts were desalted using a desalting column (Thermo Scientific) and analyzed using 10% SDS-PAGE (Bio-Rad). The proteins were then transferred to nitrocellulose membrane (Licor) at a constant voltage of 110 V for 2 h at 4°C. The blots were incubated in Licor blocking solution for 1 h and primary antibodies for 1 h. The following primary antibodies were used: mouse anti-TATA-binding protein (TBP) (Abcam), mouse anti-phosphorylated CREB (Millipore). Blots were first incubated with anti-TBP, visualized using a fluorescently conjugated anti-mouse IgG antibody using Odyssey imaging system. The blot was then stripped using Re-blot Plus stripping solution (Millipore) according to the manufacturer's instructions and re-incubated with anti-pCREB. The densitometry of the bands was analyzed using the accompanying Odyssey software. The densitometry of the TBP and pCREB bands was calculated using the accompanying Odyssey software. Results are presented as the ratio of pCREB/TBP normalized to a mock value of 1 for each blot.

6.10 Electrophoretic mobility shift assay

EMSAs to evaluated AP-1 activation were performed using the Promega Gel Shift Assay System according to the manufacturer's instructions. Nuclear extracts prepared as described previously were incubated with an equal volume of buffer C (20

mM HEPES, pH 7.9, 50 mM KCl, 0.2 mM EDTA, 0.5 mM DTT, protease inhibitor cocktail and phosphatase inhibitor cocktail), and the protein concentration was measured using the Bradford method. A total of 5 μg of nuclear protein were used in the EMSA, and the reaction products were run on a 4% native gel at 300 V at 4°C. The gel was then wrapped in saran wrap, exposed to a phospho screen, visualized using a STORM 860 system (Molecular Dynamics) and analyzed using ImageQuant 5.2 software (Molecular Dynamics).

6.11 Enzyme-linked immunosorbent assays

Polarized cells were treated as described, and both apical and basolateral supernatants were collected. A total of 100 μL of these supernatants were analyzed using IL-6 and TNFα ELISAs (BD) according to the manufacturer's instructions.

6.12 Luciferase assay

A total of 1 x 10^4 HEK293T cells were seeded into each well of a 96-well plate 16 h before transfection. Cells were then transfected with the pCRE-Luc plasmid (Stratagene) containing CRE fused to a firefly luciferase reporter gene and the pSV40-RL plasmid (Promega) containing a *Renilla* luciferase reporter fused to a constitutive promoter using Lipofectamine 2000 (Invitrogen). For a complete 96-well plate, 10 ng pCRE-Luc and 5 ng pSV40-RL were incubated in 500 μL MEM, and 20 μL Lipofectamine 2000 were incubated in another 500 μL MEM. These samples were mixed and incubated at room temperate for 15 min. A total of 5 mL MEM with 10% FBS was added to the mixture, and

the medium in the plate was replaced with 50 μL of the DNA mixture. Samples were added approximately 16 h post-transfection for the indicated time, and firefly luciferase and *Renilla* luciferase activities were determined using the Dual-Glo Luciferase Assay (Promega), according to the manufacturer's instructions. The results are presented as the ratio of firefly luciferase activity to *Renilla* luciferase activity.

6.13 Microscopy

6.13.1 Fluorescent labeling of vesicles

OMVs were fluorescently labeled with Alexa Fluor 555 as described previously (Ellis et al, 2010). The protein concentration of labeled OMVs was determined using the Bradford assay using bovine serum albumin (BSA) as a standard, and 1 μg of each OMV preparation was used in microscopy experiments.

6.13.2 Internalization and co-localization experiments

Polarized T84 cells were grown on clear polyethylene permeable inserts (Corning), and microscopy experiments were performed as described previously (Ivanov et al, 2004). For internalization assays, 1 μg of Alexa Fluor 555-labeled OMVs were added to the apical compartment of transwells for 4 h. The monolayers were then washed with PBS, fixed with 4% paraformaldehyde, permeabilized using 0.5% Triton X-100, and blocked in PBS containing 1% BSA (blocking buffer). Alexa Fluor 488-conjugated phalloidin (Invitrogen) was added to cells in blocking buffer to label F-actin. The membrane was then excised from transwells and mounted on glass slides using

ProLong Gold antifade with DAPI (Invitrogen). Z-stacks of 72 μm x 72 μm fields were acquired using a Leica SP5 confocal microscope (Leica) at 0.3-μm steps. Images were analyzed using Imaris software (Bitplane). Extended slices of xz and xz sections are shown in each figure.

For co-localization assays, polarized T84s were cooled to 4°C for 1 h, and 1 μg of labeled OMVs was added to the apical compartment at 4°C for 2 h. Cell monolayers were then washed and fixed in 4% paraformaldehyde in PBS for 10 min and permeabilized in 0.1% Triton X-100 in PBS for 5 min. Cells were then blocked in blocking buffer for 1 h and incubated with anti-GM1 (Abcam; 1:10), anti-EEA1 (Abcam), anti-M6PR (Abcam) or anti-LAMP1 (DSHB) in blocking buffer for 1 h. The LAMP-1 monoclonal antibody developed by J.T. August and J.E.K. Hildreth was obtained from the Developmental Studies Hybridoma Bank developed under the auspices of the NICHD and maintained by The University of Iowa, Department of Biology, Iowa City, IA 52242. The monolayers were washed in blocking buffer and incubated with the appropriate fluorescently conjugated secondary antibody (Invitrogen) for 1 h. Filters were washed in blocking buffer, excised, and mounted on glass slides in ProLong gold antifade with DAPI. Images were acquired using a Leica SP5 confocal microscope.

6.14 Isolation of detergent-resistant membranes

Lipid rafts were isolated essentially as described previously (Wolf et al, 2002), with some modifications. T84 cells were grown to confluence in 75 cm^2 tissue culture

flasks and incubated with 150 μg the indicated OMVs for 1 h. The cells were then washed with ice-cold PBS twice and scraped into PBS. Cells were centrifuged at 250 x g for 10 min, and the cell pellet was resuspended in TNE buffer (25 mM Tris-HCl, pH 7.5, 150 mM NaCl, 1 mM EDTA and protease and phosphatase inhibitor cocktails (1:100; Sigma)) containing 1% Triton X-100 and rotated at 4°C for 30 min. The cells were then passed through a 22 g needle 20 times, and lysates were collected after centrifugation at 1,000 g for 10 min. This process was repeated, and the post-nuclear supernatant fractions were pooled and mixed with an equal volume of 80% sucrose in TNE. The solution of 80% sucrose was heated to dissolve the sucrose. Sucrose solutions should be made freshly to minimize the risk of contamination. The mixture was layered under a step-wise gradient of 30% sucrose and 5% sucrose in TNE and centrifuged at 205,000 g for 18 h at 4°C. Gradients were fractionated into 1 mL fractions, and the total protein was precipitated using 5% trichloroacetic acid and acetone. The fractions were then analyzed using western blotting.

6.15 Animal models

6.15.1 Pig Ussing chamber studies

All pig studies were performed in collaboration with Dr. Jody Gookin at North Carolina State University essentially as described previously (Gookin et al, 2002). The ileal mucosa from a young pig was harvested, rinsed and stripped from the seromuscular layer in Ringers solution (142 mM Na^+, 5 mM K^+, 1.25 mM Ca^{2+}, 1.1 mM

Mg^{2+}, 124 mM Cl^-, 25 mM HCO^{3-}, 1.65 mM HPO_4^{2-}, and 0.3 mM $H_2PO_4^-$). The mucosa was then mounted on 1.12 cm^2 Ussing chambers in Ringers solution containing 10 mM glucose on the serosal side and 10 mM mannitol on the mucosal side at 37°C. Indomethacin (5 μM) was added to the chambers to inhibit prostaglandin production. Baseline measurements were obtained to determine ion transport and tissue permeability, and then 10 μM amiloride was added to block Na^+ entry and .1 μM tetrodotoxin was added to eliminate the activity of nerves attached to the mucosa. Various concentrations of LT and 1 μg/mL CT was added to the apical side, and the spontaneous potential difference and short-circuit current (Isc) was measured every ten minutes for four hours.

6.15.2 Rabbit ligated ileal loops

All rabbit studies were performed in collaboration with Dr. Francisco Uzal at the University of California Davis. Experiments were performed essentially as described previously (Sayeed et al, 2008). Briefly, two young adult rabbits were anesthetized, and the small intestine was exposed. Intestinal segments of approximately 2 cm were ligated on either end avoiding the occlusion of the blood supply, and toxin and OMVs standardized to 1 μg LT were directly injected into duplicate loops of each rabbit. The intestine was then replaced within the rabbits, which were kept under anesthesia for the remainder of the experiment. After 8 h, the rabbits were euthanized, and the fluid accumulation within each loop was determined.

6.15.3 Mouse studies

All mouse experiments were performed in collaboration with Dr. Herman Staats at Duke University. Mice were divided into groups of five mice each. Mice were intragastrically inoculated with different concentrations of ETEC LT^+ OMVs (.25 mg, .5 mg, 1.25 mg or 2.5 mg) or 10 μg LT with or without pretreatment with antibiotics and paregorics singly or in combination. When mice were pretreated with antibiotics, at 20 h before inoculation, food was removed, and mice were allowed access to water with 5 g/L streptomycin and 2.5 g/L kanamycin. To prevent fecal contamination, the mice were transferred to clean cages. When mice were pretreated with paregoric, they were intraperitoneally injected with 0.04 mg morphine in 250 μL 2 h before inoculation. In one set of experiments, 1.25 mg LT+ OMVs were administered in 200 μL 10% sodium bicarbonate in PBS.

Mice were inoculated for 6 and 10 h as indicated and then euthanized. The gastrointestinal tract was removed and weighed, and the fluid accumulation and gut density were calculated as follows:

$$\text{Fluid accumulation} = (G/(B-G))*1000 \qquad (1)$$

$$\text{Gut density} = G/L \qquad (2),$$

where G is the gut weight and fluid weight in grams, B is the body weight in grams, and L is the length of the gut in cm.

For cytokine experiments, mice pretreated with antibiotics were intragastrically inoculated with PBS, 1.25 mg LT+ OMVs, or 10 μg LT. At the time of inoculation, blood was collected by cheek bleed. After 6 h, the mice were euthanized, and blood and lumenal fluid was collected. The levels of IL-12 (p70), IL-4, IL-5, IL-6, IFNγ and TNFα were determined using a multiplex ELISA (BioRad).

6.16 Glycosidase treatment

Vesicles (3.8 μg) isolated from ETEC2, E9034P and E9034A were treated with PNGase F and O-glycosidase (New England Biolabs) according to the manufacturer's instructions. Samples that had been treated with glycosidase or not were analyzed using immunoblotting using a cross-reactive poly-clonal CT antibody. RNase B was used as a positive control, and a band shift was observed after glycosylation.

6.17 Y1 assay

The Y1 assay was performed as described previously (Horstman & Kuehn, 2000). A total of 4 x 10^5 Y1 adrenal cells were seeded in each well of a 24-well plate in Kaighn's media (Gibco). At 2-4 h later, vesicles or soluble LT were added to duplicate wells overnight, and the rounding of the cells was determined on a scale of 1 to 4 based on the percentage of rounding as follows: 0-25%, 1; 26-50%, 2; 51-75%, 3; and 76-100%, 4. When indicated, the LT and vesicle samples were pre-incubated with 10 ng/μL G_{M1}.

6.18 Statistical analysis

Multiple comparisons among treatments in cell culture were performed using a one-way analysis of variance (ANOVA) followed by Tukey's test. Comparisons between treated and untreated samples were performed using Student's *t*-test. For mouse experiments, multiple comparisons were performed using the non-parametric Kruskal-Wallis test followed by Dunn's multiple comparisons test. Comparisons between two conditions in mouse experiments were performed using the Mann Whitney test. All statistical analyses were performed using GraphPad InStat (GraphPad Software, Inc.). Results are presented as means ± SEM, and all experiments were performed in triplicate.

Appendix A

ETEC2 produces a toxic modified non-glycosylated protein that cross-reacts with heat-labile enterotoxin

Summary

ETEC2 is a strain of ETEC that was originally isolated from human diarrheal stool. This strain produces large amounts of OMVs and is therefore a good candidate for performing animal experiments. To standardize the amount of LT in these OMVs, we analyzed two-fold dilutions of soluble LT alongside ETEC2 OMVs to create a standard curve based on densitometry values. As described in the Materials and Methods, the bands were immunoblotted with a cross-reactive polyclonal anti-CT antibody. Figure 34 shows that the band that cross-reacted with the antibody in ETEC2 vesicles migrated more slowly than soluble LTB at 20 kDa and was quicker than soluble LTA.

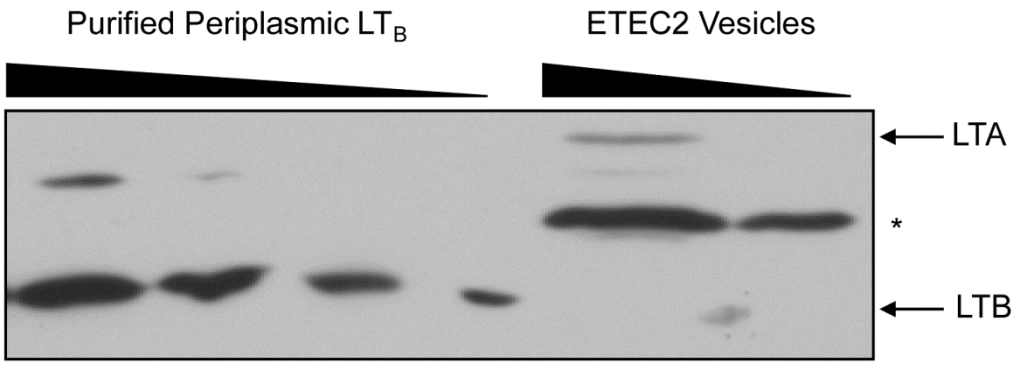

Figure 34: LT in ETEC2 vesicles show a different mobility compared to soluble LT.

Figure 34 (continued). Purified soluble LT was run in two-fold dilutions alongside two-fold dilutions of ETEC2 vesicles and immunoblotted with a cross-reactive polyclonal anti-CT antibody.

To determine whether this band was an aggregate, we treated our vesicles with 4 M urea. As shown in Figure 35A, urea treatment did not have an effect on the size of the cross-reactive band. The band was specific to the ETEC2 strain, and it was not present in E9034P, an ETEC strain that has been cured of the LT plasmid, or E9034A, which still contains the LT plasmid.

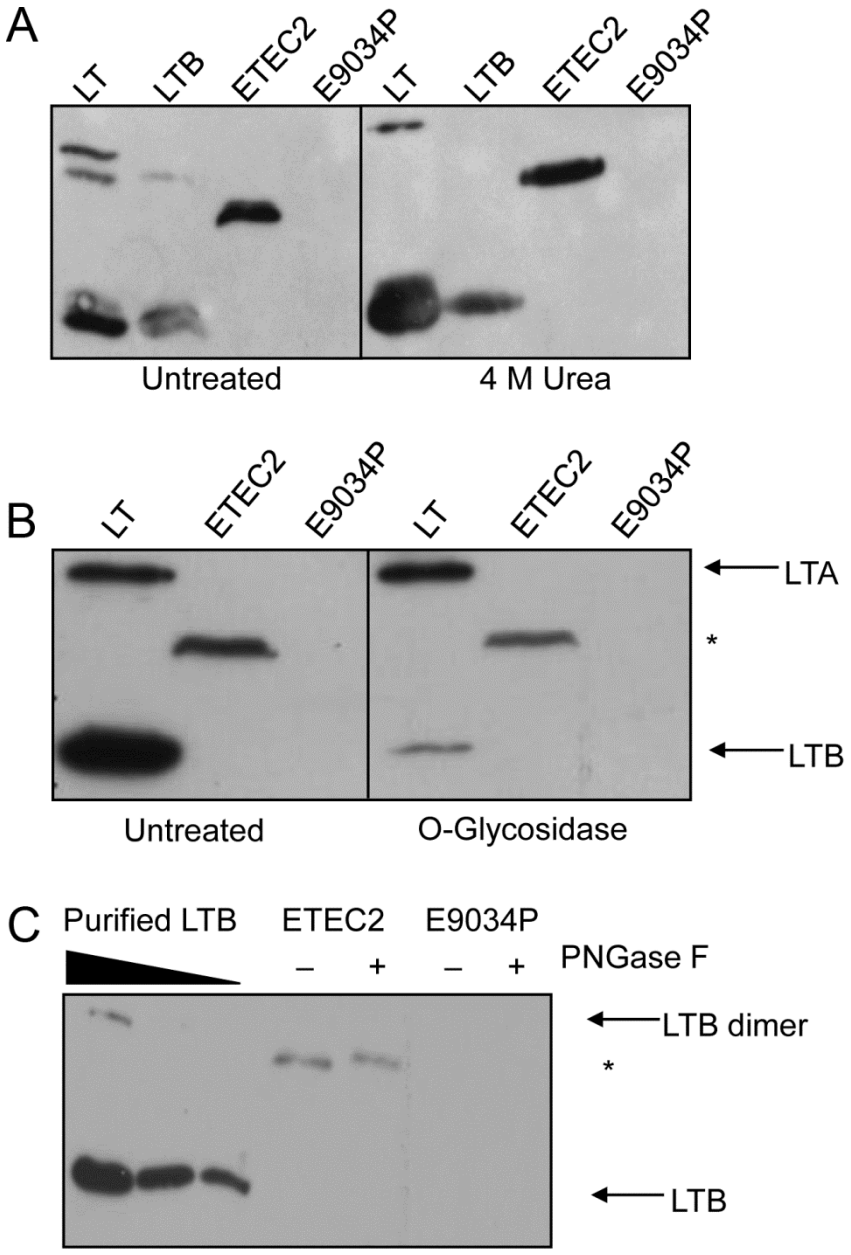

Figure 35: The slowly migrating band is not an aggregate or glycosylated.

(A) Purified LT and LTB, ETEC2 vesicles, and E9034P vesicles were incubated in 4 M urea and analyzed by immunoblotting. **(B-C)** Soluble LT, ETEC2 vesicles and E9034P vesicles were treated with **(B)** O-glycosidase and **(C)** PNGase F and analyzed using immunoblotting.

We then investigated whether the band was glycosylated. We treated ETEC2 vesicles with O-glycosidase to remove O-linked glycosylation (Figure 35B) and PNGase F to remove N-linked glycosylation (Figure 35C). Neither O-glycosidase nor PNGase F led to a difference in the size of the cross-reactive band.

In addition to the slower migrating band, no band that corresponded to the correct size of LT was observed in ETEC2. To determine whether ETEC2 could produce LT at the correct size, we transfected it with an inducible plasmid containing the sequence of canonical LT (pILT). As shown in Figure 36A, vesicles purified from ETEC2/pILT contained LT that ran at the correct size as well as the slowly migrating band. The vesicles were run alongside vesicles from strain H10407, which contains LT on a plasmid.

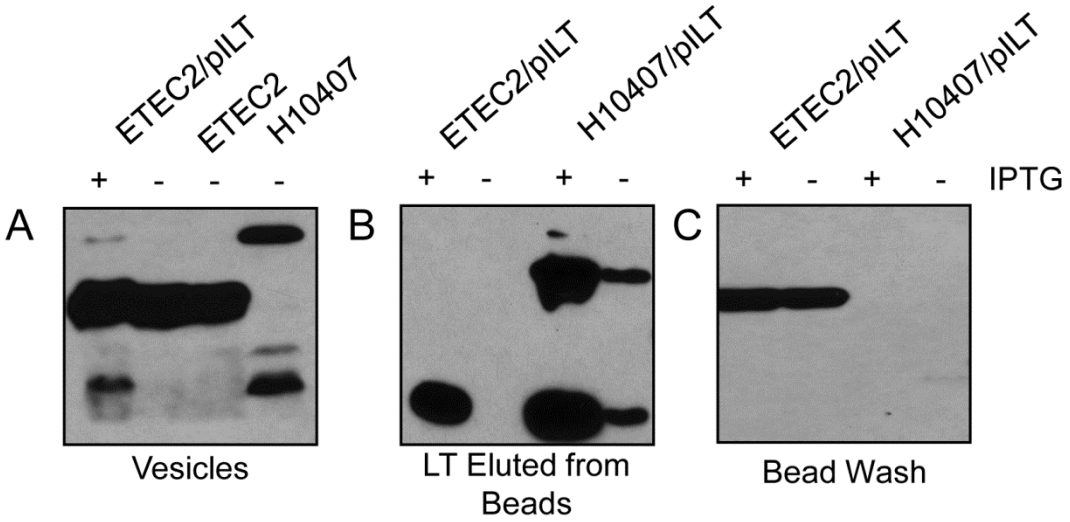

Figure 36: The vesicle-associated modified protein does not bind to galactose.

Figure 36 (continued). (A) Vesicles from strains induced with IPTG or not were immunoblotted for the presence of LT. **(B-C)** Cells were grown with or without IPTG overnight, and cells were then centrifuged, resuspended in TEN, and sonicated. The lysate was then incubated with galactose beads overnight and washed, and LT was eluted in 0.3 M galactose in TEN. The presence of LT was determined in the **(B)** eluate and **(C)** wash fractions using immunoblotting.

To determine if this modified band could bind to galactose, we purified soluble toxin from each of these strains as described in the Materials and Methods. As shown in Figure 36B, the slowly migrating band was not eluted from the beads under any of the conditions tested. Canonical LT was eluted from beads from induced ETEC2/pILT strains but not from any of the other ETEC2 strains, which suggests that LT is not produced in these strains. Figure 36C shows that the slowly migrating band remained in the wash from the ETEC2 strains, which showed that it was still produced.

We then examined the toxicity of ETEC2 strains in vitro using a Y1 adrenal cell assay. Previous results in our lab showed that vesicles containing LT led to the rounding of Y1 cells that was inhibited by pre-incubation with G_{M1} (Horstman & Kuehn, 2000). As shown in Figure 37, maximum rounding was observed in Y1 cells incubated with toxin purified from both H10407 and ETEC2 expressing pILT, and this rounding was inhibited by co-incubation of the purified toxins with G_{M1}. Similarly, when Y1 cells were incubated with vesicles from ETEC2, maximal rounding was observed regardless of the presence of the plasmid. However, this rounding was still higher than DPBSS when the vesicles were pre-incubated with G_{M1}.

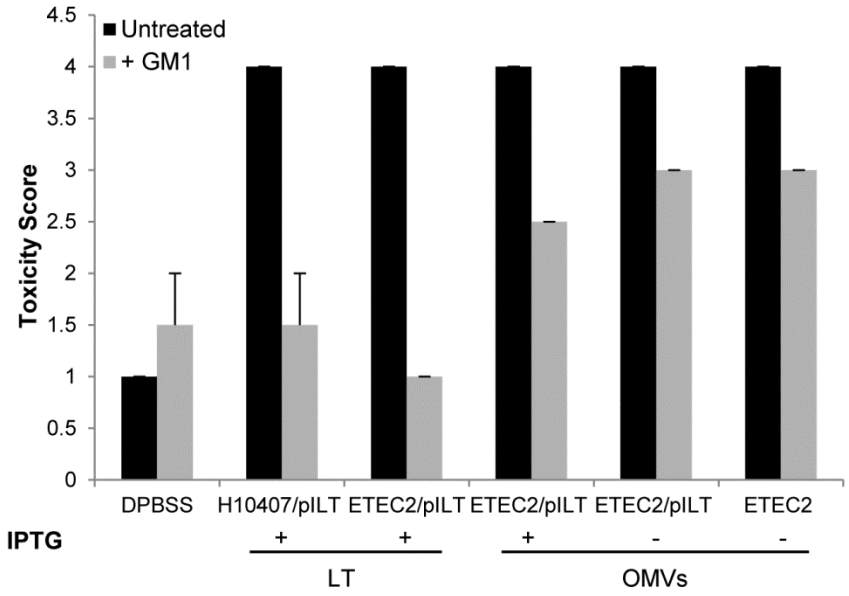

Figure 37: ETEC2 is toxic to Y1 adrenal cells.

Y1 adrenal cells incubated with purified LT or vesicles from H10407/pILT, ETEC2/pILT and ETEC2 that were pre-incubated with G_{M1} (grey bars) or not (black bars) were scored on a scale of 1-4 to determine the toxicity of the treatments.

These results suggest that the ETEC2 strain, a human diarrheal stool isolate, produces a protein that cross-reacts with the polyclonal CT antibody, does not bind galactose, and is still toxic in vitro. In studies in mice, ETEC2 vesicles, which did not show any bands corresponding to soluble LT, produced fluid accumulation (Chapter 4). Because of the difference in the size of the band, the amount of LT in these OMVs could not be determined and therefore could not be standardized to show differences between the same amount of soluble LT and vesicle-associated LT. If vesicles from this strain are to be used in mouse models, further investigations into the identity of this protein should be performed.

References

Abreu MT, Vora P, Faure E, Thomas LS, Arnold ET, Arditi M (2001) Decreased expression of Toll-like receptor-4 and MD-2 correlates with intestinal epithelial cell protection against dysregulated proinflammatory gene expression in response to bacterial lipopolysaccharide. *J Immunol* **167:** 1609-1616

Allen KP, Randolph MM, Fleckenstein JM (2006) Importance of Heat-Labile Enterotoxin in Colonization of the Adult Mouse Small Intestine by Human Enterotoxigenic Escherichia coli Strains. *Infect Immun* **74:** 869-875

Artis D (2008) Epithelial-cell recognition of commensal bacteria and maintenance of immune homeostasis in the gut. *Nat Rev Immunol* **8:** 411-420

Asensio CJA, Gaillard ME, Moreno G, Bottero D, Zurita E, Rumbo M, van der Ley P, van der Ark A, Hozbor D (2011) Outer membrane vesicles obtained from Bordetella pertussis Tohama expressing the lipid A deacylase PagL as a novel acellular vaccine candidate. *Vaccine* **29:** 1649-1656

Badizadegan K, Dickinson BL, Wheeler HE, Blumberg RS, Holmes RK, Lencer WI (2000) Heterogeneity of detergent-insoluble membranes from human intestine containing caveolin-1 and ganglioside GM1. *American Journal of Physiology - Gastrointestinal and Liver Physiology* **278:** G895-G904

Balsalobre C, Silvan JM, Berglund S, Mizunoe Y, Uhlin BE, Wai SN (2006) Release of the type I secreted α-haemolysin via outer membrane vesicles from Escherichia coli. *Molecular Microbiology* **59:** 99-112

Bauman SJ, Kuehn MJ (2009) Pseudomonas aeruginosa vesicles associate with and are internalized by human lung epithelial cells. *BMC Microbiol* **9:** 26

Beatty WL, Meresse S, Gounon P, Davoust J, Mounier J, Sansonetti PJ, Gorvel J-P (1999) Trafficking of Shigella Lipopolysaccharide in Polarized Intestinal Epithelial Cells. *J Cell Biol* **145:** 689-698

Begum YA, Talukder KA, Nair GB, Qadri F, Sack RB, Svennerholm A-M (2005) Enterotoxigenic Escherichia coli Isolated from Surface Water in Urban and Rural Areas of Bangladesh. *J Clin Microbiol* **43:** 3582-3583

Berberov EM, Zhou Y, Francis DH, Scott MA, Kachman SD, Moxley RA (2004) Relative Importance of Heat-Labile Enterotoxin in the Causation of Severe Diarrheal Disease in the

Gnotobiotic Piglet Model by a Strain of Enterotoxigenic Escherichia coli That Produces Multiple Enterotoxins. *Infect Immun* **72:** 3914-3924

Bertin A (1985) F41 Antigen as a Virulence Factor in the Infant Mouse Model of Escherichia coli Diarrhoea. *Journal of General Microbiology* **131:** 3037-3045

Binder HJ (2010) Role of colonic short-chain fatty acid transport in diarrhea. *Annual review of physiology* **72:** 297-313

Bishop DG, Work E (1965) An extracellular glycolipid produced by Escherichia coli grown under lysine-limiting conditions. *The Biochemical journal* **96:** 567-576

Bisson J-F, Hidalgo S, Rozan P, Messaoudi M (2010) Preventive Effects of Different Probiotic Formulations on Travelers' Diarrhea Model in Wistar Rats. *Digestive Diseases and Sciences* **55:** 911-919

Black R (1990) Epidemiology of travelers' diarrhea and relative importance of various pathogens. *Reviews of Infectious Diseases* **12:** S73-79

Bodero MD, Munson GP (2009) Cyclic AMP Receptor Protein-Dependent Repression of Heat-Labile Enterotoxin. *Infection and Immunity* **77:** 791-798

Bomberger JM, Maceachran DP, Coutermarsh BA, Ye S, O'Toole GA, Stanton BA (2009) Long-distance delivery of bacterial virulence factors by Pseudomonas aeruginosa outer membrane vesicles. *PLoS Pathog* **5:** e1000382

Bowman CC, Clements JD (2001) Differential Biological and Adjuvant Activities of Cholera Toxin and Escherichia coli Heat-Labile Enterotoxin Hybrids. *Infect Immun* **69:** 1528-1535

Bray J (1945) Isolation of antigenically homogeneous strains of Bact. coli neapolitanum from summer diarrhœa of infants. *The Journal of Pathology and Bacteriology* **57:** 239-247

Brown KH (2003) Diarrhea and Malnutrition. *The Journal of Nutrition* **133:** 328S-332S

Cario E, Podolsky DK (2000) Differential Alteration in Intestinal Epithelial Cell Expression of Toll-Like Receptor 3 (TLR3) and TLR4 in Inflammatory Bowel Disease. *Infection and Immunity* **68:** 7010-7017

Chakraborty S, Deokule JS, Garg P, Bhattacharya SK, Nandy RK, Nair GB, Yamasaki S, Takeda Y, Ramamurthy T (2001) Concomitant Infection of Enterotoxigenic Escherichia coli in an Outbreak of Cholera Caused by Vibrio cholerae O1 and O139 in Ahmedabad, India. *J Clin Microbiol* **39:** 3241-3246

Chen DJ, Osterrieder N, Metzger SM, Buckles E, Doody AM, DeLisa MP, Putnam D (2010) Delivery of foreign antigens by engineered outer membrane vesicle vaccines. *Proc Natl Acad Sci U S A* **107:** 3099-3104

Chen ML, Ge Z, Fox JG, Schauer DB (2006) Disruption of tight junctions and induction of proinflammatory cytokine responses in colonic epithelial cells by Campylobacter jejuni. *Infect Immun* **74:** 6581-6589

Cheng E, Cardenas L, Clements JD (2000) The role of cAMP in mucosal adjuvanticity of Escherichia coli heat-labile enterotoxin (LT). *Vaccine* **18:** 38-49

Chutkan H, Kuehn MJ (2011) Context-Dependent Activation Kinetics Elicited by Soluble versus Outer Membrane Vesicle-Associated Heat-Labile Enterotoxin. *Infect Immun* **79:** 3760-3769

Ciofu O, Beveridge TJ, Kadurugamuwa J, Walther-Rasmussen J, Høiby N (2000) Chromosomal β-lactamase is packaged into membrane vesicles and secreted from Pseudomonas aeruginosa. *Journal of Antimicrobial Chemotherapy* **45:** 9-13

Croxen MA, Finlay BB (2010) Molecular mechanisms of Escherichia coli pathogenicity. *Nat Rev Micro* **8:** 26-38

Dallas WS, Falkow S (1980) Amino acid sequence homology between cholera toxin and Escherichia coli heat-labile toxin. *Nature* **288:** 499-501

Dallas WS, Gill DM, Falkow S (1979) Cistrons encoding Escherichia coli heat-labile toxin. *Journal of Bacteriology* **139:** 850-858

Daniels NA (2006) Enterotoxigenic Escherichia coli: Traveler's Diarrhea Comes Home. *Clinical Infectious Diseases* **42:** 335-336

Dann SM, Spehlmann ME, Hammond DC, Iimura M, Hase K, Choi LJ, Hanson E, Eckmann L (2008) IL-6-Dependent Mucosal Protection Prevents Establishment of a Microbial Niche for Attaching/Effacing Lesion-Forming Enteric Bacterial Pathogens. *The Journal of Immunology* **180:** 6816-6826

De Haan L, Hirst TR (2004) Cholera toxin: a paradigm for multi-functional engagement of cellular mechanisms (Review). *Mol Membr Biol* **21:** 77-92

de Silva DG, Mendis LN, Sheron N, Alexander GJ, Candy DC, Chart H, Rowe B (1993) Concentrations of interleukin 6 and tumour necrosis factor in serum and stools of children with Shigella dysenteriae 1 infection. *Gut* **34:** 194-198

De SN, Bhattacharya K, Sarkar JK (1956) A study of the pathogenicity of strains of bacterium coli from acute and chronic enteritis. *The Journal of Pathology and Bacteriology* **71:** 201-209

Dendorfer U, Oettgen P, Libermann TA (1994) Multiple regulatory elements in the interleukin-6 gene mediate induction by prostaglandins, cyclic AMP, and lipopolysaccharide. *Mol Cell Biol* **14:** 4443-4454

Dorsey FC, Fischer JF, Fleckenstein JM (2006) Directed delivery of heat-labile enterotoxin by enterotoxigenic Escherichia coli. *Cellular Microbiology* **8:** 1516-1527

Duchet-Suchaux M (1988) Protective antigens against enterotoxigenic Escherichia coli O101:K99,F41 in the infant mouse diarrhea model. *Infection and Immunity* **56:** 1364-1370

Duchet-Suchaux M, Bertin A, Le Maitre C (1990) Differences in susceptibility of inbred and outbred infant mice to enterotoxigenic Escherichia coli of bovine, porcine and human origin. *Journal of Medical Microbiology* **31:** 185-190

DuPont HL, Evans DG, Evans Jr DJ, Satterwhite TK (1981) Antitoxic immunity in cholera and enterotoxigenic escherichia coli (ETEC) diarrhea. *Pharmacology & Therapeutics* **13:** 249-255

DuPont HL, Formal SB, Hornick RB, Snyder MJ, Libonati JP, Sheahan DG, LaBrec EH, Kalas JP (1971) Pathogenesis of Escherichia coli Diarrhea. *New England Journal of Medicine* **285:** 1-9

Ellis TN, Kuehn MJ (2010) Virulence and immunomodulatory roles of bacterial outer membrane vesicles. *Microbiol Mol Biol Rev* **74:** 81-94

Ellis TN, Leiman SA, Kuehn MJ (2010) Naturally Produced Outer Membrane Vesicles from Pseudomonas aeruginosa Elicit a Potent Innate Immune Response via Combined Sensing of Both Lipopolysaccharide and Protein Components. *Infect Immun* **78:** 3822-3831

Feng Y, Jadhav AP, Rodighiero C, Fujinaga Y, Kirchhausen T, Lencer WI (2004) Retrograde transport of cholera toxin from the plasma membrane to the endoplasmic reticulum requires the trans-Golgi network but not the Golgi apparatus in Exo2-treated cells. *EMBO Rep* **5:** 596-601

Fiocca R, Necchi V, Sommi P, Ricci V, Telford J, Cover TL, Solcia E (1999) Release of Helicobacter pylori vacuolating cytotoxin by both a specific secretion pathway and budding of outer membrane vesicles. Uptake of released toxin and vesicles by gastric epithelium. *The Journal of Pathology* **188:** 220-226

Fishman PH (1980) Mechanism of action of cholera toxin: Studies on the lag period. *Journal of Membrane Biology* **54:** 61-72

Fleckenstein JM, Hardwidge PR, Munson GP, Rasko DA, Sommerfelt H, Steinsland H (2010) Molecular mechanisms of enterotoxigenic Escherichia coli infection. *Microbes and Infection* **12:** 89-98

Flores J, DuPont HL, Lee SA, Belkind-Gerson J, Paredes M, Mohamed JA, Armitige LY, Guo D-C, Okhuysen PC (2008) Influence of Host Interleukin-10 Polymorphisms on Development of Traveler's Diarrhea Due to Heat-Labile Enterotoxin-Producing Escherichia coli in Travelers from the United States Who Are Visiting Mexico. *Clin Vaccine Immunol* **15:** 1194-1198

Fujinaga Y, Wolf AA, Rodighiero C, Wheeler H, Tsai B, Allen L, Jobling MG, Rapoport T, Holmes RK, Lencer WI (2003) Gangliosides That Associate with Lipid Rafts Mediate Transport of Cholera and Related Toxins from the Plasma Membrane to Endoplasmic Reticulm. *Mol Biol Cell* **14:** 4783-4793

Fukuta S, Magnani JL, Twiddy EM, Holmes RK, Ginsburg V (1988) Comparison of the carbohydrate-binding specificities of cholera toxin and Escherichia coli heat-labile enterotoxins LTh-I, LT-IIa, and LT-IIb. *Infection and Immunity* **56:** 1748-1753

Furuta N, Tsuda K, Omori H, Yoshimori T, Yoshimura F, Amano A (2009) Porphyromonas gingivalis Outer Membrane Vesicles Enter Human Epithelial Cells via an Endocytic Pathway and Are Sorted to Lysosomal Compartments. *Infect Immun* **77:** 4187-4196

Galka F, Wai SN, Kusch H, Engelmann S, Hecker M, Schmeck B, Hippenstiel S, Uhlin BE, Steinert M (2008) Proteomic Characterization of the Whole Secretome of Legionella pneumophila and Functional Analysis of Outer Membrane Vesicles. *Infect Immun* **76:** 1825-1836

Gewirtz AT, Navas TA, Lyons S, Godowski PJ, Madara JL (2001) Cutting edge: bacterial flagellin activates basolaterally expressed TLR5 to induce epithelial proinflammatory gene expression. *J Immunol* **167:** 1882-1885

Gill DM, Richardson SH (1980) Adenosine Diphosphate-Ribosylation of Adenylate Cyclase Catalyzed by Heat-Labile Enterotoxin of Escherichia coli: Comparison with Cholera Toxin. *Journal of Infectious Diseases* **141:** 64-70

Gookin JL, Rhoads JM, Argenzio RA (2002) Inducible nitric oxide synthase mediates early epithelial repair of porcine ileum. *Am J Physiol Gastrointest Liver Physiol* **283:** G157-168

Greenberg DE, Jiang Z-D, Steffen R, Verenker MP, DuPont HL (2002) Markers of Inflammation in Bacterial Diarrhea among Travelers, with a Focus on Enteroaggregative Escherichia coli Pathogenicity. *The Journal of Infectious Diseases* **185:** 944-949

Gribar SC, Anand RJ, Sodhi CP, Hackam DJ (2008) The role of epithelial Toll-like receptor signaling in the pathogenesis of intestinal inflammation. *Journal of Leukocyte Biology* **83:** 493-498

Guerrant DI, Moore SR, Lima AA, Patrick PD, Schorling JB, Guerrant RL (1999) Association of early childhood diarrhea and cryptosporidiosis with impaired physical fitness and cognitive function four-seven years later in a poor urban community in northeast Brazil. *Am J Trop Med Hyg* **61:** 707-713

Guerrant RL, Kosek M, Moore S, Lorntz B, Brantley R, Lima AAM (2002) Magnitude and Impact of Diarrheal Diseases. *Archives of Medical Research* **33:** 351-355

Guidry J, Cardenas L, Cheng E, Clements J (1997) Role of receptor binding in toxicity, immunogenicity, and adjuvanticity of Escherichia coli heat-labile enterotoxin. *Infect Immun* **65:** 4943-4950

Hajishengallis G, Wang M, Liang S, Triantafilou M, Triantafilou K (2008) Pathogen induction of CXCR4/TLR2 cross-talk impairs host defense function. *Proceedings of the National Academy of Sciences* **105:** 13532-13537

Hellman J, Loiselle PM, Zanzot EM, Allaire JE, Tehan MM, Boyle LA, Kurnick JT, Warren HS (2000) Release of gram-negative outer-membrane proteins into human serum and septic rat blood and their interactions with immunoglobulin in antiserum to Escherichia coli J5. *J Infect Dis* **181:** 1034-1043

Hirst TR, Randall LL, Hardy SJ (1984a) Cellular location of heat-labile enterotoxin in Escherichia coli. *J Bacteriol* **157:** 637-642

Hirst TR, Sanchez J, Kaper JB, Hardy SJ, Holmgren J (1984b) Mechanism of toxin secretion by Vibrio cholerae investigated in strains harboring plasmids that encode heat-labile enterotoxins of Escherichia coli. *Proceedings of the National Academy of Sciences* **81:** 7752-7756

Hofstra H, Witholt B (1984) Kinetics of synthesis, processing, and membrane transport of heat-labile enterotoxin, a periplasmic protein in Escherichia coli. *The Journal of biological chemistry* **259:** 15182-15187

Hofstra H, Witholt B (1985) Heat-labile enterotoxin in Escherichia coli. Kinetics of association of subunits into periplasmic holotoxin. *The Journal of biological chemistry* **260:** 16037-16044

Hokari R, Lee H, Crawley SC, Yang SC, Gum JR, Jr, Miura S, Kim YS (2005) Vasoactive intestinal peptide upregulates MUC2 intestinal mucin via CREB/ATF1. *Am J Physiol Gastrointest Liver Physiol* **289:** G949-959

Holm MM, Vanlerberg SL, Foley IM, Sledjeski DD, Lafontaine ER (2004) The Moraxella catarrhalis Porin-Like Outer Membrane Protein CD Is an Adhesin for Human Lung Cells. *Infect Immun* **72:** 1906-1913

Holmgren J, Lindblad M, Fredman P, Svennerholm L, Myrvold H (1985) Comparison of receptors for cholera and Escherichia coli enterotoxins in human intestine. *Gastroenterology* **89:** 27-35

Holmgren J, Svennerholm A-M (1998) Vaccines against diarrheal disease. In *Handbook of Experimental Pharmacology*, Perlmann P, Wigzell H (eds), Vol. 133, pp 291-328. Berlin: Springer

Holmner Å, Askarieh G, Ökvist M, Krengel U (2007) Blood Group Antigen Recognition by Escherichia coli Heat-labile Enterotoxin. *Journal of Molecular Biology* **371:** 754-764

Horstman AL, Bauman SJ, Kuehn MJ (2004) Lipopolysaccharide 3-deoxy-D-manno-octulosonic acid (Kdo) core determines bacterial association of secreted toxins. *J Biol Chem* **279:** 8070-8075

Horstman AL, Kuehn MJ (2000) Enterotoxigenic Escherichia coli secretes active heat-labile enterotoxin via outer membrane vesicles. *J Biol Chem* **275:** 12489-12496

Horstman AL, Kuehn MJ (2002) Bacterial surface association of heat-labile enterotoxin through lipopolysaccharide after secretion via the general secretory pathway. *J Biol Chem* **277:** 32538-32545

Ismail S, Hampton MB, Keenan JI (2003) Helicobacter pylori Outer Membrane Vesicles Modulate Proliferation and Interleukin-8 Production by Gastric Epithelial Cells. *Infect Immun* **71:** 5670-5675

Ivanov AI, Nusrat A, Parkos CA (2004) Endocytosis of Epithelial Apical Junctional Proteins by a Clathrin-mediated Pathway into a Unique Storage Compartment. *Mol Biol Cell* **15:** 176-188

Jacks TM, Wu BJ, Braemer AC, Bidlack DE (1973) Properties of the Enterotoxic Component in Escherichia coli Enteropathogenic for Swine. *Infect Immun* **7:** 178-189

Jarchum I, Pamer EG (2011) Regulation of innate and adaptive immunity by the commensal microbiota. *Current Opinion in Immunology* **23:** 353-360

Jiang B, Snipes-Magaldi L, Dennehy P, Keyserling H, Holman RC, Bresee J, Gentsch J, Glass RI (2003) Cytokines as Mediators for or Effectors against Rotavirus Disease in Children. *Clinical and Diagnostic Laboratory Immunology* **10:** 995-1001

Jin JS, Kwon SO, Moon DC, Gurung M, Lee JH, Kim SI, Lee JC (2011) Acinetobacter baumannii Secretes Cytotoxic Outer Membrane Protein A via Outer Membrane Vesicles. *PLoS One* **6:** e17027

Johnson AM, Kaushik RS, Francis DH, Fleckenstein JM, Hardwidge PR (2009) Heat-Labile Enterotoxin Promotes Escherichia coli Adherence to Intestinal Epithelial Cells. *J Bacteriol* **191:** 178-186

Jones F, Hall E, Tribble D, Savarino S, Cassels FJ, Porter C, Meza R, Nunez G, Espinoza N, Salazar M, Luckett R, Scott D (2006) The New World primate, Aotus nancymae, as a model for examining the immunogenicity of a prototype enterotoxigenic Escherichia coli subunit vaccine. *Vaccine* **24:** 3786-3792

Kadurugamuwa JL, Beveridge TJ (1996) Bacteriolytic effect of membrane vesicles from Pseudomonas aeruginosa on other bacteria including pathogens: conceptually new antibiotics. *J Bacteriol* **178:** 2767-2774

Kadurugamuwa JL, Beveridge TJ (1998) Delivery of the Non-Membrane-Permeative Antibiotic Gentamicin into Mammalian Cells by Using Shigella flexneri Membrane Vesicles. *Antimicrob Agents Chemother* **42:** 1476-1483

Kadurugamuwa JL, Beveridge TJ (1999) Membrane vesicles derived from Pseudomonas aeruginosa and Shigella flexneri can be integrated into the surfaces of other Gram-negative bacteria. *Microbiology* **145:** 2051-2060

Kaksonen M, Toret CP, Drubin DG (2006) Harnessing actin dynamics for clathrin-mediated endocytosis. *Nat Rev Mol Cell Biol* **7:** 404-414

Kaper JB, Nataro JP, Mobley HLT (2004) Pathogenic Escherichia coli. *Nat Rev Micro* **2:** 123-140

Kato S, Kowashi Y, Demuth DR (2002) Outer membrane-like vesicles secreted by Actinobacillus actinomycetemcomitans are enriched in leukotoxin. *Microbial Pathogenesis* **32:** 1-13

Kesty NC, Kuehn MJ (2004) Incorporation of heterologous outer membrane and periplasmic proteins into Escherichia coli outer membrane vesicles. *J Biol Chem* **279:** 2069-2076

Kesty NC, Mason KM, Reedy M, Miller SE, Kuehn MJ (2004) Enterotoxigenic Escherichia coli vesicles target toxin delivery into mammalian cells. *EMBO J* **23:** 4538-4549

Koeberling O, Welsch JA, Granoff DM (2006) Improved immunogenicity of a H44/76 group B outer membrane vesicle vaccine with over-expressed genome-derived Neisserial antigen 1870. *Vaccine* **In Press, Corrected Proof**

Kohler K, Zahraoui A (2005) Tight junction: a co-ordinator of cell signalling and membrane trafficking. *Biol Cell* **97:** 659-665

Kolling GL, Matthews KR (1999) Export of Virulence Genes and Shiga Toxin by Membrane Vesicles of Escherichia coli O157:H7. *Appl Environ Microbiol* **65:** 1843-1848

Kondo A, Koshihara Y, Togari A (2001) Signal Transduction System for Interleukin-6 Synthesis Stimulated by Lipopolysaccharide in Human Osteoblasts. *Journal of Interferon & Cytokine Research* **21:** 943-950

Kouro T, Takatsu K (2009) IL-5- and eosinophil-mediated inflammation: from discovery to therapy. *International Immunology* **21:** 1303-1309

Kuehn MJ, Kesty NC (2005) Bacterial outer membrane vesicles and the host-pathogen interaction. *Genes Dev* **19:** 2645-2655

Kulp A, Kuehn MJ (2010) Biological functions and biogenesis of secreted bacterial outer membrane vesicles. *Annu Rev Microbiol* **64:** 163-184

Kunkel SL, Robertson DC (1979) Factors affecting release of heat-labile enterotoxin by enterotoxigenic Escherichia coli. *Infect Immun* **23:** 652-659

Lajoie P, Nabi IR (2010) Chapter 3 - Lipid Rafts, Caveolae, and Their Endocytosis. In *International Review of Cell and Molecular Biology*, Kwang WJ (ed), Vol. Volume 282, pp 135-163. Academic Press

Lariviere S, Gyles CL, Barnum DA (1973) Preliminary characterization of the heat-labile enterotoxin of Escherichia coli F11(P155). *The Journal of Infectious Diseases* **128:** 312-320

Lee TH, Linstedt AD (2000) Potential Role for Protein Kinases in Regulation of Bidirectional Endoplasmic Reticulum-to-Golgi Transport Revealed by Protein Kinase Inhibitor H89. *Mol Biol Cell* **11:** 2577-2590

Lieb K, Schaller H, Bauer J, Berger M, Schulze-Osthoff K, Fiebich BL (1998) Substance P and Histamine Induce Interleukin-6 Expression in Human Astrocytoma Cells by a Mechanism Involving Protein Kinase C and Nuclear Factor-IL-6. *Journal of Neurochemistry* **70:** 1577-1583

Lindmark B, Rompikuntal P, Vaitkevicius K, Song T, Mizunoe Y, Uhlin B, Guerry P, Wai S (2009) Outer membrane vesicle-mediated release of cytolethal distending toxin (CDT) from Campylobacter jejuni. *BMC Microbiology* **9:** 220

Lu L, Khan S, Lencer W, Walker WA (2005) Endocytosis of cholera toxin by human enterocytes is developmentally regulated. *American journal of physiology Gastrointestinal and liver physiology* **289:** G332-341

McBroom AJ, Johnson AP, Vemulapalli S, Kuehn MJ (2006) Outer Membrane Vesicle Production by Escherichia coli Is Independent of Membrane Instability. *J Bacteriol* **188:** 5385-5392

McBroom AJ, Kuehn MJ (2007) Release of outer membrane vesicles by Gram-negative bacteria is a novel envelope stress response. *Mol Microbiol* **63:** 545-558

McMahon HT, Boucrot E (2011) Molecular mechanism and physiological functions of clathrin-mediated endocytosis. *Nat Rev Mol Cell Biol* **12:** 517-533

Moss J, Osborne JC, Fishman PH, Nakaya S, Robertson DC (1981) Escherichia coli heat-labile enterotoxin. Ganglioside specificity and ADP-ribosyltransferase activity. *Journal of Biological Chemistry* **256:** 12861-12865

Mudrak B, Kuehn MJ (2010) Heat-labile enterotoxin: beyond g(m1) binding. *Toxins* **2:** 1445-1470

Mudrak B, Rodriguez DL, Kuehn MJ (2009) Residues of heat-labile enterotoxin involved in bacterial cell surface binding. *J Bacteriol* **191:** 2917-2925

Mundell DH, Anselmo CR, Wishnow RM (1976) Factors influencing heat-labile Escherichia coli enterotoxin activity. *Infect Immun* **14:** 383-388

Muralinath M, Kuehn MJ, Roland KL, Curtiss R, 3rd (2011) Immunization with Salmonella enterica serovar Typhimurium-derived outer membrane vesicles delivering the pneumococcal protein PspA confers protection against challenge with Streptococcus pneumoniae. *Infection and Immunity* **79:** 887-894

Mynott TL, Guandalini S, Raimondi F, Fasano A (1997) Bromelain prevents secretion caused by Vibrio cholerae and Escherichia coli enterotoxins in rabbit ileum in vitro. *Gastroenterology* **113:** 175-184

Nazli A, Wang A, Steen O, Prescott D, Lu J, Perdue MH, Söderholm JD, Sherman PM, McKay DM (2006) Enterocyte Cytoskeleton Changes Are Crucial for Enhanced Translocation of Nonpathogenic Escherichia coli across Metabolically Stressed Gut Epithelia. *Infection and Immunity* **74:** 192-201

Niyogi S (2005) Shigellosis. *Journal of Microbiology* **43:** 133-143

O'Donnell EK, Sedlacek RL, Singh AK, Schultz BD (2000) Inhibition of enterotoxin-induced porcine colonic secretion by diarylsulfonylureas in vitro. *Am J Physiol Gastrointest Liver Physiol* **279:** G1104-1112

Oh P, McIntosh DP, Schnitzer JE (1998) Dynamin at the Neck of Caveolae Mediates Their Budding to Form Transport Vesicles by GTP-driven Fission from the Plasma Membrane of Endothelium. *The Journal of Cell Biology* **141:** 101-114

Ohno A, Marui A, Castro ES, Reyes AAB, Elio-Calvo D, Kasitani H, Ishii Y, Yamaguchi K (1997) Enteropathogenic Bacteria in the La Paz River of Bolivia. *The American Journal of Tropical Medicine and Hygiene* **57:** 438-444

Oprins JCJ, Meijer HP, Groot JA (2000) TNF-α potentiates the ion secretion induced by muscarinic receptor activation in HT29cl.19A cells. *American Journal of Physiology - Cell Physiology* **278:** C463-C472

Palva ET, Hirst TR, Hardy SJ, Holmgren J, Randall L (1981) Synthesis of a precursor to the B subunit of heat-labile enterotoxin in Escherichia coli. *Journal of Bacteriology* **146:** 325-330

Parissi-Crivelli A, Parissi-Crivelli JM, Giron JA (2000) Recognition of enteropathogenic Escherichia coli virulence determinants by human colostrum and serum antibodies. *Journal of clinical microbiology* **38:** 2696-2700

Park SB, Jang HB, Nho SW, Cha IS, Hikima J, Ohtani M, Aoki T, Jung TS (2011) Outer Membrane Vesicles as a Candidate Vaccine against Edwardsiellosis. *PLoS One* **6:** e17629

Parker H, Chitcholtan K, Hampton MB, Keenan JI (2010) Uptake of Helicobacter pylori Outer Membrane Vesicles by Gastric Epithelial Cells. *Infect Immun* **78:** 5054-5061

Parton RG, Simons K (2007) The multiple faces of caveolae. *Nat Rev Mol Cell Biol* **8:** 185-194

Pearson A, Colville-Nash P, Kwan J, Dockrell M (2008) Albumin induces interleukin-6 release from primary human proximal tubule epithelial cells. *Journal of Nephrology* **21:** 887-893

Peeters CCAM, Rümke HC, Sundermann LC, Rouppe van der Voort EM, Meulenbelt J, Schuller M, Kuipers AJ, van der Ley P, Poolman JT (1996) Phase I clinical trial with a hexavalent PorA containing meningococcal outer membrane vesicle vaccine. *Vaccine* **14:** 1009-1015

Petri WA, Miller M, Binder HJ, Levine MM, Dillingham R, Guerrant RL (2008) Enteric infections, diarrhea, and their impact on function and development. *The Journal of Clinical Investigation* **118:** 1277-1290

Prados-Rosales R, Baena A, Martinez LR, Luque-Garcia J, Kalscheuer R, Veeraraghavan U, Camara C, Nosanchuk JD, Besra GS, Chen B, Jimenez J, Glatman-Freedman A, Jacobs WR, Porcelli SA, Casadevall A (2011) Mycobacteria release active membrane vesicles that modulate

immune responses in a TLR2-dependent manner in mice. *Journal of Clinical Investigation* **121:** 1471-1483

Prestle J, Pfizenmaier K, Brenner J, Johannes FJ (1996) Protein kinase C mu is located at the Golgi compartment. *The Journal of Cell Biology* **134:** 1401-1410

Qadri F, Das SK, Faruque ASG, Fuchs GJ, Albert MJ, Sack RB, Svennerholm A-M (2000) Prevalence of Toxin Types and Colonization Factors in Enterotoxigenic Escherichia coli Isolated during a 2-Year Period from Diarrheal Patients in Bangladesh. *J Clin Microbiol* **38:** 27-31

Qadri F, Svennerholm A-M, Faruque ASG, Sack RB (2005) Enterotoxigenic Escherichia coli in Developing Countries: Epidemiology, Microbiology, Clinical Features, Treatment, and Prevention. *Clin Microbiol Rev* **18:** 465-483

Rao MC (1985) Toxins which activate guanylate cyclase: heat-stable enterotoxins. *Ciba Found Symp* **112:** 74-93

Renelli M, Matias V, Lo RY, Beveridge TJ (2004) DNA-containing membrane vesicles of Pseudomonas aeruginosa PAO1 and their genetic transformation potential. *Microbiology* **150:** 2161-2169

Ricci V, Chiozzi V, Necchi V, Oldani A, Romano M, Solcia E, Ventura U (2005) Free-soluble and outer membrane vesicle-associated VacA from Helicobacter pylori: two forms of release, a different activity. *Biochemical and Biophysical Research Communications* **337:** 173-178

Rivera J, Cordero RJB, Nakouzi AS, Frases S, Nicola A, Casadevall A (2010) Bacillus anthracis produces membrane-derived vesicles containing biologically active toxins. *Proceedings of the National Academy of Sciences* **107:** 19002-19007

Roberts R, Moreno G, Bottero D, Gaillard ME, Fingermann M, Graieb A, Rumbo M, Hozbor D (2008) Outer membrane vesicles as acellular vaccine against pertussis. *Vaccine* **26:** 4639-4646

Rompikuntal PK, Thay B, Khan MK, Alanko J, Penttinen A-M, Asikainen S, Wai SN, Oscarsson J (2011) Perinuclear localization of internalized Outer Membrane Vesicles carrying active Cytolethal Distending Toxin (CDT) from Aggregatibacter actinomycetemcomitans. *Infect Immun*: IAI.06069-06011

Round JL, O'Connell RM, Mazmanian SK (2010) Coordination of tolerogenic immune responses by the commensal microbiota. *Journal of Autoimmunity* **34:** J220-J225

Rumbo M, Anderle P, Didierlaurent A, Sierro F, Debard N, Sirard J-C, Finke D, Kraehenbuhl J-P (2004) How the Gut Links Innate and Adaptive Immunity. *Annals of the New York Academy of Sciences* **1029:** 16-21

Sack RB (1975) Human diarrheal disease caused by enterotoxigenic Escherichia coli. *Annu Rev Microbiol* **29:** 333-353

Sack RB, Gorbach SL, Banwell JG, Jacobs B, Chatterjee BD, Mitra RC (1971) Enterotoxigenic Escherichia coli Isolated from Patients with Severe Cholera-like Disease. *Journal of Infectious Diseases* **123:** 378-385

Saleh M, Trinchieri G (2011) Innate immune mechanisms of colitis and colitis-associated colorectal cancer. *Nat Rev Immunol* **11:** 9-20

Sánchez J, Holmgren J (2005) Virulence factors, pathogenesis and vaccine protection in cholera and ETEC diarrhea. *Current Opinion in Immunology* **17:** 388-398

Sayeed S, Uzal FA, Fisher DJ, Saputo J, Vidal JE, Chen Y, Gupta P, Rood JI, McClane BA (2008) Beta toxin is essential for the intestinal virulence of Clostridium perfringens type C disease isolate CN3685 in a rabbit ileal loop model. *Molecular Microbiology* **67:** 15-30

Schaar V, de Vries SP, Perez Vidakovics ML, Bootsma HJ, Larsson L, Hermans PW, Bjartell A, Morgelin M, Riesbeck K (2011) Multicomponent Moraxella catarrhalis outer membrane vesicles induce an inflammatory response and are internalized by human epithelial cells. *Cellular Microbiology* **13:** 432-449

Schlegel A, Volonté D, Engelman JA, Galbiati F, Mehta P, Zhang X-L, Scherer PE, Lisanti MP (1998) Crowded Little Caves: Structure and Function of Caveolae. *Cellular Signalling* **10:** 457-463

Schooling SR, Beveridge TJ (2006) Membrane Vesicles: an Overlooked Component of the Matrices of Biofilms. *J Bacteriol* **188:** 5945-5957

Schreiber E, Matthias P, Muller MM, Schaffner W (1989) Rapid detection of octamer binding proteins with 'mini extracts', prepared from a small number of cells. *Nucl Acids Res* **17:** 6419-

Sharpe SW, Kuehn MJ, Mason KM (2011) Elicitation of Epithelial Cell-Derived Immune Effectors by Outer Membrane Vesicles of Nontypeable Haemophilus influenzae. *Infect Immun* **79:** 4361-4369

Soriani M, Bailey L, Hirst TR (2002) Contribution of the ADP-ribosylating and receptor-binding properties of cholera-like enterotoxins in modulating cytokine secretion by human intestinal epithelial cells. *Microbiology* **148:** 667-676

Spangler BD (1992) Structure and function of cholera toxin and the related Escherichia coli heat-labile enterotoxin. *Microbiol Mol Biol Rev* **56:** 622-647

Steffen R, Castelli F, Dieter Nothdurft H, Rombo L, Jane Zuckerman N (2005) Vaccination against Enterotoxigenic Escherichia coli, a Cause of Travelers Diarrhea. *Journal of Travel Medicine* **12:** 102-107

Subramanian S, Rhodes JM, Hart CA, Tam B, Roberts CL, Smith SL, Corkill JE, Winstanley C, Virji M, Campbell BJ (2008) Characterization of epithelial IL-8 response to inflammatory bowel disease mucosal E. coli and its inhibition by mesalamine. *Inflamm Bowel Dis* **14:** 162-175

Svennerholm A-M, Steele D (2004) Progress in enteric vaccine development. *Best Practice & Research Clinical Gastroenterology* **18:** 421-445

Takashi K, Fujita I, Kobari K (1989) Effects of short chain fatty acids on the production of heat-labile enterotoxin from enterotoxigenic Escherichia coli. *Japanese journal of pharmacology* **50:** 495-498

Taxt A, Aasland R, Sommerfelt H, Nataro J, Puntervoll P (2010) Heat-Stable Enterotoxin of Enterotoxigenic Escherichia coli as a Vaccine Target. *Infect Immun* **78:** 1824-1831

Tebbutt NC, Giraud AS, Inglese M, Jenkins B, Waring P, Clay FJ, Malki S, Alderman BM, Grail D, Hollande F, Heath JK, Ernst M (2002) Reciprocal regulation of gastrointestinal homeostasis by SHP2 and STAT-mediated trefoil gene activation in gp130 mutant mice. *Nat Med* **8:** 1089-1097

Teneberg S, Hirst TR, Ångström J, Karlsson K-A (1994) Comparison of the glycolipid-binding specificities of cholera toxin and porcine<i>Escherichia coli</i> heat-labile enterotoxin: identification of a receptor-active non-ganglioside glycolipid for the heat-labile toxin in infant rabbit small intestine. *Glycoconjugate Journal* **11:** 533-540

Triadafilopoulos G, Pothoulakis C, Weiss R, Giampaolo C, Lamont JT (1989) Comparative study of Clostridium difficile toxin A and cholera toxin in rabbit ileum. *Gastroenterology* **97:** 1186-1192

van der Ley P, Heckels JE, Virji M, Hoogerhout P, Poolman JT (1991) Topology of outer membrane porins in pathogenic Neisseria spp. *Infect Immun* **59:** 2963-2971

Van der Ley P, Van den Dobbelsteen G (2011) Next-generation outer membrane vesicle vaccines against Neisseria meningitidis based on nontoxic LPS mutants. *Human Vaccines* **7:** 886-890

Vassilieva EV, Gerner-Smidt K, Ivanov AI, Nusrat A (2008) Lipid rafts mediate internalization of β1-integrin in migrating intestinal epithelial cells. *American Journal of Physiology - Gastrointestinal and Liver Physiology* **295:** G965-G976

Vermeulen L, De Wilde G, Van Damme P, Vanden Berghe W, Haegeman G (2003) Transcriptional activation of the NF-[kappa]B p65 subunit by mitogen- and stress-activated protein kinase-1 (MSK1). *Embo J* **22:** 1313-1324

Vieira FS, Corrêa G, Einicker-Lamas M, Coutinho-Silva R (2010) Host-cell lipid rafts: a safe door for micro-organisms? *Biology of the Cell* **102:** 391-407

Viswanathan VK, Hodges K, Hecht G (2009) Enteric infection meets intestinal function: how bacterial pathogens cause diarrhoea. *Nat Rev Microbiol* **7:** 110-119

Wachsmuth K, Wells J, Shipley P, Ryder R (1979) Heat-labile enterotoxin production in isolates from a shipboard outbreak of human diarrheal illness. *Infection and Immunity* **24:** 793-797

Wai SN, Lindmark B, Söderblom T, Takade A, Westermark M, Oscarsson J, Jass J, Richter-Dahlfors A, Mizunoe Y, Uhlin BE (2003) Vesicle-Mediated Export and Assembly of Pore-Forming Oligomers of the Enterobacterial ClyA Cytotoxin. *Cell* **115:** 25-35

Wai SN, Takade A, Amako K (1995) The release of outer membrane vesicles from the strains of enterotoxigenic Escherichia coli. *Microbiology and Immunology* **39:** 451-456

Walker RI, Steele D, Aguado T (2007) Analysis of strategies to successfully vaccinate infants in developing countries against enterotoxigenic E. coli (ETEC) disease. *Vaccine* **25:** 2545-2566

Wang L, Walia B, Evans J, Gewirtz AT, Merlin D, Sitaraman SV (2003) IL-6 Induces NF-κB Activation in the Intestinal Epithelia. *The Journal of Immunology* **171:** 3194-3201

Wenneras C, Erling V (2004) Prevalence of enterotoxigenic Escherichia coli-associated diarrhoea and carrier state in the developing world. *Journal of Health, Population and Nutrition* **22:** 370-382

Wensink J, Gankema H, Jansen WH, Guinée PAM, Witholt B (1978) Isolation of the membranes of an enterotoxigenic strain of Escherichia coli and distribution of enterotoxin activity in different subcellular fractions. *Biochimica et Biophysica Acta (BBA) - Biomembranes* **514:** 128-136

Wensink J, Witholt B (1981) Outer-Membrane Vesicles Released by Normally Growing *Escherichia coli* Contain Very Little Lipoprotein. *European Journal of Biochemistry* **116:** 331-335

Wolf AA, Fujinaga Y, Lencer WI (2002) Uncoupling of the Cholera Toxin-GM1 Ganglioside Receptor Complex from Endocytosis, Retrograde Golgi Trafficking, and Downstream Signal

Transduction by Depletion of Membrane Cholesterol. *Journal of Biological Chemistry* **277:** 16249-16256

Wolf AA, Jobling MG, Wimer-Mackin S, Ferguson-Maltzman M, Madara JL, Holmes RK, Lencer WI (1998) Ganglioside Structure Dictates Signal Transduction by Cholera Toxin and Association with Caveolae-like Membrane Domains in Polarized Epithelia. *The Journal of Cell Biology* **141:** 917-927

Yeung C-Y, Lee H-C, Lin S-P, Fang S-B, Jiang C-B, Huang F-Y, Chuang C-K (2004) Serum cytokines in differentiating between viral and bacterial enterocolitis. *Annals of Tropical Paediatrics: International Child Health* **24:** 337-343

Zhang W, Robertson DC, Zhang C, Bai W, Zhao M, Francis DH (2008) Escherichia coli Constructs Expressing Human or Porcine Enterotoxins Induce Identical Diarrheal Diseases in a Piglet Infection Model. *Appl Environ Microbiol* **74:** 5832-5837

Biography

Halima Jane Chutkan was born on June 1, 1984 in Kingston, Jamaica. She moved to Lehigh Acres, Florida in 1998 and was the valedictorian of the 2001 class of Riverdale High School. She attended the University of Florida and graduated summa cum laude in 2005 with a B.S. in Microbiology and Cell Science. Halima matriculated at Duke University through the Cell and Molecular Biology program and affiliated with the Department of Molecular Genetics and Microbiology. She met her husband Ace Hatch when they were both rotating in the Kuehn lab, which she eventually joined. Halima has been awarded grants to present at the American Society for Microbiology General Meeting and at Mid-Atlantic Microbial Pathogenesis Meetings. She defended her thesis on December 14, 2011, a gift to everyone who loves her.

Publications

Chutkan, H and M.J. Kuehn. 2011. Context-Dependent Activation Kinetics Elicited by Soluble versus Outer Membrane Vesicle-Associated Heat-Labile Enterotoxin. *Infection and Immunity.* 79(9): 3760-3769.

Chutkan, H and M.J. Kuehn. 2011. Heat labile enterotoxin- and GM1-dependent intracellular trafficking and signaling of enterotoxigenic Escherichia coli outer membrane vesicles. Submitted.